PERFORMANCE OF NANO SILICA GEL PRODUCED FROM RISE HUSK ASH (RHA) IN CEMENTITIOUS MEDIA

By

BAKUL BARUA [B.Sc. Eng.]

Student ID: 21MCE031P

A thesis submitted in partial fulfilment of the requirements for the degree of

MASTER of ENGINEERING in CIVIL ENGINEERING

Department of Civil Engineering

CHITTAGONG UNIVERSITY OF ENGINEERING AND TECHNOLOGY

July 2025

Declaration

I hereby declare that the work contained in this thesis has not been previously submitted to meet the requirements for an award at this or any other higher education institution. To the best of my knowledge and belief, the Thesis contains no material previously published or written by another person except where due reference is cited. Furthermore, the Thesis complies with PLAGIARISM and ACADEMIC INTEGRITY regulations of CUET.

Bakul Barua
21MCE031P
Department of Civil Engineering
Chittagong University of Engineering & Technology (CUET)

Copyright © Bakul Barua, 2025.
This work may not be copied without the permission of the author or Chittagong University of Engineering & Technology.

Dedication

To my amazing mentors and friends, whose guidance and encouragement have been invaluable.

and

To my beloved family, who are infinitely supportive and always believe in me.

List of Publications

Conference

Barua B. and Islam G. M. S. (2025) "Fresh properties of nano-silica gel-induced cementitious media." *8th International Conference on Engineering Research, Innovation and Education*, 24-26 April 2025, School of Applied Sciences & Technology, Shahjalal University of Science and Technology (SUST), Sylhet, Bangladesh.

Declaration by the Supervisor

This is to certify that **Bakul Barua** has carried out this research work under my supervision and that he has fulfilled the relevant Academic Ordinance of the Chittagong University of Engineering and Technology so that he is qualified to submit the following Thesis in the application for the degree of MASTER of ENGINEERING in CIVIL ENGINEERING. Furthermore, the Thesis complies with the PLAGIARISM and ACADEMIC INTEGRITY regulations of CUET.

Prof. Dr. G. M. Sadiqul Islam

Department of Civil Engineering

Chittagong University of Engineering & Technology.

Acknowledgement

My most profound appreciation goes to my thesis supervisor, Prof. Dr. G.M. Sadiqul Islam, from the Department of Civil Engineering. Thank you for your exceptional guidance, unwavering support, and constant encouragement during this process. Your thoughtful feedback and mentorship have been vital in helping me achieve the success of this thesis.

I am deeply thankful to the Civil Engineering Department at CUET for providing the resources and a conducive environment that is necessary for conducting this research. Special thanks to the lab staff and colleagues who assisted with experiments and analysis.

To my family, I am eternally thankful for your unwavering love, patience, and encouragement. Your encouragement gave me the drive and determination to see this endeavour through to completion.

Lastly, I want to thank my friends and peers who stood by me, offering encouragement and assistance whenever needed. This journey would not have been possible without each of you.

Bakul Barua

July 2025

Abstract

This study investigates the use of Nano-Silica Gel (NSG) derived from Rice Husk Ash (RHA) as a sustainable alternative in cement-based composites. RHA, rich in amorphous silica, is an eco-friendly source for NSG production, which can enhance cement performance and reduce environmental impact. Experimental tests were conducted on pastes and mortars by replacing cement with NSG dosages of 1%, 2%, 3%, and 5% to evaluate flowability, density, setting time, compressive strength, flexural strength, shrinkage, soundness, electrical resistivity, and pozzolanic activity. Scanning Electron Microscopy (SEM) and X-ray Diffraction (XRD) were also used to analyze microstructural changes at 7, 28, and 90 days.

Results showed that 1% NSG significantly improved compressive strength (53.9 MPa) and flexural strength (6.94 MPa) at 90 days, compared to the control mix. This improvement is due to the highly reactive nature of NSG, which accelerates the formation of calcium-silicate-hydrate (C-S-H) gel, enhancing the matrix and pore structure. However, higher NSG dosages (≥3%) decreased strength and stability due to increased water demand and particle agglomeration. Pozzolanic activity was moderate at 1–2% NSG but declined at 5%. The Frattini test confirmed moderate pozzolanic activity at lower dosages; however, the benefits diminished at the highest replacement level (5%). Lower NSG levels improved electrical resistivity, while higher dosages increased porosity. In conclusion, NSG derived from RHA could be a viable and effective supplementary cementitious material when used at optimal replacement levels. Specifically, a 1% NSG substitution shows the best balance of enhanced strength and other relevant properties. The use of RHA-derived NSG also contributes to sustainability goals by reducing the demand for cement, an energy-intensive material. This work offers valuable insights into advancing sustainable practices in the construction industry by promoting waste utilization and reducing the carbon footprint associated with cement production.

Table of Content

Abstract vi

Table of Content vii

List of Figures x

List of Tables xii

Nomenclature xiii

Chapter 1: INTRODUCTION 1

1.1 BACKGROUND 1

1.2 CONTEXT 3

1.3 AIMS AND OBJECTIVES 5

1.4 SIGNIFICANCE OF THE STUDY 5

1.5 SCOPE OF THE WORK 6
- 1.5.1 Material Characterization 6
- 1.5.2 Experimental condition 6
- 1.5.3 Mechanical Performance Testing 6
- 1.5.4 Indirect Durability Assessment 7
- 1.5.5 Environmental and Sustainability Impact 7

1.6 DEFINITIONS 7

1.7 THESIS OUTLINE 8

Chapter 2: LITERATURE REVIEW 10

2.1 CEMENTITIOUS MATERIALS AND SUSTAINABILITY CHALLENGES 10

2.2 DIFFERENT SCMS USED IN CEMENTITIOUS MEDIA 11

2.3 RICE HUSK 13

2.4 RICE HUSK ASH 14

2.5 SYNTHESIS OF NANO SILICA FROM RHA 14

2.6 EFFECT OF NSG ON FRESH PROPERTIES 17

2.7 MICROSTRUCTURE 19

2.8 STRENGTH CHARACTERISTICS 21

2.9 DURABILITY PERFORMANCE 24

2.10 SUSTAINABILITY AND ENVIRONMENTAL BENEFITS 27

2.11 SUMMARY OF LITERATURE REVIEW AND RESEARCH GAPS 30

Chapter 3: MATERIALS AND METHODOLOGY 35

3.1 MATERIALS 35
- 3.1.1 Ordinary Portland Cement 36
- 3.1.2 Nano Silica Gel 38

3.1.3 Fine Aggregate 39
3.1.4 Water 40
3.2 METHODOLOGY 41
3.3 NSG Characterization Tests 46
3.3.1 Particle Size Distribution 46
3.3.2 Scanning Electron Microscopy for morphology and EDX 47
3.3.3 Mineralogical composition (XRD) 48
3.3.4 Chemical composition (XRF) 48
3.3.5 Loss on Ignition 48
3.4 NSG Paste Sample Test 50
3.4.1 Frattini Test for Pozzolanic Activity 50
3.4.2 Normal Consistency 52
3.4.3 Setting Time 53
3.4.4 Soundness (Le Chatelier Method) 54
3.4.5 Autoclave Expansion Test 54
3.5 MORTAR Tests 56
3.5.1 Mix Design 56
3.5.2 Specimen Preparation 57
3.5.3 Flow Table Test 59
3.5.4 Fresh Density of Mortar 60
3.5.5 Hardened Density of Mortar 60
3.6 CURING ENVIRONMENT 60
3.7 TESTING PROGRAM 62
3.7.1 Compressive Strength Test of Mortar 62
3.7.2 Flexural Strength Test of Mortar 63
3.7.3 Drying shrinkage 65
3.7.4 Electrical Resistivity 67
Chapter 4: RESULTS AND DISCUSSION 69
4.1 MATERIAL TEST RESULT 69
4.1.1 Particle Size Distribution 69
4.1.2 Chemical Analysis by XRF 70
4.1.3 Mineralogy by X-ray Diffraction (XRD) 72
4.1.4 Loss on Ignition 73
4.1.5 Frattini Test for Pozzolanic Activity 74
4.2 PASTE TEST RESULT 75
4.2.1 Scanning electron microscopy (SEM) 75
4.2.2 Energy-Dispersive X-ray Spectroscopy (EDX) Analysis 81
4.2.3 Normal Consistency 85
4.2.4 Setting Time 86
4.2.5 Soundness 88
4.2.6 Autoclave expansion 89
4.4 MORTAR TEST RESULT 90
4.4.1 The Flow Table Test 90
4.4.2 Fresh density of mortar 92
4.4.3 Hardened Density of Mortar 94
4.4.4 Flexural Strength Analysis 95
4.4.5 Compressive Strength Analysis 97
4.4.6 Strength Activity Index (SAI) 99
4.4.7 Drying Shrinkage 100
4.4.8 Electrical Resistivity 102

4.5 SUMMARY OF EXPERIMENTAL RESULTS 103
Chapter 5: CONCLUSIONS 105
5.1 GENERAL 105
5.2 KEY FINDINGS 106
5.3 LIMITATION OF THE STUDY 107
5.4 PRACTICAL IMPLICATION 107
5.5 RECOMMENDATION FOR FURTHER STUDY 108
Reference 109
Appendices 115

List of Figures

Fig. No.	Figure Caption	Page No.
Figure 3.1	The physical appearance of CEM-I	36
Figure 3.2	Physical appearance of NSG	38
Figure 3.3	Physical appearance of EN Standard Sand	40
Figure 3.4	General outline of the methodology and research program	44
Figure 3.5	Experimental program at different levels	45
Figure 3.6	Malvern Hydro EV analyzer	46
Figure 3.7	Scanning Electron Microscopy for morphology and EDX analysis	47
Figure 3.8	Programmable muffle furnace	49
Figure 3.9	Diagram for assessing pozzolanicity	50
Figure 3.10	Frattini test of pozzolanic activity	51
Figure 3.11	Normal consistency, setting time, and soundness tests	53
Figure 3.12	Autoclave expansion test	55
Figure 3.13:	Mortar specimen preparation	58
Figure 3.14	Curing of specimens	61
Figure 3.15	Compressive strength testing.	63
Figure 3.16	Flexural test on standard mortar prism	65
Figure 3.17	Drying shrinkage of paste	66
Figure 3.18	Electrical resistivity test of mortar	68
Figure 4.1	Particle size distribution curve of NSG	70
Figure 4.2	XRD pattern of nano silica [(Intensity) vs 2 Theta]	72
Figure 4.3	Frattini test result	75
Figure 4.4	SEM image of the control paste	76
Figure 4.5	SEM image of 1% replacement of CEM-1 with NGS	77
Figure 4.6	SEM image of 2% replacement of CEM-1 with NGS	78
Figure 4.7	SEM image of 3% replacement of CEM-1 with NGS	79
Figure 4.8	SEM image of 5% replacement of CEM-1 with NGS	80
Figure 4.9	EDX of control sample	82

Figure 4.10 EDX of 1% CEM I replacement with NGS 82
Figure 4.11 EDX of 2% CEM I replacement with NGS 83
Figure 4.12 EDX of 3% CEM I replacement with NGS 83
Figure 4.13 EDX of 5% CEM I replacement with NGS 84
Figure 4.14 Normal consistency result 85
Figure 4.15 Setting Time Result 87
Figure 4.16 Soundness test results 88
Figure 4.17 Autoclave expansion result 89
Figure 4.18 Flow value result 91
Figure 4.19 Water demand result 91
Figure 4.20 Fresh density of mortar 93
Figure 4.21 Hardened density test results 95
Figure 4.22 Flexural strength of NGS induced mortars at different ages 96
Figure 4.23 Compressive strength of mortars 98
Figure 4.24 Drying shrinkage result 101
Figure 4.25 Surface resistivity of mortar 102

List of Tables

Table No. **Table Caption** **Page No.**

Table 3.1: Chemical composition of CEM-I 37
Table 3.2: Physical properties of OPC 37
Table 3.3 Mix proportions for Frattini test 51
Table 3.4 Mortar mix proportions.....56
Table 3.5: Number of samples for mortar 56
Table 4.1: The chemical composition of NSG analyzed using the XRF. 71
Table 4.2: Wet Physical Properties of Formulation analysis results of nano silica....72

Nomenclature

Symbol / Term	Meaning
NSG	Nano Silica Gel
RHA	Rice Husk Ash
SCM	Supplementary Cementitious Material
LCA	Life Cycle Assessment
OPC	Ordinary Portland Cement
C-S-H	Calcium Silicate Hydrate
C-H	Calcium Hydroxide
UV	Ultraviolet
CO_2	Carbon Dioxide
w/c	Water to Cement Ratio
ρ	Density
CEN	European Committee for Standardization
SEM	Scanning Electron Microscopy
XRD	X-ray Diffraction
XRF	X-ray Fluorescence
EDX	Energy-Dispersive X-ray Spectroscopy
LOI	Loss on Ignition
Frattini Test	Test for Pozzolanic Activity (BS EN 196-5:1995)
NaOH	Sodium Hydroxide
H_2SO_4	Sulfuric Acid
HCl	Hydrochloric Acid
ASTM	American Society for Testing and Materials
EN	European Standard
SEAL	Sustainable Energy & Agro-Resource Ltd

Chapter 1: INTRODUCTION

The growing demand for sustainable construction has given impetus to research on advanced materials that enhance performance and promote environmental sustainability. One such innovation is nano-silica gel, which enhances cement-based composites through its pozzolanic activity. Producing this material using eco-friendly approaches is crucial, and rice husk ash (RHA), a byproduct of rice milling, offers an ideal solution due to its high silica content. Converting RHA into nano silica gel not only utilizes agricultural waste but also optimizes the mechanical and durability properties of cementitious materials.

Nano silica gel interacts at the nanoscale, accelerating cement hydration and refining pore structures. These interactions enhance compressive strength, reduce permeability, and improve overall durability. Its finer particle size and larger surface area set it apart from conventional silica fume, offering superior reactivity and performance in concrete applications. While RHA has shown promise as a supplementary cementitious material (SCM), its direct use presents challenges, including inconsistent composition and incomplete reactions. Transforming RHA into nano-silica gel could mitigate these issues, ensuring better dispersion and reactivity within the cement matrix. This process also addresses environmental concerns by reducing agricultural waste and minimizing carbon emissions tied to cement production.

This study aims to evaluate the effectiveness of nano silica gel derived from RHA, focusing on hydration, workability, strength, and durability. By bridging the gap between sustainable practices and high-performance materials, this research contributes to greener construction methods while addressing ecological and engineering challenges. Findings are expected to provide valuable insights for improving cement-based infrastructure and promoting eco-friendly waste utilization strategies.

1.1 BACKGROUND

The rising demand for eco-friendly and high-performance construction materials has driven extensive research into alternative cementitious materials. Cement

production is a significant source of carbon dioxide (CO_2) emissions, accounting for approximately 8% of global CO_2 emissions (Scrivener et al., 2018). Consequently, researchers and engineers are exploring supplementary cementitious materials (SCMs) that can partially replace cement while improving its mechanical and durability properties. Among these SCMs, nano silica has attracted significant attention for its ability to refine pore structure, accelerate hydration, and enhance the overall performance of cement-based materials (Liu et al., 2022). Nano silica gel produced from rice husk ash (RHA) offers a sustainable and cost-effective approach to reducing cement usage while enhancing concrete properties.

Rice husk, an agricultural rice milling residue, accounts for approximately 20% of the total mass of rice grains (Ali et al., 2021). The production of rice husk ash (RHA) is formed by the combustion of rice husks under monitored conditions, which carries up to 90% amorphous silica (Zareei et al., 2017). RHA is a suitable precursor for producing nano silica gel due to its high silica content. Traditional uses of RHA in cementitious systems have shown promising results, enhancing compressive strength, resistance and durability to chemical attack (Amran et al., 2021). However, the direct use of RHA presents challenges, such as composition variability and incomplete reaction with cement, which can reduce its effectiveness as an SCM. The cement matrix is better able to disperse and react by transforming RHA into nano silica gel, which addresses these issues (Singh & Murmu, 2011).

Nano silica, with its massive surface area and ultrafine particle size, interacts more effectively with calcium hydroxide (CH) generated during cement hydration, resulting in the formation of a greater amount of calcium silicate hydrate (C-S-H) gel. This strengthens the microstructure of cementitious materials (Calabria-Holley et al., 2015). Studies have shown that incorporating nano silica gel into cement paste can significantly enhance mechanical properties,

such as compressive strength and durability, while reducing porosity and permeability (Zhang et al., 2017). Moreover, nano silica gel enhances early-age strength development, which is vital for projects requiring fast-setting concrete (Lu & Poon, 2018).

From an ecological perspective, incorporating nano silica gel made from rice husk ash (RHA) promotes sustainable building practices by cutting down on agricultural waste and lowering cement usage. Recent research indicates that rice farming generates approximately 150 million tons of rice husks annually, a substantial portion of which is improperly disposed of, resulting in environmental pollution (Moraes et al., 2014). By transforming RHA into nano silica gel, this waste can be utilized as a valuable construction material, lessening its environmental footprint and improving the quality of concrete.

This study focuses on evaluating the effectiveness of nano-silica gel sourced from RHA in cementitious media, specifically examining its impact on hydration, workability, strength, and durability. Through exploring potential applications, this research supports the development of sustainable, high-performance cement-based materials, providing an effective solution to both environmental and engineering challenges.

1.2 CONTEXT

The construction industry is one of the largest consumers of raw materials and a significant source of carbon dioxide (CO_2) releases, primarily from cement manufacture. Traditional Portland cement (OPC) clinker accounts for approximately 8% of global CO_2 emissions, underscoring the urgent need for an alternative cementitious material that can enhance sustainability while maintaining or improving concrete performance (Scrivener et al., 2018). The development of sustainable building materials has garnered considerable attention due to growing ecological concerns and the need to reduce carbon

footprints. Cement, a widely used material in construction, is especially linked to a high environmental impact because of its energy-heavy production process and considerable carbon emissions. As a result, researchers have been exploring the use of industrial by-products as partial alternatives to cement.

Rice husk, a by-product of rice milling produced in large amounts, has emerged as a promising material for the construction industry. When rice husks are burned under controlled conditions, they produce Rice Husk Ash (RHA), which is high in silica. RHA has been studied for its reactive properties, making it a valuable ingredient in cementitious materials. When processed at the nanoscale, RHA can be converted into nano-silica gel, which exhibits enhanced reactivity, improved pozzolanic activity, and the ability to enhance the strength and longevity of cement-based composites.

Nano-silica gel, owing to its fine particle size and extensive surface area, has been shown to enhance the micro-level composition of cementitious materials. It can accelerate the hydration process, increase compressive strength, decrease permeability and strengthen resistance to chemical attacks. The use of nano-silica gel derived from rice husk ash not only offers an eco-friendly alternative to conventional cement but also helps to address the environmental challenges connected with agricultural waste.

This study aims to evaluate the performance of nano-silica gel derived from rice husk ash (RHA) in cementitious materials. Specifically, the study focuses on investigating the mechanical characteristics, durability, and microstructural features of cement-based materials, such as nano-silica gel. By examining how nano-silica gel enhances the properties of cementitious materials, this study aims to advance the development of more sustainable and high-performance construction materials.

By exploring this innovative application of rice husk ash, this research tackles the dual goals of reducing agricultural by-product waste and enhancing the performance of cement-based materials. The results of this study could lead to more sustainable and cost-effective solutions in the construction industry, with broader implications for minimizing the environmental impact of building materials.

1.3 AIMS AND OBJECTIVES

This study aims to assess the effectiveness of Nano Silica Gel (NSG) derived from Rice Husk Ash (RHA) in cement-based materials and examine its viability as a partial substitute for Ordinary Portland Cement (OPC). The key objectives to achieve this goal are as follows:

a. Conducting chemical, physical, and morphological characterization of Nano Silica Gel (NSG)
b. Evaluating the fresh properties of NSG-modified cementitious materials
c. Evaluating the mechanical, microstructural, and durability properties of NSG-modified cementitious materials

By accomplishing these objectives, this study aims to advance the development of sustainable cementitious materials and encourage the utilization of agricultural waste in eco-friendly construction solutions.

1.4 SIGNIFICANCE OF THE STUDY

This study is important as it offers a sustainable solution to the environmental issues linked to cement production. This research uses nano-silica gel (NSG) derived from rice husk ash (RHA), an agricultural residue, to address waste reduction and the environmental challenges of cement. The inclusion of NSG in cementitious materials can improve the mechanical properties, durability, and

overall performance of concrete, providing a more sustainable and high-performance alternative to conventional cement.

Beyond its environmental benefits, NSG's small particle size and high reactivity enhance strength, reduce permeability, and increase chemical resistance in cement-based materials. This study aims to evaluate these improvements, offering valuable insights into how NSG can optimize concrete performance and contribute to more durable, eco-friendly construction practices.

1.5 SCOPE OF THE WORK

This research covers material characterization, experimental investigations, and performance evaluation of NSG in cement-based composites, with a focus on mechanical, microstructural, and durability aspects.

1.5.1 Material Characterization

The characterization involves analysing the chemical, mineralogical, and morphological properties of NSG, as well as assessing its pozzolanic activity and microstructural features.

1.5.2 Experimental condition

To assess NSG as a partial substitute for Ordinary Portland Cement (OPC) at varying levels (1%, 2%, 3%, and 5%). Perform a performance analysis of cement paste and cement mortar through laboratory experiments. Investigate hydration products and the interface between NSG and aggregates in the transition zone.

1.5.3 Mechanical Performance Testing

To evaluate the compressive, flexural, and split tensile strengths at curing ages of 7, 28, and 90 days.

1.5.4 Indirect Durability Assessment

Examining the pore structure modifications due to NSG incorporation. To assess water absorption, drying shrinkage, and electrical resistivity. To investigate the potential for improved long-term durability and sustainability benefits.

1.5.5 Environmental and Sustainability Impact

To assess the potential reduction in carbon footprint through the partial replacement of cement with NSG and promote sustainable waste management by utilizing RHA, a widely available agricultural by-product. Explore the potential for large-scale applications in eco-friendly and cost-effective construction. This study did not cover the economic feasibility of large-scale commercial production of nano silica gel, as the primary focus is on the scientific and engineering aspects of its performance in cementitious media.

1.6 DEFINITIONS

To establish clarity, the following key terms used in this study are defined:

Rice Husk Ash (RHA): A byproduct from rice milling, generated by burning rice husks under regulated conditions, it contains up to 90% amorphous silica, making it an important supplementary cementitious material (Mosaberpanah & Umar, 2020).

Supplementary Cementitious Materials (SCMs): Materials such as fly ash, silica fume, and RHA interact with calcium hydroxide during cement hydration to form calcium silicate hydrate (C-S-H) gel, enhancing concrete properties (Al-saffar et al., 2023).

Nano Silica Gel (NSG): A colloidal form of silica nanoparticles with a high surface area, known for its high reactivity in cementitious materials, enhancing hydration and strength development (Singh et al., 2011).

Hydration Process: A reaction occurs between cement and water, leading to the formation of C-S-H gel, the primary binding phase responsible for the development of strength in concrete (Thomas & Jennings, 2006).

Pozzolanic Activity: The chemical reactivity of silica-based materials involves their reaction with calcium hydroxide, producing more C-S-H gel, which improves the mechanical strength and durability of cementitious materials. (Tang et al., 2021)

Carbon Footprint: The carbon footprint of a product or process represents the total amount of CO_2 emissions associated with it, measured in terms of its environmental impact (Scrivener et al., 2018).

By defining these key terms and outlining the scope of the study, this research establishes a comprehensive framework for evaluating the performance of nano silica gel derived from RHA as a sustainable cementitious additive.

1.7 THESIS OUTLINE

The layout of this thesis is structured as follows:

Chapter 1: Introduction – This chapter provides an overview of the background and outlines the research problem, objectives, and significance of the study on the performance of NGS in cementitious media.

Chapter 2: Literature Review – This chapter reviews previous studies on nano-silica, RHA-based materials, and their role in cementitious media.

Chapter 3: Materials and Methodology – It describes the synthesis of NSG, experimental setup, testing procedures, and analytical techniques.

Chapter 4: Results and Discussion – It presents findings on NSG characterization, hydration kinetics, and mechanical properties of cementitious media. Analyzes

and interprets the results, discussing their implications and comparing them with existing research.

Chapter 6: Conclusions and Recommendations – It summarizes key findings, discusses practical applications, and suggests directions for future research.

Chapter 2: LITERATURE REVIEW

This chapter provides a thorough literature review relevant to the research. It begins with an overview of cementitious materials and the sustainability challenges (Section 2.1). The subsequent sections cover different SCMs used in cementitious media (Section 2.2), rice husk (Section 2.3), rice husk ash (Section 2.4), synthesis of nano silica from RHA (Section 2.5), effect of NSG on fresh properties (Section 2.6), microstructure (Section 2.7), strength characteristics (Section 2.8), durability performance (Section 2.9) and its sustainability and environmental benefit (Section 2.10). Finally, Section 2.11 presents a summary of the literature review and identifies research gaps.

2.1 CEMENTITIOUS MATERIALS AND SUSTAINABILITY CHALLENGES

Approximately 8% of global CO_2 emissions are attributed to the cement industry (Scrivener et al., 2018), driving the search for alternatives such as Supplementary Cementitious Materials (SCMs). Materials such as fly ash, slag, and silica fume can help reduce cement consumption and CO_2 emissions, while also enhancing the durability of concrete (Bajpai et al., 2020). Fly ash enhances workability and durability, while ground granulated blast furnace slag (GGBFS) improves the mechanical properties of concrete (Li & Zhao, 2002). However, challenges such as material availability, cost, and variability hinder their widespread use. Geopolymer concrete, produced from industrial byproducts, presents additional potential for reducing CO_2 emissions (Azad & Samarakoon, 2021a). Life Cycle Assessment (LCA) studies show that SCMs can reduce emissions, although some, such as silica fume, may involve high production energy (Fallah-Valukolaee et al., 2022).

2.2 DIFFERENT SCMS USED IN CEMENTITIOUS MEDIA

Supplementary Cementitious Materials (SCMs) are incorporated into cement mixes to improve concrete properties, minimize the environmental effects of cement production, and support sustainability efforts. SCMs, which can be sourced from industrial byproducts or natural materials, are often utilized in cement-based blends. These include fly ash, slag, silica fume, natural pozzolans, and geopolymers, with each providing distinct advantages for the durability, workability, strength, and overall sustainability of concrete.

Fly Ash: While produced from the combustion of coal in power plants, it is one of the most common supplementary cementitious materials (SCMs). It primarily consists of fine, spherical particles that significantly enhance the workability and durability of concrete (Li et al., 2022). Fly ash helps to reduce the heat of hydration, making it ideal for large pours or use in hot climates. Moreover, it improves concrete's ability to withstand chemical attacks, such as those caused by sulfate and chloride corrosion, by decreasing permeability (Shaikh & Supit, 2015).

Ground Granulated Blast Furnace Slag (GGBFS): GGBFS, an important SCM, is created by quickly cooling of molten iron slag from blast furnaces. It enhances concrete's mechanical properties, particularly its compressive strength and durability, when applied in the right proportions. GGBFS helps to develop a denser concrete microstructure, enhancing its durability against chemical corrosion and reducing long-term shrinkage (Bernal et al., 2017a). GGBFS is particularly effective in concrete exposed to severe environmental conditions, such as in seawater or high-sulfate environments.

Rice Husk Ash (RHA): RHA is an emerging SCM derived from the combustion of rice husks, a widely available agricultural waste product. RHA is rich in silica, which makes it highly reactive when combined with calcium hydroxide in

cement. This reaction forms additional cementitious compounds that enhance the mechanical properties of concrete. RHA improves workability, strength, and durability, particularly in terms of chemical and heat resistance (Davidovits, 2013). Moreover, incorporating RHA in concrete supports sustainability by reusing agricultural waste and reducing CO_2 emissions from traditional cement production. However, the reactivity of RHA can vary depending on production conditions, like the burning temperature (Azad & Samarakoon, 2021b).

SBA: Sugarcane Bagasse Ash (SBA) is another agricultural byproduct that has demonstrated potential as a Supplementary Cementitious Material (SCM). It is produced by burning sugarcane bagasse, the fibrous byproduct from sugarcane juice extraction. Like other ash-based materials, SBA is rich in silica, which imparts pozzolanic properties to the concrete. The incorporation of SBA can enhance the mechanical properties of concrete, particularly its compressive strength, and improve its durability against sulfate and chloride attacks. Additionally, SBA helps to reduce the heat released during hydration in concrete mixtures, making it suitable for large-scale construction projects. The SBA also provides an effective method for disposing of agricultural waste, contributing to both environmental sustainability and reducing carbon emissions in cement production (Azad & Samarakoon, 2021b). However, its reactivity and performance depend on the ignition temperature and the chemical composition of the bagasse ash, which can vary widely.

Metakaolin: Metakaolin is a highly reactive pozzolanic material obtained by heating kaolin clay at controlled temperatures (typically between 600°C and 800°C). When used as an SCM, metakaolin significantly improves the mechanical properties, workability, and durability of concrete (Davidovits, 2013). It enhances the strength of concrete by filling voids and creating additional binding phases when reacting with calcium hydroxide in the mix. Metakaolin also contributes to a dense microstructure, which reduces permeability and increases the resistance

of concrete to sulfate attack, chloride-induced corrosion, and freeze-thaw cycles (Hossam et al., 2017). Although it is an excellent enhancer of concrete's properties, metakaolin can be more expensive than other SCMs, and its use may be limited by cost and availability. However, it is especially valuable in high-performance concrete where exceptional durability and strength are needed (Azad & Samarakoon, 2021a).

Silica Fume: Silica fume, a byproduct of silicon metal or ferrosilicon alloy manufacturing, is a fine, highly reactive substance that significantly enhances the strength and durability of concrete (Scrivener et al., 2018). In high-performance concrete, silica fume enhances density and reduces porosity, significantly improving resistance to chemical attacks such as chloride-induced corrosion and freeze-thaw damage. However, the high energy consumption and cost of silica fume production can restrict its widespread use (Hamada et al., 2023).

2.3 RICE HUSK

Rice Husk is the outer protective layer of rice grains, a residue from rice milling that is produced in vast quantities globally. Although typically considered waste, the potential of rice husk in sustainable construction has gained significant attention from other industries. It is primarily used in the formation of Rice Husk Ash (RHA), which, when burned at high temperatures, is rich in silica. This silica content makes RHA a highly effective Supplementary Cementitious Material (SCM) in concrete, enhancing its strength and durability (Davidovits, 2013). Beyond concrete, rice husks are also explored for applications in biofuels, insulation, and as fillers in composite materials, contributing to a circular economy by turning agricultural waste into valuable products (Azad & Samarakoon, 2021a).

In construction, rice husks can be used directly as lightweight aggregates or fillers in bricks and mortars. The insulating properties of rice husk make it particularly

useful in thermal applications (Scrivener et al., 2018). However, challenges remain regarding the cost-effective processing of rice husks on a large scale, though their availability in rice-producing countries offers significant potential for sustainable construction practices

2.4 RICE HUSK ASH

Rice Husk Ash (RHA) is produced by burning rice husks, a byproduct of the rice milling process. When rice husks are burned at temperatures typically between 500°C and 700°C, they create an ash rich in silica (SiO_2), making it highly reactive and valuable as a Supplementary Cementitious Material (SCM) in concrete. Calcium hydroxide in cement reacts with the silica in RHA, forming more calcium silicate hydrate (C-S-H) gel, a crucial compound that enhances concrete strength and durability (Davidovits, 2013). As a SCM, RHA improves concrete's mechanical properties, enhances its resistance to chemical degradation, including sulfate and chloride-induced corrosion, while reducing the material's overall permeability (Scrivener et al., 2018).

Beyond improving the properties of concrete, RHA offers environmental benefits by utilizing rice husks, a byproduct of agriculture, thereby reducing its environmental impact. The mixture of RHA in concrete also reduces the amount of Portland cement required, contributing to lower CO_2 emissions during production (Azad & Samarakoon, 2021a). However, the efficiency of RHA depends on variables such as combustion temperature and silica content, which can vary according to the origin of the rice husks.

2.5 SYNTHESIS OF NANO SILICA FROM RHA

Rice Husk Ash (RHA), a byproduct of rice milling, has recently gained significant attention as a valuable source of silica. When rice husks are burned at high temperatures, they produce RHA, which is rich in amorphous silica (SiO_2). This silica can be further processed to produce nano-silica, a material renowned for its

exceptional characteristics, including a large surface area, reactivity, and versatility, with applications in various fields such as construction, biomedicine, and electronics.

The process of synthesizing nano-silica from RHA generally includes extracting silica from RHA and reducing the particle size to the nanoscale. The initial step is the extraction of silica, typically achieved through chemical methods like alkaline extraction or acid leaching. In the alkaline extraction method, RHA is treated with sodium hydroxide (NaOH) to dissolve the silica. This results in a soluble silicate solution, which is then neutralized and further processed to produce silica gel. In the acid leaching method, sulfuric acid (H_2SO_4) is used to extract silica from RHA, followed by washing and filtration to remove impurities, resulting in pure silica gel (Azad & Samarakoon, 2021a).

Once the silica is extracted, it undergoes a precipitation process to form silica nanoparticles. This can be accomplished through various chemical processes, including sol-gel, co-precipitation, or hydrothermal methods. Among the different approaches, the sol-gel technique is the most popular for synthesizing nano-silica from RHA. In this method, a silica precursor, typically sodium silicate, is converted into a gel by the addition of an acid such as hydrochloric acid (HCl). The gel is then dried and calcined at elevated temperatures to produce fine nano-silica particles. Compared to conventional silica, these nano-silica particles exhibit a high surface area and greater reactivity, which makes them suitable for numerous applications (Davidovits, 2013).

The properties of nano-silica synthesized from RHA are strongly influenced by the synthesis conditions, including temperature, pH, and the chemical reagents used. Nano-silica derived from RHA typically features a high surface area, small particle size, and excellent dispersion properties, making it ideal for use in composite materials, adhesives, and as an additive in concrete. In particular,

nano-silica improves mechanical properties, durability, and ability to withstand chemical attacks, particularly in high-performance concrete mixes (Scrivener et al., 2018). Its incorporation strengthens the bonding between cement particles and reduces the porosity of concrete, resulting in stronger and more durable structures.

Furthermore, nano-silica synthesized from RHA is also being investigated for other applications such as drug delivery systems, antimicrobial coatings, and sensors, due to its biocompatibility and high reactivity. The biomedical and environmental benefits of nano-silica have been extensively studied, with promising results in controlled drug release, wound healing, and water purification (Azad & Samarakoon, 2021a).

One of the main advantages of synthesizing nano-silica from RHA is its sustainability. RHA is an abundant and inexpensive byproduct, and using it to produce valuable materials like nano-silica helps to reduce waste and promotes the recycling of agricultural byproducts. This method also presents an environmentally sustainable alternative to traditional nano-silica production, which typically involves energy-intensive processes and the use of hazardous chemicals (Davidovits, 2013).

To conclude, the production of nano-silica from rice husk ash offers a sustainable and efficient method for creating high-performance materials with applications in various industries, including construction, biomedicine, and electronics. This process not only adds value to agricultural waste but also helps to reduce environmental impact, making it a crucial area of research for future technological advancements.

2.6 EFFECT OF NSG ON FRESH PROPERTIES

The incorporation of Nano Silica Gel (NSG) into concrete has gained significant attention due to its ability to enhance the mechanical properties and durability of hardened concrete. However, understanding the impact of NSG on the fresh properties of concrete, such as workability, consistency, and setting time, is crucial for its practical use. Fresh properties refer to the characteristics of concrete during mixing, transportation, and placement, which directly affect the ease of handling and the overall performance of the material once it has hardened. The effect of NSG on these properties can be both positive and negative, depending on factors like dosage, particle size, and the specific mix design.

One of the most significant impacts of NSG on fresh concrete is its influence on workability. Nano-silica, with its fine particle size, increases the viscosity of the mix, resulting in reduced workability. The high surface area of NSG particles demands more water to preserve the same flowability as regular concrete mixes (Scrivener et al., 2018). This reduction in workability can make the mix stiffer, potentially making it more difficult to place, especially in intricate forms or areas requiring detailed finishing. However, this challenge can be mitigated by adjusting the mix proportions, such as increasing water content or incorporating superplasticizers to maintain the desired workability (Li & Zhao, 2003)

Despite the potential reduction in workability, NSG can positively impact the consistency of the mix. The small particle size and highly reactive nature of NSG particles enhance the dispersion of the solid phase in the mix, resulting in a more homogeneous concrete. This improvement is particularly beneficial when incorporating other SCMs (Supplementary Cementitious Materials), such as fly ash or slag, as NSG helps distribute these materials more evenly throughout the mix (Azad & Samarakoon, 2021a). Furthermore, the uniform dispersion of NSG in the fresh mix facilitates more effective chemical reactions during hydration,

which can contribute to the enhanced strength and durability of hardened concrete.

Setting time is another critical fresh property influenced by NSG. The addition of NSG typically accelerates the setting time of concrete due to the increased reactivity of the nano-sized silica particles. The primary reason for this is the improved pozzolanic reaction between NSG and calcium hydroxide ($Ca(OH)_2$), which is produced during cement hydration, leading to a faster formation of additional calcium silicate hydrate (C-S-H) gel (Davidovits, 2013). This characteristic can be helpful in applications that need rapid setting and early-stage strength development. However, if not carefully controlled, the accelerated setting time may shorten the workability period, posing challenges for large-scale pours or extended placement durations.

Bleeding and segregation are important fresh properties when the addition of NSG can also influence. Due to its large surface area and reactivity, NSG decreases the bleeding rate of concrete by improving particle bonding and minimizing water segregation from the mix. This helps to improve both the durability and consistency of the concrete (Scrivener et al., 2018). However, excessive amounts of NSG without proper adjustments to the mix could accelerate segregation, causing heavier particles to settle and leaving water and fines on top.

In summary, the influence of Nano Silica Gel (NSG) on the fresh properties of concrete is multifaceted and wide-ranging. While NSG can reduce workability and increase viscosity, it also enhances consistency and reduces bleeding. The rapid setting time induced by NSG can be advantageous for specific applications, but it requires careful control to prevent premature setting. By adjusting the mix design and incorporating admixtures, these challenges can be managed, allowing the beneficial effects of NSG to enhance the long-term performance of concrete.

Further research and optimization are essential to fully understand the best practices for using NSG in fresh concrete, balancing its impact on workability, setting time, and durability.

2.7 MICROSTRUCTURE

The microstructure of materials refers to the arrangement of their constituents at the microscopic level, including the distribution of phases, grain size, crystal shape and orientation, and the occurrence of imperfections such as dislocations, pores, and voids. This microstructural arrangement directly influences the material's physical, mechanical, and thermal properties, such as strength, ductility, electrical conductivity, and corrosion resistance. Understanding the microstructure of materials is crucial for enhancing their performance in various applications, including metals, polymers, ceramics, and composites.

At the atomic or molecular scale, the microstructure defines how the building blocks—atoms or molecules—interact with each other, governing the material's overall behavior. For example, in metals, the arrangement of atoms within the crystal lattice affects mechanical properties. Grain boundaries, which are regions where crystals of different orientations meet, play an essential part in determining the material’s strength and ductility. Materials with smaller grains are typically stronger because the grain boundaries impede the movement of dislocations—defects in the crystal lattice that enable deformation (Hu et al., 2023). These grain sizes can be manipulated through heat treatment or cold working processes, which subsequently affect the material's performance, particularly in structural uses

In polymers, the microstructure refers to the arrangement and orientation of polymer chains. Polymers with well-organized, crystalline regions generally display higher strength and better thermal resistance, while those with amorphous regions are usually more flexible and transparent (Lin et al., 2012).

The level of crystallinity in polymers greatly affects properties such as melting point, hardness, and resistance to solvents. In composite materials, the microstructure is determined by the alignment of fibers or particles within the matrix, which can be adjusted to optimize specific properties, such as strength-to-weight ratios or thermal conductivity (Nurazzi et al., 2021).

Porosity is another key aspect of the microstructure that affects material performance. Materials with high porosity, such as foams or certain ceramics, typically have low density and thermal conductivity, making them well-suited for insulation applications. Excessive porosity, however, can reduce a material's structural strength, increase the risk of fracture or failure when subject to stress (Liu et al., 2017). In contrast, tightly packed microstructures with minimal voids tend to be more resistant to degradation and wear. Methods such as scanning electron microscopy (SEM) and X-ray diffraction (XRD) are commonly used to examine porosity, providing in-depth analysis of pore size distribution, connectivity, and surface morphology.

The microstructure of materials can be optimized during processing to meet specific performance goals. For example, in metal alloys, heat treatment processes such as annealing or quenching refine the microstructure by controlling grain size and precipitate formation, improving properties like hardness, tensile strength, and fatigue resistance (Anil Kumar et al., 2022). Due to their nanometer-scale grains, nanomaterials exhibit remarkable mechanical properties, including high strength, electrical conductivity, and wear resistance, which are attributed to their fine microstructure and large surface-to-volume ratio (Sulka, 2023).

To study the microstructure of materials, advanced characterization techniques such as scanning electron microscopy (SEM), transmission electron microscopy (TEM), and atomic force microscopy (AFM) are used. These tools enable the

precise observation of atomic arrangements, grain structures, and other features, providing valuable data for designing materials with tailored properties. The evolution of microstructures is a dynamic process, shaped by temperature, pressure, composition, and processing methods. By optimizing these factors, materials can be engineered to satisfy particular application requirements.

In conclusion, the microstructure of materials has a significant impact on their macroscopic properties and performance. The ability to manipulate and control the microstructure through various processing methods enables the development of materials that meet the high-performance requirements of sectors including aerospace, automotive, biomedical, and electronics.

2.8 STRENGTH CHARACTERISTICS

The strength characteristics of materials are essential to their performance in structural applications. Strength defines a material's resistance to applied forces without failing, deforming excessively, or breaking. It is a crucial property for materials used in construction, engineering, and manufacturing because it directly influences the safety, durability, and service life of structures. Strength can be categorized into several types, including compressive strength, tensile strength, shear strength, and flexural strength, each of which is important for assessing how materials perform under different loading conditions.

Compressive Strength is perhaps the most widely measured strength characteristic, especially in construction materials like concrete, ceramics, and metals. It is defined as the material's capability to resist axial compressive forces without failing. For concrete, compressive strength is a primary indicator of its quality and is typically determined through standard testing methods, such as the uniaxial compression test (Bernal et al., 2017b). Several factors influence the compressive strength of concrete, including the water-cement ratio, type of aggregates, and curing conditions. Higher water-cement ratios usually result in

lower compressive strength due to the formation of larger pores and voids, which reduce the material's density and overall strength (Scrivener et al., 2018).

Tensile strength evaluates a material's ability to resist tension or stretching forces. This is particularly important for materials that are subjected to stretching or bending. Unlike compressive strength, tensile strength is typically lower in materials like concrete, which tends to fail under tensile stress more readily. To increase tensile strength, concrete is generally reinforced with materials such as steel. In metals, tensile testing is commonly performed using a tensile test machine, which measures the material's elongation and the point at which it fractures (Olivito & Zuccarello, 2010). Reinforcing fibers, such as carbon or glass fibers, can significantly improve the tensile strength of concrete and other materials, increasing their resistance to stretching and bending stresses (Scheibe et al., 2025).

Shear strength is the ability of a material to resist forces that act parallel to its surface, which often cause sliding between layers. Shear strength is crucial in materials such as metals, soil, and concrete, particularly when subjected to forces like earthquakes or uneven loads. The microstructure, grain boundary interactions, and the presence of defects in the material all influence shear strength. In concrete, shear strength is typically enhanced by adding fibers or admixtures that improve bonding and reduce crack propagation under stress (Li & Zhao, 2003). Testing shear strength is often done using methods such as the direct shear test or triaxial shear test, where lateral forces are applied to the material to measure its resistance to sliding.

Flexural Strength measures a material's ability to resist bending. This property is significant for materials subjected to bending stress, such as beams or slabs in construction. Flexural strength is commonly tested using a three-point or four-point bending test, where the material is subjected to a central load while being

supported at two points. In concrete, flexural strength is often assessed using the modulus of rupture, which serves as a key indicator of its resistance to cracking (Davidovits, 2013). Like tensile strength, flexural strength can be improved by incorporating reinforcing materials or modifying the mix design to reduce porosity and enhance overall density.

The effect of additives and Supplementary Cementitious Materials (SCMs) on strength properties has been widely researched. Incorporating materials such as fly ash, slag, silica fume, and nano-silica can significantly enhance the strength of concrete by improving its microstructure and reducing porosity. For instance, nano-silica refines the pore structure, resulting in increased compressive and tensile strength along with enhanced durability (Scrivener et al., 2018). Similarly, fly ash and slag enhance long-term strength by reacting with calcium hydroxide to form more calcium silicate hydrate (C-S-H) gel, which fills the voids in the concrete matrix and improves its density (Azad & Samarakoon, 2021a).

In metals, the strength characteristics are significantly influenced by the microstructure, which encompasses factors such as grain size, phase distribution, and defects, including dislocations and voids. Heat treatments, such as annealing or quenching, can be used to modify the microstructure, thereby enhancing the strength and toughness of materials (Langebeck et al., 2020). For instance, reducing grain size through rapid cooling or introducing precipitates into the matrix can increase the strength of alloys and improve their resistance to fatigue and fracture.

In conclusion, the strength characteristics of materials are essential to understanding their behavior under various loads and conditions. The ability to measure and optimize these characteristics allows engineers to design materials that meet specific performance requirements. The strength of materials can be significantly influenced by their composition, microstructure, and processing

methods, as well as by the incorporation of additives and reinforcing fibers. Advancements in material science continue to provide innovative ways to enhance strength, leading to the production of stronger, more reliable materials for a wide array of applications.

2.9 DURABILITY PERFORMANCE

The durability performance of materials refers to their ability to withstand degradation over time when exposed to environmental factors, mechanical stress, chemical reactions, and thermal cycles. Durability is a key factor in assessing the longevity and maintenance requirements of materials used in construction, infrastructure, and industrial sectors. It is influenced by factors such as microstructure, chemical composition, environmental conditions, and the stresses to which a material is subjected. A clear understanding of durability performance is essential for creating materials that retain their functionality and aesthetics over time, while reducing the frequency of repairs and replacements.

Concrete, being widely used in infrastructure such as bridges, roads, and buildings, is one of the most studied materials in terms of durability. Concrete's durability is primarily governed by its permeability and porosity, as they control the infiltration of harmful agents (such as water, chlorides, and sulfates) that can weaken the material. Low permeability is crucial for resisting water and chemical penetration, which can lead to problems such as steel reinforcement corrosion, freeze-thaw damage, and sulfate attack (Mehta & Monteiro, 2021). Factors such as the water-cement ratio, curing conditions, and the use of Supplementary Cementitious Materials (SCMs) significantly influence permeability and, consequently, the durability of concrete (Scrivener et al., 2018).

The incorporation of SCMs, such as fly ash, slag, silica fume, and nano-silica, has been shown to improve concrete's durability by reducing its permeability and promoting the formation of calcium silicate hydrate (C-S-H) gel. This gel serves

as a dense and durable binder (Azad & Samarakoon, 2021a). For example, the inclusion of fly ash boosts concrete's resistance to sulfate and chloride attacks by reducing porosity and filling voids in the matrix. Nano-silica, due to its high surface area and fine particle size, refines the pore structure and strengthens the bond between cement particles, creating a denser and more durable microstructure (Scrivener et al., 2018). These enhancements enable concrete to withstand environmental stresses, including exposure to seawater or extreme weather conditions.

In addition to concrete, the durability of metals is a crucial concern, especially in environments prone to corrosion, high temperatures, or exposure to aggressive chemicals. Corrosion, particularly rusting in ferrous materials exposed to moisture and oxygen, is the most common form of degradation in metals. Corrosion not only weakens the mechanical strength of metals but can also lead to structural failure. Strategies to enhance the durability of metals include the addition of corrosion inhibitors, the application of protective coatings, or the development of corrosion-resistant alloys. For example, stainless steels are designed to resist corrosion in moist or acidic environments due to the addition of chromium, which forms a passive oxide layer on the surface (Scheibe et al., 2025). Similarly, titanium and aluminum alloys are known for their exceptional corrosion resistance, especially in marine environments.

Polymers and composites also encounter durability challenges, particularly when exposed to UV radiation, high temperatures, and moisture. Over time, the chemical bonds in these materials can degrade, resulting in a reduction in their mechanical properties. UV degradation of polymers, for example, causes polymer chains to break and form free radicals, resulting in cracking, discolouration, and embrittlement (Maraveas et al., 2024). To improve their durability, stabilizers and UV inhibitors are added to polymers to prevent chain scission and maintain the material's integrity. Fiber-reinforced polymers (FRPs),

commonly used in concrete repair, offer enhanced durability due to their resistance to corrosion, moisture, and chemical attacks (Scheibe et al., 2025).

Thermal stability is another essential factor when evaluating durability. Materials used in high-temperature environments, such as those in aerospace and automotive sectors, must endure significant thermal cycling without compromising their mechanical properties. For example, certain ceramics exhibit high thermal stability, making them well-suited for use in jet engines and power plants. The emergence of nanomaterials has enhanced the durability of high-temperature materials, improving their resistance to thermal shock and creep deformation (Nalwa, 2017).

The durability performance of materials is also evaluated from the perspective of environmental sustainability. Life Cycle Assessment (LCA) provides a comprehensive evaluation of a material's environmental impact, encompassing energy consumption, CO_2 emissions, and waste generation throughout its entire lifecycle. Sustainable materials that are durable and require minimal maintenance are crucial for reducing the carbon footprint of the built environment. For instance, materials such as geopolymers and nano-silica are more sustainable alternatives to traditional Portland cement, as they require less energy to produce and release fewer greenhouse gases (Davidovits, 2013).

In conclusion, the durability performance of materials is crucial in determining their suitability for various applications. Understanding how factors such as composition, microstructure, environmental conditions, and additives influence durability is essential for developing materials that can endure harsh environments and maintain their functionality over time. Advances in materials science, including the incorporation of nanotechnology and the development of new composites and alloys, continue to enhance the durability and sustainability of materials across industries.

2.10 SUSTAINABILITY AND ENVIRONMENTAL BENEFITS

In materials science, sustainability refers to the ability of materials to be produced, utilized, and disposed of in a manner that minimizes their environmental impact while enhancing their performance and durability. As environmental concerns continue to grow globally, the importance of sustainable materials remains paramount. Challenges such as resource depletion, energy use, pollution, and climate change have drawn attention to the need for materials that are efficient in terms of resource consumption, energy consumption, and recycling. Sustainable materials are crucial in reducing the carbon footprint in industries such as construction, manufacturing, and transportation.

One keyway that materials contribute to sustainability is through energy efficiency. For example, cement, a crucial component in construction, accounts for a significant portion of global CO_2 emissions. According to Scrivener et al., (2018), cement production contributes to about 7-8% of global CO_2 emissions, mainly because of the energy-intensive production of clinker and the chemical decomposition of limestone. To mitigate this, Supplementary Cementitious Materials (SCMs), such as fly ash, slag, and silica fume, have been introduced as a more sustainable alternative. These byproducts from other industries can substitute for a portion of Portland cement, thereby lowering energy consumption during concrete production and reducing its environmental impact (Azad & Samarakoon, 2021a). Additionally, incorporating nano-silica into concrete not only strengthens the material but also enhances its durability, thereby reducing the need for repairs and replacements over time (Li & Zhao, 2002).

The environmental benefits of sustainable materials go beyond reducing CO_2 emissions during production. Recycling and reusing materials are essential components of sustainability. Materials that can be recycled or repurposed lower the demand for virgin raw materials, conserving natural resources and reducing

the environmental impact of extraction and processing. For instance, recycled concrete aggregates (RCA), extracted from demolished concrete structures, can be recycled into new concrete, lowering the requirement for fresh aggregates and minimizing construction waste (Mehta & Monteiro, 2021). Similarly, recycling metals and plastics helps reduce the environmental harm caused by mining and refining, offering more sustainable alternatives for various applications.

The use of renewable resources is another important facet of sustainable materials. Agricultural byproducts, such as rice husk ash (RHA), sugarcane bagasse ash (SBA), and hemp fibers, offer eco-friendly alternatives to conventional materials. For example, RHA, when processed into nano-silica, can replace traditional silica sources in concrete, resulting in both environmental and cost benefits (Davidovits, 2013). Furthermore, biodegradable polymers and composites derived from natural fibers like jute, hemp, and flax provide an eco-friendly alternative to petroleum-based plastics, reducing the environmental impact of plastic waste (Lin et al., 2012). These materials are both renewable and biodegradable, which helps reduce the accumulation of non-biodegradable waste in landfills.

Life Cycle Assessment (LCA) is now an essential method for evaluating the environmental impacts of materials at every stage of their lifecycle, from raw material extraction through to production, use, and disposal. LCA provides an in-depth analysis of a material's environmental footprint, including energy use, water consumption, greenhouse gas emissions, and waste generation. By applying LCA, manufacturers and researchers can identify opportunities for improvement and select processes and materials that minimize environmental impact (Hendriks et al., 2004). Eco-efficiency, the concept of achieving economic value while reducing environmental impact, is a key principle of sustainable material development. Materials with high eco-efficiency contribute to both

financial and environmental sustainability, benefiting industries, consumers, and the planet.

Sustainable materials typically provide increased durability and longevity, minimizing the need for frequent maintenance, repairs, and replacements. For instance, geopolymers, made from industrial byproducts such as fly ash and slag, not only help to reduce CO_2 emissions but also enhance concrete resistance to chemical attacks, temperature fluctuations, and wear, leading to longer-lasting structures and fewer resource-intensive repairs (Davidovits, 2013). Similarly, nanomaterials and advanced composites offer superior mechanical properties and resistance to degradation, increasing the material's service life while reducing the need for additional resources over time (Scheibe et al., 2025).

In addition to their environmental benefits, eco-friendly materials are often linked to improved health and safety. Materials free from toxic chemicals or pollutants, such as low-VOC paints or non-toxic insulation materials, contribute to healthier indoor air quality and safer living environments (Nalwa, 2017). The use of sustainable materials also reduces workers' exposure to harmful chemicals during manufacturing and construction, improving safety at construction sites and manufacturing facilities.

In conclusion, the sustainability and environmental benefits of materials are crucial in addressing issues like resource depletion, climate change, and pollution. The development and adoption of sustainable materials—such as SCMs, recycled products, renewable resources, and bio-based materials—offer substantial opportunities to reduce environmental impacts while improving the performance, durability, and functionality of materials. Advances in material science, alongside tools like Life Cycle Assessment (LCA), continue to provide valuable insights into developing eco-efficient materials that support both environmental and economic sustainability.

2.11 SUMMARY OF LITERATURE REVIEW AND RESEARCH GAPS

The cement industry is a significant contributor to global CO_2 emissions, responsible for approximately 8% of the total emissions. This has sparked growing interest in sustainable alternatives, such as Supplementary Cementitious Materials (SCMs). Materials such as fly ash, slag, and silica fume provide notable benefits by reducing cement consumption and CO_2 emissions, while simultaneously enhancing the durability of concrete. Fly ash improves workability and durability, while Ground Granulated Blast Furnace Slag (GGBFS) strengthens the mechanical properties of concrete. However, challenges such as availability, cost, and material variability limit their widespread adoption. Emerging alternatives, such as geopolymer concrete made from industrial byproducts, show potential for further reducing CO_2 emissions. Life Cycle Assessment (LCA) studies have shown that while SCMs are effective in reducing emissions, some, such as silica fume, have high energy requirements during production.

Different types of SCMs, derived from both industrial byproducts and natural materials, are used to enhance concrete properties while reducing its environmental impact. Fly ash, a byproduct of coal combustion, significantly enhances the workability and durability of concrete, particularly in large pours and hot climates. GGBFS, produced by rapidly cooling molten iron slag, improves mechanical properties and durability, particularly in aggressive environments. Materials like Rice Husk Ash (RHA) and Sugarcane Bagasse Ash (SBA) offer sustainable options by utilizing agricultural waste to enhance the strength and chemical resistance of concrete. However, the performance of these materials can vary depending on their production conditions, which affect their reactivity. Metakaolin, a highly reactive pozzolanic material, enhances concrete's strength and durability but is typically more expensive than other SCMs.

Derived from burning rice husks, Rice Husk Ash (RHA) is a promising SCM. Its high silica content reacts with calcium hydroxide in cement, improving mechanical properties and strengthening resistance to chemical attack. Using RHA also supports sustainability by reducing CO_2 emissions in cement production. However, the performance of RHA can be inconsistent due to variations in combustion temperature and silica content, which complicates its large-scale adoption. Additionally, RHA can be processed into nano-silica, a material with broad applications, especially in high-performance concrete, where it improves strength, durability, and chemical resistance. This process adds value to agricultural waste and provides an environmentally friendly alternative to traditional, energy-intensive methods for producing silica.

The addition of Nano Silica Gel (NSG) to concrete greatly enhances its mechanical and durability properties. However, NSG influences the fresh properties of concrete, such as workability and setting time. The fine particle size of NSG increases the mix's viscosity, reducing workability and making the concrete harder to handle. This can be mitigated by adjusting the mix proportions, such as improving water content or using superplasticizers. Despite reducing workability, refining the concrete microstructure enhances consistency and boosts both strength and durability. Additionally, it accelerates the formation of calcium silicate hydrate (C-S-H) gel, resulting in faster strength development, which is beneficial for rapid-strength applications but requires careful control to prevent premature setting.

The microstructure of materials, including concrete, plays a vital role in their overall performance, affecting strength, durability, and resistance to degradation. SCMs, such as fly ash and nano-silica, refine the concrete's microstructure by improving pore structure, reducing permeability, and enhancing durability. Understanding of the effect of SCMs on the microstructure is essential for optimizing concrete performance. Strength characteristics, particularly

compressive strength, are crucial in determining the quality of concrete. Incorporating SCMs enhances both compressive and tensile strength by filling voids and strengthening the bond between particles, thereby contributing to long-term durability.

Durability performance refers to a material's ability to resist deterioration over time, particularly in concrete exposed to environmental stressors such as moisture, chemicals, and temperature fluctuations. SCMs enhance concrete durability by decreasing permeability and improving resistance to chemical attacks. Materials such as fly ash, silica fume, and nano-silica contribute to the formation of a denser, more durable microstructure, thereby increasing the resistance of concrete to sulfate and chloride attacks. These improvements are especially advantageous in challenging environments, such as seawater exposure or freeze-thaw conditions.

Sustainability and environmental benefits are fundamental to the development of materials in the construction industry. By using SCMs such as fly ash, slag, and silica fume, CO_2 emissions are reduced through partial replacement of Portland cement. Moreover, the recycling and reuse of materials, such as recycled concrete aggregates, promote sustainability by conserving natural resources and minimizing waste. The use of renewable resources, such as agricultural byproducts like RHA and SBA, also supports eco-friendly construction practices. Life Cycle Assessment (LCA) has become a vital tool in assessing the environmental impact of materials, aiding the development of more sustainable and environmentally efficient solutions.

In conclusion, while the potential of SCMs to enhance concrete performance and sustainability is well-established, challenges remain, including material variability, cost, and production conditions. Further research is essential to optimize the use of SCMs, particularly emerging materials such as RHA and

nano-silica, to realize their environmental and performance benefits fully. A deeper understanding of their behavior in both fresh and hardened concrete will help foster more sustainable building methods, lowering CO_2 emissions while improving the durability and longevity of the structure.

Chapter 3: MATERIALS AND METHODOLOGY

This chapter outlines the methods, strategies, and materials employed in this research to achieve the objectives, which are detailed in Sections 3.1 and 3.2. Sections 3.1 and 3.2 discuss the materials used, namely OPC, nano silica gel, fine aggregates, water, and their physical and chemical properties, outlining the methodology employed in this study through a workflow diagram and an overview flow diagram. The parameters of cement and nano silica gel, like specific gravity and moisture content, were studied in the Engineering Materials Laboratory at Chittagong University of Engineering Technology (CUET). Tests on the nano silica gel chemical and physical characteristics were conducted at the Bangladesh Council of Scientific and Industrial Research Laboratory (BCSIR) in Dhaka. Section 3.3 provides a detailed explanation of the trial mix proportioning procedure. Following that, Section 3.4 discusses the curing environment, and Section 3.5 provides a detailed procedure for all the tests conducted in this study.

3.1 MATERIALS

The materials used in this study include:

1. Ordinary Portland Cement (CEM-I 42.5N):
    - Serves as the control binder.
2. Nano Silica Gel (NSG):
    - Sourced from SEAL to ensure high purity and uniformity.
    - Derived from RHA, aligning with sustainability goals.
3. Fine Aggregate:
    - Standard CEN sand, for use in standard mortar mixes.
4. Water:
    - Water of drinking quality is used for mixing and curing

3.1.1 Ordinary Portland Cement

The binder serves as the fundamental component in all types of concrete, with cement being one of the most widely used materials, which is found suitable for this purpose. This study aims to minimize the clinker content in cement production, making it a relevant focus. Portland cement was used to evaluate the intended effects. To assess the effectiveness of nano silica gel on mortar and paste properties, the cement chemical composition data supplied by the providing industry was standard for ensuring accuracy and consistency in material characterization.



Figure 3.1 The physical appearance of CEM-I

The study utilized 42.5-grade CEM I (OPC) cement, conforming to BDS EN 197-1 standards, as the primary binder and the reference material. Based on the data supplied by the cement manufacturer, the cement composition consisted of 95–100% clinker and 0–5% gypsum. The properties, both physical and chemical, of CEM I were analyzed using the provided data, ensuring alignment with industry standards and real-world production conditions**.** Tables 3.1 and 3.2 present the chemical composition and physical properties of the OPC used in this study.

Table 3.1: Chemical composition of CEM-I

Components	Chemical Composition %
CaO	63.78
SiO_2	20.42
Al_2O_3	5.35
Fe_2O_3	3.44
TiO_3	-
MgO	1.32
SO_3	2.57
Insoluble residue	1.33
Loss on ignition	0.92
Free Lime	1.08
C_3S	56.20
C_2S	16.66
C_3A	8.36

Table 3.2: Physical properties of OPC

Properties	Test result
Soundness	sound
Fineness	3800 cm^2/gm
Specific gravity	3.10
Initial setting time	1hours 25minutes
Final setting time	2 hours 48 minutes
Consistency	27%
Standard	BDS EN 197-1:2003

In this study, the specific gravity of Ordinary Portland Cement (OPC) was determined following ASTM C188 (Standard Test Method for Density of

Hydraulic Cement). The measured specific gravity of cement was found to be 3.10, which is within the typical range of 3.10 to 3.15 for CEM I Portland cement. This value indicates that the cement used conforms to standard properties, ensuring accurate volumetric calculations in the mix design process.

3.1.2 Nano Silica Gel

Nano silica gel, produced from rice husk ash (RHA), is a sustainable and economical material, as RHA contains 85–95% amorphous silica (SiO_2). The process begins with the controlled combustion of rice husks at 500–700°C, producing high-purity silica. The silica is extracted with an alkaline solution (NaOH or KOH), resulting in sodium silicate, which is subsequently acidified to precipitate nano-silica gel. The resulting nano silica has a particle size ranging from 1 to 100 nm, making it highly reactive and suitable for various applications. It enhances concrete strength and durability by reducing porosity and increasing hydration efficiency. Fig 3.2 shows the NSG sample used in the study.



Figure 3.2 Physical appearance of NSG

In industrial coatings and paints, it improves UV resistance and anti-corrosion properties. It is also used in wastewater treatment for removing heavy metals

and in drug delivery platforms for the controlled release of medications. The production of nano-silica gel from rice husk ash helps reduce agricultural waste while offering a high-value material for construction, environmental, and biomedical applications. Its high purity and sustainability make it a superior alternative to synthetic silica. With its wide-ranging benefits, nano silica gel from RHA is a promising material for future technological advancements.

The specific gravity of NSG was determined in conformity with ASTM C188, and the experimental results indicated a value of 1.97. This lower specific gravity compared to cement highlights the lightweight nature of nano silica, which can influence workability, hydration, and overall material properties. The reduced density means that, for the same mass, NSG occupies a larger volume than cement, which can lead to modifications in the rheology of the cement paste and the development of its microstructure.

3.1.3 Fine Aggregate

CEN Standard Sand is a premium, standardized reference material extensively utilized in research and testing laboratories for assessing the mechanical properties of cementitious materials, including compressive strength, flexural strength, and setting times.

The term 'CEN Standard Sand' refers to sand that meets the specifications defined in the European Standard EN 196-1, which plays a crucial role in ensuring the quality control of cement testing. This sand is produced following the EN 196-1:2016 standard, which sets the requirements for standard sand used in mortar preparation for cement strength testing (EN 196-1, 2016). The sand is meticulously controlled for factors such as grain size distribution, silica content, and purity, ensuring consistency and reliability in laboratory tests. For this research, the product is manufactured by Société Nouvelle du Littoral (SNL) in

France and is certified to meet both ISO 679:2009 and EN 196-1 standards. Fig 3.3 shows the EN standard sand sample.



Figure 3.3 Physical appearance of EN Standard Sand

3.1.4 Water

In cementitious material research and construction practices, Water is essential in both the mixing and curing processes of concrete and mortar. To ensure the consistency and reproducibility of test results, it is standard practice to use drinking quality water for mixing and curing purposes. According to various cement testing standards, such as EN 196-1:2016, ASTM C1602, and IS 456, the water used in these processes must be free from impurities that could interfere with cement hydration or negatively impact the mechanical properties of the hardened concrete.

The clean tap water, sourced from the Engineering Material lab CUET, is suitable for construction purposes. Throughout the study, the same high-quality potable water was consistently used for all mortar preparations and concrete curing procedures, maintaining uniformity and ensuring the reliability of the results. The use of clean, uncontaminated water was crucial for ensuring that the focus of the inquiry remained on the performance of the nano silica gel derived from

RHA in the cementitious media, without external factors influencing the outcome.

3.2 METHODOLOGY

An experimental research design is followed in this study to determine the pozzolanic activity and cementitious effectiveness of NSG. The study is structured into three levels:

Level 0: Characterization of Binder Materials

Collection and processing of NSG and Ordinary Portland Cement (CEM-I). Characterization of NSG through specific gravity, particle size distribution (PSD), XRF, XRD, and pozzolanic activity tests.

Level 1: Cement Paste with NSG

Partial replacement of CEM-I with NSG at 1%, 2%, 3%, and 5% (by volume). Evaluation of consistency, setting time, soundness, and microstructural properties.

Level 2: Cement Mortar with NSG

Preparation of mortar specimens using CEM-I, CEN sand, and NSG. Assessment of workability, flexural and compressive strength, drying shrinkage, and electrical resistivity. The research methodology is divided into systematic experimental stages, as follows:

Stage 1: Collection and Preparation of Materials

Nano Silica Gel (NSG): Sourced from Sustainable Energy & Agro-resource Ltd. (SEAL) to ensure quality and processed through chemical treatment of RHA.

Cementitious Materials: Ordinary Portland Cement (CEM-I 42.5N) – serves as the primary binder.

Fine Aggregates: Standard CEN sand conforming to BS EN 196-1.

Water: Safe water for mixing and curing.

Stage 2: Characterization of NSG and Cement (Level 0 Analysis)

Before incorporating NSG into cementitious materials, detailed characterization is performed:

- Specific Gravity (ASTM C188)
- Particle Size Distribution (Laser Diffraction Method)
- Chemical Composition (X-ray Fluorescence - XRF)
- Mineralogical Phases (X-ray Diffraction - XRD)
- Pozzolanic Activity (Frattini and Strength Activity Index - SAI Tests)

Stage 3: Cement Paste Preparation and Testing (Level 1 Analysis)

- Mixing Proportions:
    - CEM-I replacement levels: 0%, 1%, 2%, 3%, and 5% (by volume).
- Tests Conducted:
    - Normal Consistency, Setting Time, and Soundness (BS EN 196-3)
    - Autoclave Expansion Test (ASTM C151)
    - Scanning Electron Microscopy (SEM) for Microstructural Analysis

Stage 4: Cement Mortar Preparation and Testing (Level 2 Analysis)

- Mixing Proportions:
    - Binder: Fine aggregate ratio maintained at 1:3.
    - NSG replacement levels: 2.5%, 5%, 7.5%, and 10%.
- Tests Conducted on Mortar Specimens:
    - Flow Table Test (BS EN 1015-3) – Evaluates workability.
    - Fresh and Hardened Density (BS EN 1015-6, BS EN 1015-10).

- Flexural and Compressive Strength (BS EN 196-1) – Tested at 7, 28, 90, and 180 days.
- Drying Shrinkage (ASTM C596) – Assesses volume stability.
- Electrical Resistivity (ASTM C1760-12) – Measures durability.

This section outlines the methodological procedure and standards employed in conducting the study, collecting information, reviewing sources, and presenting the results. The methodology describes the key components and provides an overview of the overall approach. Initially, the problem was identified by reviewing relevant research. The next stage was to write a research proposal, which was accepted before material collection could begin. Materials were collected in accordance with guidance from various sources. After that, the mix design was selected on a trial basis. The overall summary of the procedure and test program is given in Figures 3.4 and 3.5.

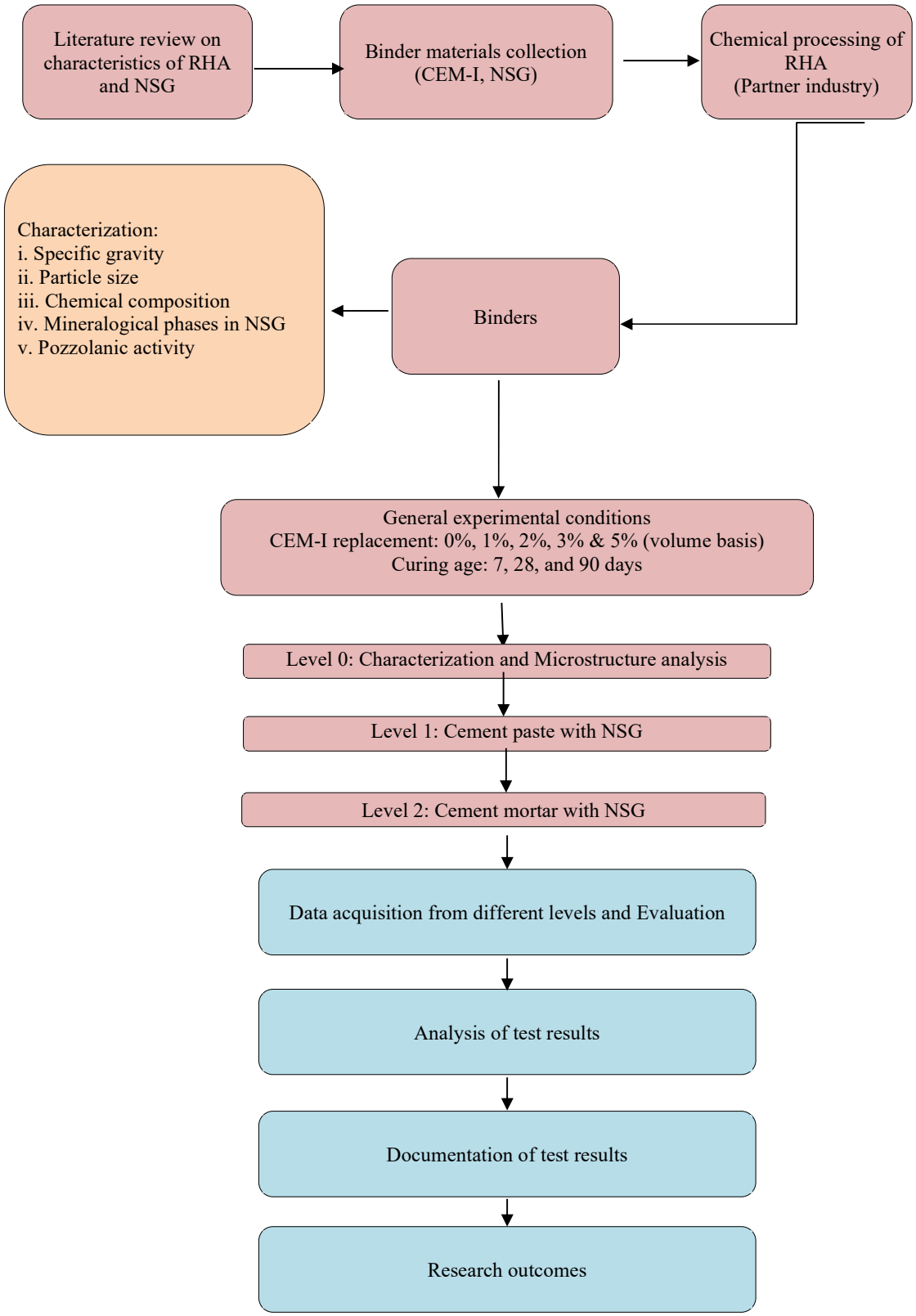


Figure 3.4 General outline of the methodology and research program

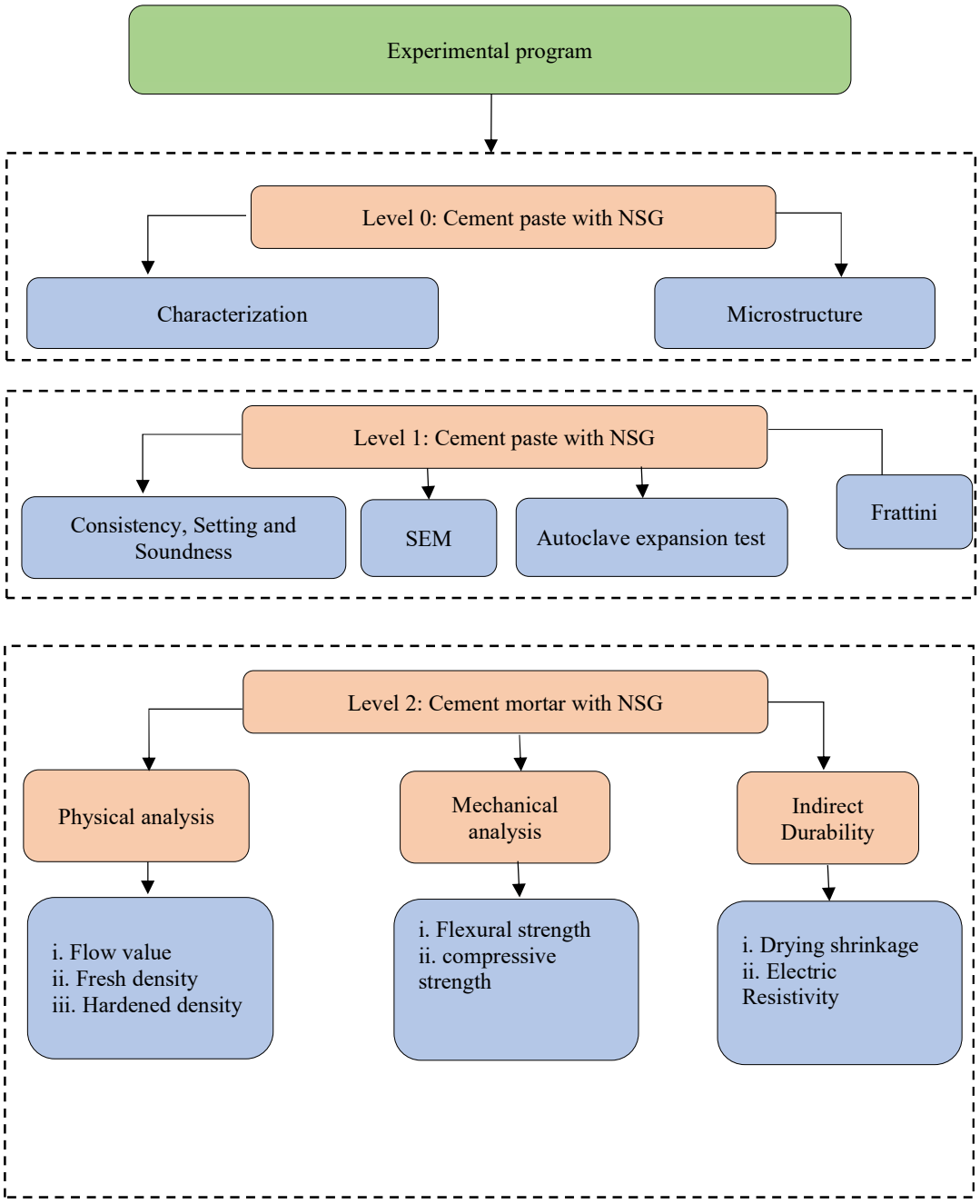


Figure 3.5 Experimental program at different levels

3.3 NSG CHARACTERIZATION TESTS

3.3.1 Particle Size Distribution

The particle size distribution (PSD) of the nano silica gel particles was evaluated by dynamic light scattering (DLS) using the Malvern Hydro EV analyzer (as shown in the image of Fig 3.6). Before measurement, the dry powder was dispersed in deionized water at a concentration of 0.05 wt% and sonicated for 10 minutes to break up any weak agglomerates. The suspension was then introduced into the Hydro EV's measurement cell at 25 °C under automatic optimization of measurement parameters.

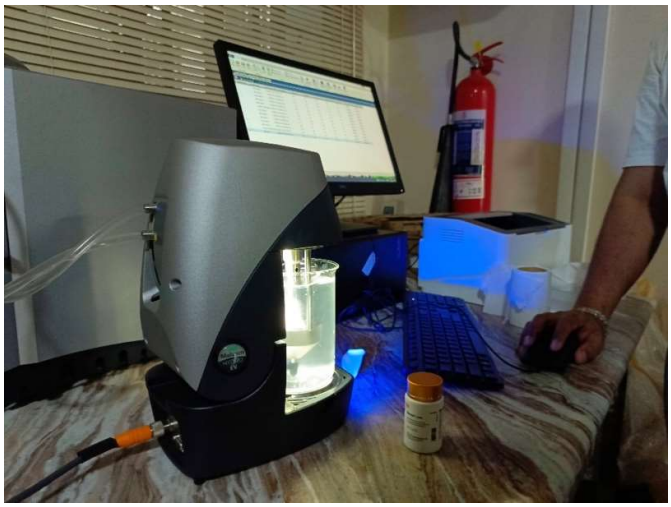


Figure 3.6 Malvern Hydro EV analyzer

DLS examines fluctuations in the intensity of scattered light as the nanoparticles undergo Brownian motion; these fluctuations are converted via the Stokes–Einstein equation into a hydrodynamic-diameter distribution. Both intensity- and volume-weighted PSDs were recorded, from which the characteristic diameters D_{10} (10th percentile), D_{50} (median), and D_{90} (90th percentile) were extracted. In this study, the volume-weighted PSD was unimodal and relatively narrow, with $D_{10} \approx 90$ nm, $D_{50} \approx 150$ nm, and $D_{90} \approx 260$ nm. Such a tight distribution confirms a largely monodisperse population of nano silica gel

particles. A narrow, monomodal PSD is highly desirable for applications in cementitious systems and aerogel fabrication. It ensures a high and consistent specific surface area for rapid dissolution or interaction, promotes uniform pore development in aerogels, and yields reproducible pozzolanic reactivity during use as a supplementary cementitious material.

3.3.2 Scanning Electron Microscopy for morphology and EDX

A ZEISS Sigma300 scanning electron microscope (SEM) was used to perform the morphological analysis and elemental composition of the test materials. High-resolution images were captured using the SEM, which operated at an accelerating voltage of 5 kV, as shown in Figure 3.7. Additionally, the instrument featured an energy-dispersive X-ray spectroscopy (EDX) system for elemental analysis, which was employed to analyse the crystalline deposits present on the surfaces of selected samples. This test was conducted at Jashore University of Science and Technology. Figure 3.7 shows the SEM used for imaging and EDX analysis.



a) b)

Figure 3.7 Scanning Electron Microscopy for morphology and EDX analysis

3.3.3 Mineralogical composition (XRD)

X-ray diffraction (XRD) analysis was conducted to identify the crystalline phases in the nano-silica. The sample was finely ground for uniformity and placed on a low-background sample holder. For XRD measurements, a diffractometer with a Cu Kα radiation source (λ = 1.5406 Å), operating at 40 kV and 30 mA, was used. The scan range was between 5° and 90° 2θ, with a step size of 0.02° and a counting time of 1 second per step to achieve high resolution. The diffraction data were analysed using specialized software, with the measured patterns compared to the ICDD database for phase identification. Rietveld refinement was employed to determine the phase distribution, calculate lattice parameters, and evaluate macrostrain values.

3.3.4 Chemical composition (XRF)

To determine the elemental composition of the nano-silica powder, X-ray fluorescence (XRF) analysis was conducted. The sample was first finely ground to ensure homogeneity, then pressed into a stable pellet using a hydraulic press at approximately 10 tons pressure. XRF analysis was carried out using a spectrometer with a Rhodium (Rh) anode tube, operated at 50 kV and 50 mA. The instrument was calibrated using certified reference materials (CRMs) to ensure accuracy. Measurements were conducted under vacuum to enhance sensitivity, especially for lighter elements. Data were analysed using dedicated software to identify and quantify principal oxides (expressed as weight percentages) and trace elements (expressed in parts per million).

3.3.5 Loss on Ignition

The loss-on-ignition (LOI) of a powdered sample is measured in compliance with ASTM C114/C114M to assess its volatile and carbonaceous content. First, a representative portion of the dried material (approximately 1.00 g) is accurately weighed to 0.1 mg and placed in a clean, tared platinum or porcelain crucible. The crucible is then transferred into a muffle furnace preheated to 950 ± 25 °C

and held at that temperature for 60 minutes. This dwell time ensures complete combustion of organic matter and removal of loosely bound water. Figure 3.8 shows the muffle furnace used for the LoI test.



Figure 3.8 Programmable muffle furnace

Immediately after ignition, the crucible is removed and cooled in a desiccator to room temperature to prevent moisture uptake. The cooled crucible and its residue are weighed, and the LOI is determined as the percentage mass loss relative to the original sample mass:

$$LOI = \frac{Winitial - Wfinal}{Winitial} x100 \qquad \text{Eq. 3.1}$$

Where $W_{initial}$ is the mass before ignition, and $W_{ignited}$ is the mass after ignition. Care is taken to ensure reproducibility by repeating the procedure on duplicate specimens and reporting the average LOI. A low and consistent LOI indicates minimal volatile impurities, while elevated values may signal excessive moisture.

3.4 NSG PASTE SAMPLE TEST

3.4.1 Frattini Test for Pozzolanic Activity

The pozzolanic activity of Nano Silica Gel (NSG) in cementitious materials was evaluated using the Frattini test (BS EN 196-5). This test assesses whether NSG reacts with calcium hydroxide ($Ca(OH)_2$) in an alkaline solution, a crucial indicator of pozzolanic behavior. It involves measuring the concentrations of calcium oxide (CaO) and hydroxyl ions (OH^-) in a cement-containing solution after a fixed hydration period. These results are then compared to a calcium hydroxide saturation curve (Fig. 3.9) to determine if NSG effectively consumes calcium hydroxide, thereby indicating its pozzolanic activity. Table 3.3 shows the mix proportion used for the Frattini test.

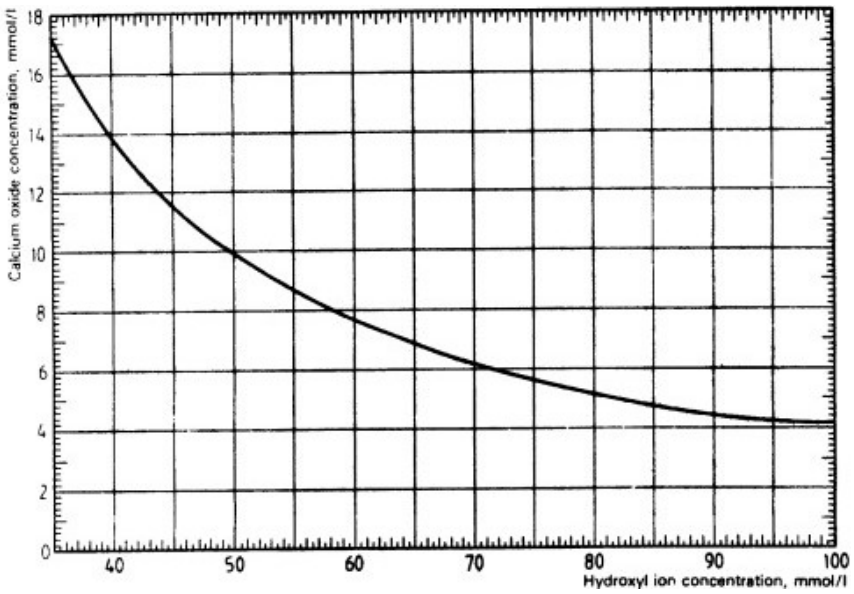


Figure 3.9 Diagram for assessing pozzolanicity

For the test, a 20 g sample of cement (CEM-I or NSG-blended) was blended with 100 mL of distilled water and placed in a sealed plastic container to prevent CO_2 absorption. The sample was stored in a thermostatically controlled enclosure at 40 ± 0.5°C for 8 and 15 days, ensuring sufficient time for hydration and chemical equilibrium. After the designated hydration period, the solution was immediately filtered under vacuum using a Büchner funnel with low-porosity

filter paper (mean pore size ~2 μm) to separate undissolved solids. The filtration was completed within 30 seconds to prevent interference from atmospheric CO_2, and the filtrate was collected in a sealed flask for subsequent chemical analysis. Figure 3.10 demonstrates the Frattini test of the pozzolanic activity of NSG blended cement.

Table 3.3 Mix proportions for Frattini test

Mix ID	Cement, gm	NSG, replacing cement	Water, gm
Control	20.00	---	100
N1	19.80	1% (0.127 gm)	
N2	19.60	2% (0.254 gm)	
N2	19.40	3% (0.381 gm)	
N5	19.00	5% (0.635 gm)	



Figure 3.10 Frattini test of pozzolanic activity

To determine the hydroxyl ion concentration, a 50 mL sample of the filtrate was titrated with a 0.1 mol/L solution of hydrochloric acid (HCl) using methyl orange as an indicator. The endpoint was identified by a transition in colour from yellow to orange, and the hydroxyl ion concentration was calculated based on the volume of acid used. For CaO concentration, the same filtrate was treated with 5 mL of NaOH solution to maintain a pH above 13. A murexide indicator was introduced to the solution, and titration was performed using 0.025 mol/L EDTA until the colour changed from purple to violet. The CaO concentration was then determined from the amount of EDTA consumed.

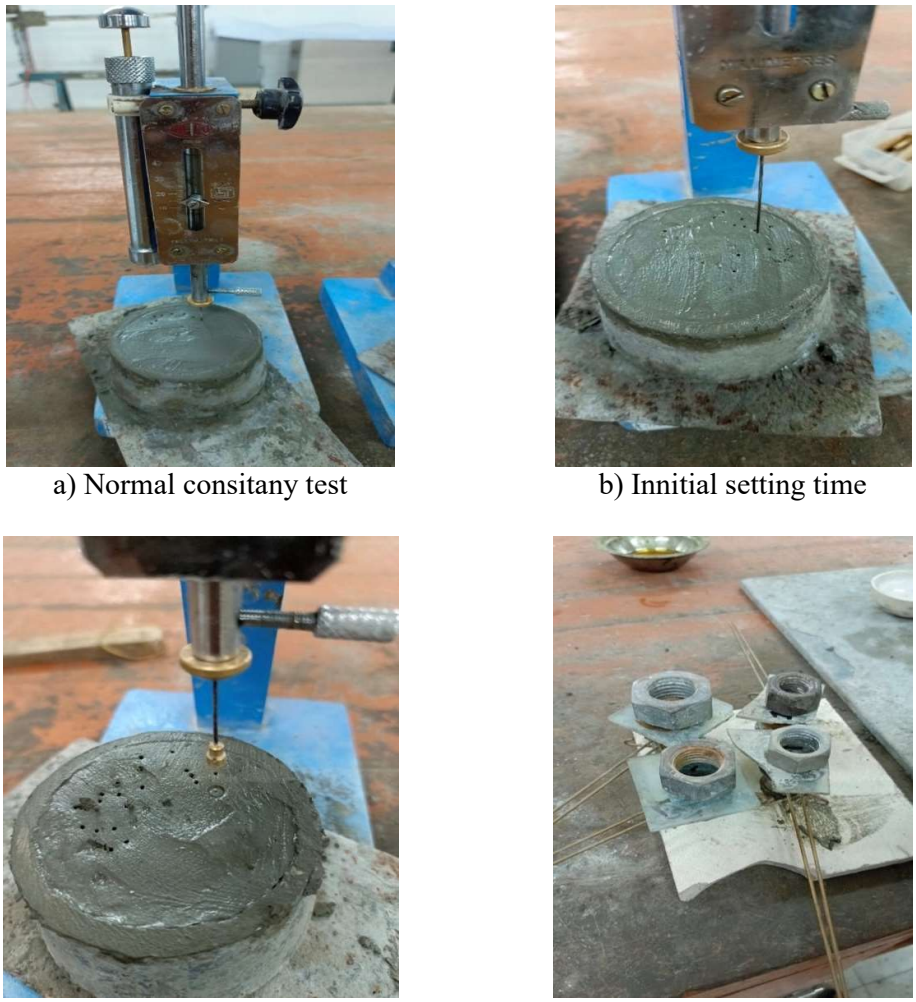
To evaluate the test results, the calcium oxide concentration was plotted against the hydroxyl ion concentration on a Frattini saturation curve. If the plotted point falls under the calcium hydroxide solubility curve, it signifies that NSG effectively consumed $Ca(OH)_2$, confirming its pozzolanic activity. However, if the point was above the curve, it indicated that NSG did not significantly react with $Ca(OH)_2$, suggesting low pozzolanicity. This analysis was crucial in evaluating the viability of NSG as a supplementary cementitious material (SCM) and its potential to enhance cement hydration and improve long-term durability.

3.4.2 Normal Consistency

For each trial, 400 grams of cement were weighed and mixed with a calculated amount of water, starting with an approximate water-to-cement ratio of 25% by weight. A cement paste was then prepared using a standard Vicat apparatus. The Vicat mould was filled with the freshly mixed paste, ensuring the surface was level with the top of the mould. The Vicat plunger, measuring 10 mm in diameter and 50 mm in length, was inserted into the paste and released. The depth of penetration was measured precisely. If the plunger did not reach a depth of 10 ± 1 mm, the water content was adjusted, and the steps were repeated until the desired penetration depth was achieved. The water content at this point was recorded as the normal consistency of the cement paste.

3.4.3 Setting Time

To determine the setting times of the cement paste, a paste was first prepared using cement and water at normal consistency. The Vicat mould was then filled with the prepared paste, and the stopwatch was started immediately after the mixing process was completed. The Vicat needle was inserted at equal intervals into the paste to determine the initial setting time. The initial setting time was defined as the point at which the needle's penetration reached 25 ± 1 mm. For the final setting time, the annular needle attachment was used, and the setting time was recorded when the needle ceased to leave an impression on the paste surface. Fig 3.11 illustrates the determination of normal consistency, setting time and soundness of cement.



a) Normal consitany test

b) Innitial setting time

c) Final setting test

d) Soundness test

Figure 3.11 Normal consistency, setting time, and soundness tests

3.4.4 Soundness (Le Chatelier Method)

A cement paste was prepared using water at normal consistency. Next, the Le Chatelier mould was filled with the paste in two layers, each layer gently compacted to eliminate air voids. Once filled, the mould was covered with a glass plate and submerged in water held at 20 ± 1°C for 24 hours. After curing, the distance between the indicator points on the mould was measured.

The specimen was subsequently boiled in water for three hours to test its soundness. After boiling, the specimen was cooled and dried, and the final distance between the indicator points was measured again. The expansion of the specimen was then calculated as the difference between the initial and final measurements. It was verified that the expansion remained within the permissible limit, which is commonly set at a maximum of 10 mm.

3.4.5 Autoclave Expansion Test

The procedure for conducting the Autoclave Expansion Test begins with the preparation of the cement paste specimens. A standard batch of cement paste is prepared by mixing 650 g of cement with sufficient water to produce a paste of normal consistency in accordance with ASTM C 187. The mixing is done as per ASTM C 305. The paste is then immediately molded into specimens of 25.4 mm x 25.4 mm (1 inch) cross-section, as specified in ASTM C 490.

The specimens are stored in a moist room for at least 20 hours but no more than 24 hours, as specified in ASTM C 511. At 24 hours ± 30 minutes, the specimens are removed from the moist atmosphere, and the initial length is measured using a length comparator. The specimens are then placed in an autoclave at room temperature. The autoclave is filled with water at an initial temperature of 20°C to 28°C to maintain a saturated steam environment during the entire test. The water should occupy 7 to 10% of the total volume of the autoclave.

During the heating phase, the vent valve is initially left open to allow air to escape. Once steam begins to escape, the vent valve is closed, and the temperature is gradually raised. The autoclave is heated to a pressure of 295 ± 10 psi (2 MPa), which corresponds to a temperature of 216 ± 2°C. This process takes between 45 and 75 minutes. After reaching the target pressure, the pressure is maintained at 295 ± 10 psi for 3 hours.

At the end of the 3-hour holding period, the heat is turned off, and the autoclave is cooled. The pressure inside the autoclave is reduced to less than 10 psi within 90 minutes, and any remaining pressure is slowly released by partially opening the vent valve. After the pressure is released, the specimens are removed and placed in water at a temperature above 90°C to cool. The temperature of the water is gradually reduced to 23°C within 15 minutes, and the specimens are then held at this temperature for an additional 15 minutes.

Finally, the length comparator reading is taken again, and the change in length is calculated by subtracting the initial reading from the final reading. The autoclave expansion is reported as the percentage increase in length to the nearest 0.01%, with a minus sign prefixed if a decrease in length occurs. Fig. 3.12 shows the autoclave expansion test process.



a) Autoclave



b) Placement of the prism



c) Length comparator

Figure 3.12 Autoclave expansion test

3.5 MORTAR TESTS

3.5.1 Mix Design

Mix designs with different percentages of nano silica gel (0%, 1%, 2%, 3%, and 5%) were prepared at various levels to investigate the effects of nano silica gel on mortar properties. Mix design involves selecting the appropriate ingredient proportions that meet the required performance characteristics. CEN Standard Sand (EN 196-1) was used to create the specimens for this study. Laboratory tests were conducted to determine the necessary characteristics of fine and coarse aggregates, as well as the binder material. After gathering all the required data, the mix design was finalized. Table 3.4 presents the mortar mix design, where additional water is added to ensure the flow value control is within ± 5 mm. Due to volumetric replacement, the total weight of materials is slightly reduced as NSG has a lower specific gravity. Table 3.5 shows the number of mortar specimens.

Table 3.4 Mortar mix proportions

Mix ID	Cement, gm	NSG, replacing cement	Sand, gm	Water, gm	Added Water, gm
Control	450.0	---	1350	225.0	---
N1	445.5	1% (27.29 gm)	1350	200.57	15
N2	441.0	2% (54.58 gm)	1350	176.14	35
N3	436.5	3% (81.87 gm)	1350	151.71	40
N5	427.5	5% (136.36 gm)	1350	103.0	60

Table 3.5: Number of samples for mortar

Mix ID	**NSG, replacing cement**	**Curing Days**	**Sample No**	
			Compressive	**Flexural**
Control	---	7,28,90	6	3
N1	1%	7,28,90	6	3
N2	2%	7,28,90	6	3
N3	3%	7,28,90	6	3
N5	5%	7,28,90	6	3

3.5.2 Specimen Preparation

The preparation of 40 x 40 x 160 mm mortar specimens was conducted in accordance with the BDS EN 196-1:2003 standard to ensure consistency in strength testing. The process was carried out in several sequential steps. Firstly, to facilitate easy demolding, the steel moulds were coated with mould oil before casting. The required quantities of materials for producing three prism specimens were measured according to the standard guidelines. The mortar mixer machine was set up properly before the mixing process began. Water was first poured into the mixing bowl, and subsequently, cement was added.

The mixer was run at low speed for 30 seconds, followed by the gradual introduction of sand into the bowl over the next 30 seconds. The mixture was then stirred at maximum speed for another 30 seconds. After this initial mixing, the machine was paused for 90 seconds to allow the mixture to rest. During this pause, any mortar clinging to the walls of the mixing bowl was scraped back into the mixture. The mixing process resumed for an additional 60 seconds at high speed, ensuring a uniform mortar consistency. When the mixing process was finished, the fresh mortar was transferred into the steel moulds. To confirm proper compaction, the moulds were placed on a jolting table and securely fastened. Two layers were used to fill the moulds. The first layer was approximately 20 mm thick, and the jolting table was activated for 60 jolts to compact the mortar. The second layer was then added in the same manner, followed by another 60 jolts for proper compaction. After placing the second layer, any excess mortar was removed using a metal straightedge. The straightedge was moved across the surface with a gentle sawing motion in both directions to ensure a smooth, level top surface.

After casting, the moulds containing fresh mortar were put in a moist environment for 24 hours to maintain proper curing conditions. After the initial 24-hour period, the test specimens were carefully removed from the moulds.

Each specimen was properly labelled and documented before transferring to a water-curing tank controlled at (20 ± 2)°C. Fig. 3.13 shows mortar specimen preparation and associated tests.



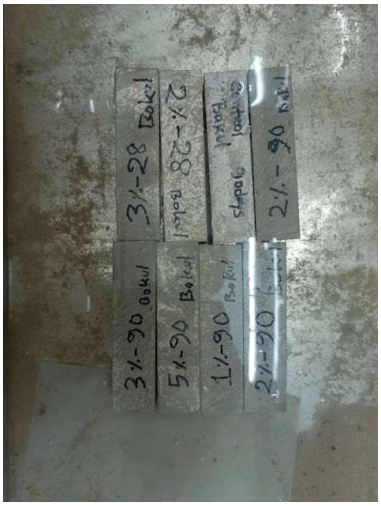
a) Automatic mixture machine



b) Flow table test



c) Sample preparation



d) Underwater curing

Figure 3.13: Mortar specimen preparation

The mortar specimens were immersed in water at controlled temperature conditions until their designated test dates. Specimens underwent flexural and compressive strength tests at 7, 28, and 90 days, in accordance with the EN 196-1 testing procedure.

3.5.3 Flow Table Test

The Flow Table Test, performed in accordance with standard test methods, is a standard method used to evaluate the consistency and workability of fresh mortar for masonry applications. This test helps assess the fluidity, which directly influences its ease of application and performance in construction.

The test procedure begins with the preparation of the mortar mix as per the standard test, ensuring it meets the required proportions and consistency. The flow table, a 300 mm diameter circular metal plate, is placed on a level surface. A cone-shaped mould, with a base diameter of 100 mm, a top diameter of 70 mm, and a height of 60 mm, is positioned at its centre. The fresh mortar is then placed into the mould in two layers, with each layer being tamped using a normal test tamping rod to ensure proper compaction.

The mould is filled and levelled. It is then raised in a controlled vertical motion, allowing the mortar to spread evenly on the table. The next step involves dropping the table check normal teal from a height of which facilitates the flow and expansion of the final diameter of the mortar spread is measured in two orthogonal directions, and the average value is noted. The flow percentage is then calculated using the formula:

$$\text{Flow (\%)} = (D - D_O)/D_O \text{x} 100 \qquad \text{Eq. 3.2}$$

where D is the average spread diameter and D_0 is the initial base diameter of the mould (100 mm). Typically, the required flow percentage for masonry mortar falls between 140% and 200%, depending on the application. Due to the high surface area, increased cohesion, water absorption, and effect on particle packing and pozzolanic activity of nano silica gel, the flow value tends to decrease with a higher replacement level (Labaran et al., 2024). The flow value is adjusted using excess water (as mentioned in Table 3.4) within a control range of ±5 mm to maintain consistency and ensure adequate mix workability.

3.5.4 Fresh Density of Mortar

The fresh density of mortar is a crucial parameter influencing its consistency, workability, and overall performance. As per BS EN 1015-6, the density is determined by measuring the mass of a known volume of fresh mortar. This involves filling a container of known volume with the mortar, compacting it through tamping or vibration, and then weighing the filled container. The fresh density is then calculated using the formula:

$$\text{Fresh Density} = \frac{\text{Mass of mortar}}{\text{Volume of container}} \qquad \text{Eq. 3.3}$$

3.5.5 Hardened Density of Mortar

The hardened density of mortar is a crucial parameter that significantly influences its strength, durability, and overall performance in construction. According to BS EN 1015-10, the hardened density is calculated by measuring the mass and volume of a mortar specimen after it has undergone the curing process. The test begins with the preparation of mortar specimens, which are typically cast into standard moulds and cured under controlled conditions for a specified period, usually 28 days. Once the curing period is complete, the specimens are placed in an oven at 105°C ± 5°C and dried until they reach a constant mass, ensuring that all free moisture is removed.

After drying, the specimens are weighed using a precise balance, and their volume is measured either by taking their physical dimensions or by using the water displacement method. The hardened density is then calculated using the formula:

$$\text{Fresh Density}(\varrho) = \frac{Mass\ of\ specimen\ (kg)}{Volume\ of\ specimen(m^3)} \qquad \text{Eq. 3.4}$$

3.6 CURING ENVIRONMENT

Curing is the process of preserving the proper moisture levels and temperature in concrete during its initial stages to ensure adequate strength development.

This process not only prevents plastic and drying shrinkage cracks from forming on the surface after placement but also contributes to the concrete's long-term durability by promoting the appropriate strength gain both initially and over time. Concrete typically consists of cement and water, which react and harden over time. Proper curing helps to retain moisture in the concrete, slowing the hardening process and enabling the material to settle and gain strength. Early surface drying without proper curing can lead to shrinkage and cracking. Therefore, the chemical reactions between the cement components and water during curing must proceed adequately to form a dense microstructure and a strong pore network within the concrete. In this study, the specimens were initially cured at a temperature range of 25–27°C with a relative humidity of >90%. After this initial curing period, the specimens were demolded and allowed to continue curing in water. After one day of water curing, the specimens were placed in a water tank at ambient temperature for further curing. Samples were taken from the curing tank at 7, 28, and 90-day intervals for additional testing. Fig. 3.14 shows the underwater curing of mortar specimens.



Figure 3.14 Curing of specimens

3.7 TESTING PROGRAM

A thorough testing scheme was developed to evaluate the mechanical properties of cast mortar specimens, focusing on their behaviour under different stress conditions. The process started with preparing the test specimens using a standard mortar mix, which was then cast into moulds of specific dimensions. To ensure accurate and reliable results, the specimens underwent an essential air-drying process. This step was crucial for removing any remaining moisture in the mortar, as water content could significantly influence the test outcomes. The air-drying took place in a controlled environment, with the specimens allowed to dry for a designated period.

Once the drying process was complete, each specimen was carefully placed at the center of the testing apparatus. This apparatus was specifically designed to apply uniform loads and accurately measure the specimens' responses to the forces applied during the tests. The specimens were then subjected to various mechanical tests to evaluate their strength properties:

3.7.1 Compressive Strength Test of Mortar

Compressive strength is an essential factor in understanding the mechanical behaviour of materials, particularly in the context of construction applications. In the case of mortar, compressive strength refers to the maximum axial load that the material can resist before failing due to compression. It is measured as the uniaxial compressive stress at failure, which occurs when the material fails to resist the applied load and fractures. The determination of compressive strength of mortar involves performing a set of compressive tests. Fig 3.15 shows the test set up and testing process of the mortar specimen under compressive loading. In this study, six separate specimens underwent testing for each data point, and the average of these measurements was reported to ensure a more reliable and statistically sound result. This method minimizes the potential for errors and provides a more representative measure of the material's behaviour.



a) Before loading b) After loading c) The testing machine

Figure 3.15 Compressive strength testing.

A calibrated compression testing machine was utilized to conduct the tests, applying a steadily increasing and uniform load to the mortar specimens. The testing machine accurately measures the load applied and records the corresponding deformation of the mortar until failure occurs. The failure point is considered the point at which the specimen can no longer bear the compressive load and begins to crack or fracture.

The fundamental equation used to calculate the compressive stress is as follows:

$$\sigma = \frac{F}{A} \qquad \text{Eq.3.5}$$

Where,

σ = Compressive stress [Pa] (Pascals)

F = Crushing load [N], indicating the total compressive force applied to the test specimen upon failure

A = Specimen cross-sectional area [m²]

3.7.2 Flexural Strength Test of Mortar

To determine the flexural strength of mortar, flexural tests were conducted in accordance with the BS EN 196-1:2005 standard. Flexural strength is a key parameter for assessing the tensile capacity of mortar and its resistance to bending failure in the absence of reinforcement. Also referred to as the modulus

of rupture, flexural strength is determined by applying a bending load to the material until failure occurs. This property is essential for evaluating how mortar performs in structural applications subjected to bending stress. Tensile stresses in mortar can arise from external loads, temperature changes, shrinkage, and the presence of moisture. The test was conducted on standard mortar prisms measuring 40 mm x 40 mm x 160 mm. The specimens were cast in moulds and cured according to the specified procedures.

The testing procedure was conducted in a series of systematic steps. Initially, the specimens were prepared and subjected to water-based curing for durations of 7, 28, and 90 days to ensure proper hydration and strength development. Once the curing periods were complete, the specimens were carefully removed from the curing tank. Their surfaces were gently dried to reach a saturated surface-dry (SSD) condition, ensuring consistency in testing.

Each 40 × 40 × 160 mm specimen was then accurately oriented and positioned in the testing apparatus. A reference line was marked on the surface of each specimen to guarantee correct alignment during the testing process. Specimens were placed in the apparatus, maintaining their original moulded orientation, ensuring that the specimen was centred on the bearing block and properly aligned with the loading system about the applied force.

Next, the load application block was brought into contact with the specimen surface, specifically at the center point between the supports, to ensure uniform load distribution. A constant load was then applied at a controlled rate, gradually increasing the stress in the extreme fibers until failure occurred. During this process, the appearance of the fractured faces was closely observed, and the type of fracture was documented for further analysis. Fig. 3.16 shows flexural strength test process. Flexural strength was determined using equation 3.5.

$$f=\frac{3F.L}{2b^2} \qquad \text{Eq. 3.5}$$

Where, f = flexural strength

F = Maximum load applied during testing, in Newtons (N)

L = Distance between supports (100 mm)

b = Width of the specimen (40 mm)



a) Before loading



b) After loading

Figure 3.16 Flexural test on standard mortar prism

3.7.3 Drying shrinkage

The preparation of the test specimens began with the mixing of mortar, following the specified proportions of 750 g of cement and 1500 g of graded standard sand, with an amount of mixing water sufficient to produce a flow of 110 ± 5%. The mixture was prepared using a mechanical mixer as specified in ASTM C 305. The mortar was then cast into molds with dimensions of 25 mm x 25 mm x 285 mm, conforming to the requirements of ASTM C 490, to form prisms with an effective gage length of 250 mm.

After the specimens were molded, they were stored under moist conditions for 24 hours ± 30 minutes, as specified in ASTM C 511, to allow for initial curing. In the case that the strength of the specimens was insufficient to allow proper demolding after 24 hours, the curing time was extended for 48 hours ± 30 minutes. Upon removal from the molds, the specimens were immersed in lime-saturated water for 48 hours. If the specimens were initially moist cured for 48 hours, they were instead immersed for only 24 hours.

At 72 hours ± 30 minutes, the specimens were removed from the water, wiped with a damp cloth, and immediately subjected to a length comparator reading to measure the initial length. Following this, the specimens were stored in air at 23 ± 2°C and 50 ± 5% relative humidity for the remainder of the testing period. Length comparator readings were taken at intervals of 4, 11, 18, and 25 days, with each reading being recorded for further analysis of drying shrinkage. Fig 3.17 shows the experimental setup for shrinkage measurement.



a) Comparator measurement b) Curing

Figure 3.17 Drying shrinkage of paste

Finally, the drying shrinkage was calculated by subtracting the initial comparator reading (taken after removal from water) from the comparator readings at the

specified drying intervals. The results were expressed as millionths of the effective gage length and as a percentage. The average drying shrinkage from the four specimens was calculated and reported as the drying shrinkage of the mortar.

$$\text{Drying Shrinkage} = \frac{Initial\ Length - Final\ Leng}{Initial\ Length} \text{x}100 \qquad \text{Eq. 3.6}$$

The result will be expressed as the percentage shrinkage over the drying period.

3.7.4 Electrical Resistivity

The testing procedure commenced with the preparation of concrete specimens in the form of cores or cylinders, with diameters of either 100 mm or 150 mm, and nominal lengths of either 200 mm or 300 mm (as per ASTM C1760-12). Each specimen was moist-cured for 28 days before testing to ensure proper hydration and strength development, although an accelerated moist-curing method could be employed if necessary. Before testing, it was ensured that all specimens were thoroughly saturated with water and maintained in a 100% relative humidity environment from the time of mould removal until the test commenced. This ensured consistent moisture conditions, which are crucial for reliable measurements.

The test environment was carefully controlled, with air temperatures maintained between 20°C and 25°C to prevent fluctuations that could affect the results. During testing, specimens were kept in a moist room or immersed in water to prevent drying. For each specimen, the finished surface was marked at four positions: 0°, 90°, 180°, and 270°, using permanent marks to facilitate consistent placement and measurement during testing (see Fig. 3.18). Before measurement, the surface of each specimen was cleaned using a saturated sponge or towel to obtain a saturated surface-dry condition.

The Wenner array probe was then positioned in contact with the specimen, ensuring that the longitudinal centre of the sample was aligned with the two inner probe pins and that the probe was accurately placed at the 0° mark (Fig. 3.16). Once the reading stabilized, the displayed resistivity value was recorded. The specimen was then rotated by 90°, and the measurement process was repeated at 90°, 180°, and 270°, with readings taken at each position.

After completing this first set of readings, the specimen was rotated back to 0°, and the same measurement sequence was redone to acquire a second set of resistivity values at each marked position. The average resistivity for each sample was calculated using both sets of readings, ensuring consistency and accuracy. If the relative standard deviation (%RSD) of the readings exceeded 7.5%, the specimen was immersed in water at a temperature range of 20°C to 25°C (68°F to 77°F) for two hours before repeating the test.



a) Specimen preparation



b) Resistivity Measurement

Figure 3.18 Electrical resistivity test of mortar

Finally, the surface resistivity values were documented, and the average resistivity for each specimen was determined. A correction factor was applied based on the curing conditions: multiply the result by 1.1 for limewater curing or by 1.0 for moist room curing, thereby finalizing the resistivity assessment.

Chapter 4: RESULTS AND DISCUSSION

This chapter discusses the laboratory test findings of nano silica gel as a partial replacement material for cement. The cementitious characteristics of nano silica gel were evaluated with control (0%), 1%, 2%, 3% and 5% substitution of cement contents. Tests conducted on Paste Samples include Normal consistency, setting time, soundness, Autoclave expansion test, Scanning electron microscopy (SEM), and Loss on ignition. The experimental results are also presented in both tabular and graphical forms. Tests conducted on mortar samples are the flow table test, fresh density of mortar, hardened density of mortar, flexural strength, compressive strength, drying shrinkage and electrical resistivity.

4.1 MATERIAL TEST RESULT

4.1.1 Particle Size Distribution

The particle size distribution analysis of nano silica gel particles conducted using the Malvern Mastersizer (v3.88) revealed a broad, multimodal size distribution. The sample, analysed under the conditions specified, showed a concentration of 0.1438% and a defined surface area of 101.2 m^2/kg. The distribution parameters revealed a span of 4.720 and a uniformity value of 1.400, indicating the presence of a wide range of particle sizes within the sample. The volume-based diameters at key percentiles were recorded as D [3,2] at 59.3 μm, D [4,3] at 166 μm, Dv(10) at 26.4 μm, Dv(50) at 85.8 μm, and Dv(90) at 431 μm. The distribution curve revealed a strong presence of particles under 10 μm, with a notable portion exceeding 100 μm, suggesting a polydisperse nature of the sample. Fig. 4.1 shows the particle size distribution of NSG.

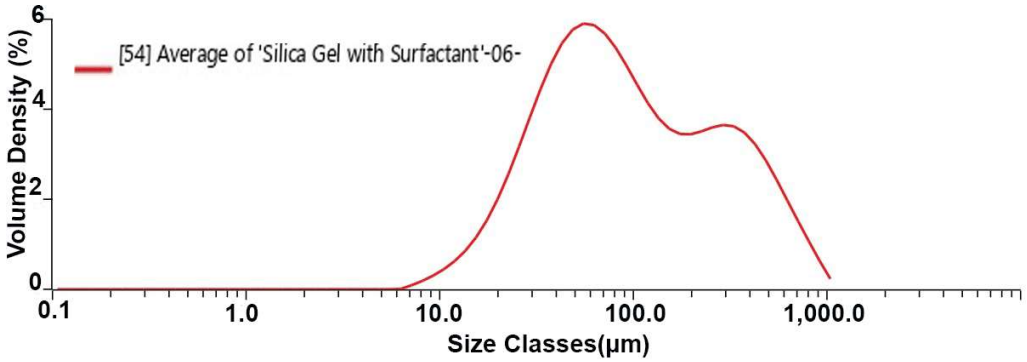


Figure 4.1 Particle size distribution curve of NSG

These results underscore the heterogeneity characteristic of silica gel produced through sol-gel methods, reflecting how synthesis conditions influence the resulting particle size distribution. Analysis of nano silica gel particles using the Malvern Mastersizer (v3.88) revealed a broad, multimodal size distribution. The observations are in line with earlier findings, such as those by Singh et al. (2014a), who documented narrower distributions in silica particles. However, the sample displayed higher polydispersity, with both sub-10 µm and larger particles (Singh et al., 2014b).

Additional studies, including those by Rahman & Padavettan (2012) and Lin et al. (2023). reported broad size distributions in sol-gel synthesized silica, supporting this finding. These works emphasize the influence of synthesis conditions on the resulting particle size distribution, which tends to vary in sol-gel processes, as evidenced by the notable presence of larger particles in the sample of this study.

4.1.2 Chemical Analysis by XRF

The chemical composition of the nano silica was examined using XRF techniques, and the results are presented in Table 4.1. The sample was predominantly composed of SiO_2 (83.60%), with minor constituents including Cl (12.90%), Na_2O (2.04%), and K_2O (0.62%). Other oxides detected at trace

levels included Al_2O_3 (0.29%), P_2O_5 (0.22%), and SO_3 (0.10%). Several minor metallic oxides were also detected at parts per million (ppm) levels, including CaO (749 ppm), Fe_2O_3 (479 ppm), Cr_2O_3 (138 ppm), and CuO (92.9 ppm).

Table 4.1: The chemical composition of NSG analyzed using the XRF.

Parameter	Value obtained
SiO_2	83.60%
Cl	12.90%
Na_2O	2.04%
K_2O	0.62%
Al_2O_3	0.29%
P_2O_5	0.22%
SO_3	0.10%
CaO	749 PPM
Fe_2O_3	479 PPM
Cr_2O_3	138 PPM
CuO	92.9 PPM

The high SiO_2 content (83.60%) confirms the successful synthesis of nano silica with a high purity level, a crucial attribute for enhancing reactivity and performance in various applications (Yuvakkumar et al., 2014). Chlorine and other minor oxides commonly found in rice husk ash (RHA)-derived nano silica are typically attributed to residual processing chemicals and natural impurities (PC, n.d.). The presence of trace amounts of CaO, Fe_2O_3, Cr_2O_3, and CuO, as detected in ppm, suggests a possible influence on the material's reactivity and performance in cement-based systems (Al-Abboodi et al., 2020). Although these levels are generally low enough to avoid adverse effects, further purification might be required for specialized applications demanding high purity (Mahdikhani & Ramezanianpour, 2014). Overall, the XRF results confirm the expected composition and high purity of RHA-derived nano silica, supporting its potential for use in pozzolanic and advanced material applications.

4.1.3 Mineralogy by X-ray Diffraction (XRD)

X-ray Diffraction (XRD) analysis of the nano silica sample (G-203) showed the presence of multiple crystalline phases, evidenced by distinct peaks in the diffractogram. The major phase detected was cristobalite (SiO_2), accounting for 41.4% by weight. Sodium silicate (Na_2SiO_3) was also identified as a notable phase, making up 20.0%,

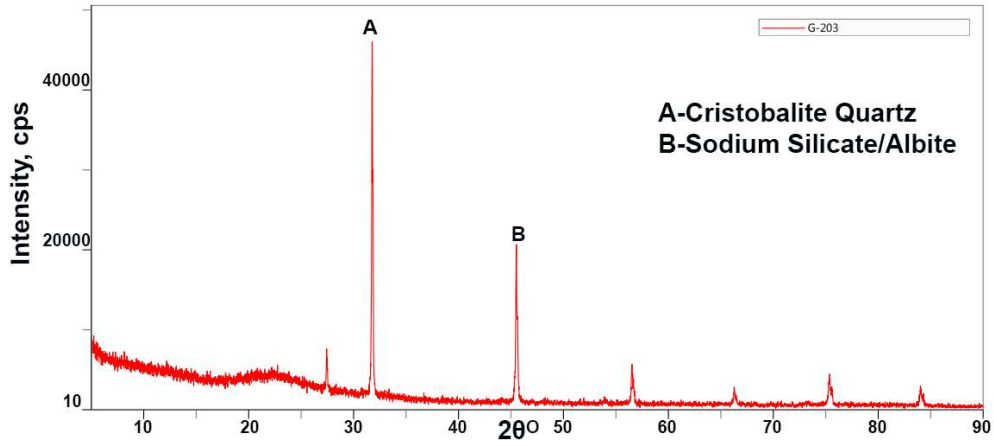


Figure 4.2 XRD pattern of nano silica [(Intensity) vs 2 Theta]

quartz (SiO_2) at 20.7%, tridymite (SiO_2) at 12.42%, sodium-alumino-silicate at 5.0%, and amorphous silica at 8.28%. Rietveld refinement results indicated good crystallinity, with lattice strain values ranging from 0.18% to 0.25% across the identified crystalline phases. Variations in lattice parameters (A, B, C) and unit cell volumes further confirmed the presence of multiple polymorphs and complex silicate structures. Table 4.2 presents the wet physical properties of the nano silica formulation analysis results.

Table 4.2: Wet Physical Properties of Formulation analysis results of nano silica

Phase	Weight Fraction (wt%)	a (Å)	b (Å)	c (Å)	α (°)	β (°)	γ (°)	Lattice Volume (Å³)	Strain (%)
Cristobalite (SiO_2)	41.4	4.98	4.98	6.92	90	90	90	171.7	0.25
Sodium Silicate (Na_2SiO_3)	20.0	5.38	5.38	10.72	90	90	90	310.6	0.20
Quartz (SiO_2)	20.7	4.91	4.91	5.40	90	90	90	122.9	0.18
Tridymite (SiO_2)	12.42	5.05	5.05	8.18	90	90	90	208.7	0.22
Sodium-Alumino-Silicate	5.0	5.24	5.24	7.68	90	90	90	210.8	0.21
Amorphous Silica	8.28	-	-	-	90	90	90	-	-

The high proportions of cristobalite and quartz phases indicate effective crystallization during synthesis, likely facilitated by the applied thermal treatment (Yuvakkumar et al., 2014). The presence of sodium silicate and sodium-alumino-silicate suggests contributions from synthesis additives or residual sodium originating from the rice husk ash precursor (Thuadaij & Nuntiya, 2008). Notably, the detection of 8.28% amorphous silica points to incomplete crystallization and suggests enhanced pozzolanic potential due to its higher reactivity compared to crystalline forms (Al-Abboodi et al., 2020). The low lattice strain values (0.18–0.25%) across the crystalline phases reflect strong crystallinity and structural stability, which may enhance the material's mechanical and thermal performance (Mahdikhani & Ramezanianpour, 2014). In summary, the XRD analysis confirms that the G-203 nano silica powder contains a complex blend of crystalline and amorphous phases, supporting its suitability for use in pozzolanic and advanced functional materials.

4.1.4 Loss on Ignition

The loss on ignition (LOI) of the nano silica was found to be 14.5%. This was determined by heating a measured sample in a muffle furnace at high temperature, driving off volatile components, mainly moisture and residual organic matter, and recording the resulting weight loss.

A high LOI of 14.5% suggests a notable presence of moisture and organic residues, which is typical for sol-gel-derived nano silica due to remaining surface hydroxyl groups and incomplete condensation during synthesis (Iqbal Khan, 2018). Elevated LOI values can negatively affect performance in high-temperature or composite applications by influencing reactivity, thermal resistance, and mechanical behaviour (Zhang et al., 2017). To mitigate these effects, post-synthesis treatments such as calcination are often employed to

eliminate volatiles, reduce LOI, and enhance material purity and consistency (Zhang et al., 2017).

4.1.5 Frattini Test for Pozzolanic Activity

The pozzolanic activity of nano silica gel (NSG) was determined using the Frattini test, with results detailed in Table 7.10. Figure 4.3 illustrates the concentrations of calcium oxide (CaO) and hydroxide ions (OH^-) in the testing solution. For the NSG sample, CaO was recorded at 6.48 mmol/L, while OH^- reached 155.34 mmol/L. In comparison, the control cement sample showed a CaO concentration of 12.96 mmol/L and an OH^- concentration of 73.7 mmol/L, indicating lower calcium but higher hydroxide levels in the NSG sample. For cement blends containing 1%, 2%, 3%, and 5% NSG, CaO concentrations ranged from 8.91 to 12.89 mmol/L, and OH^- values ranged from 65.74 to 97.83 mmol/L.

The Frattini test results confirm the high pozzolanic reactivity of nano silica gel (NSG). Across all replacement levels, CaO concentrations were significantly lower than those in the control sample, indicating a strong reaction between NSG and calcium hydroxide (CH), which promotes the formation of additional C–S–H gel. This observation aligns with (Khan, 2018), who indicated that nano silica's fine particle size and elevated surface energy enhance its reactivity compared to conventional pozzolans. Additionally, the rise in OH^- concentrations at lower NSG dosages (1–2%) indicates rapid CH consumption, consistent with the findings of Zhang et al. (2017), and reflects improved early-stage hydration. These results demonstrate that even minimal NSG incorporation can significantly enhance pozzolanic activity and improve mechanical performance in cement-based materials.

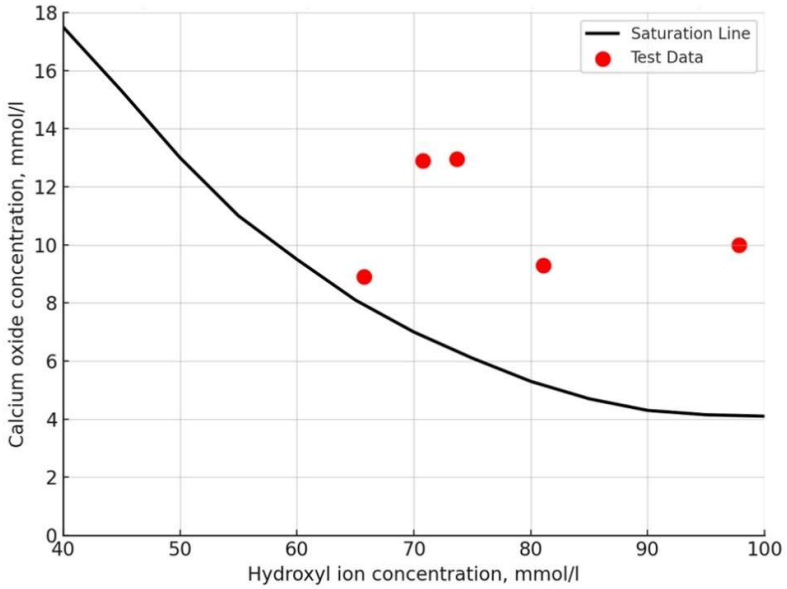
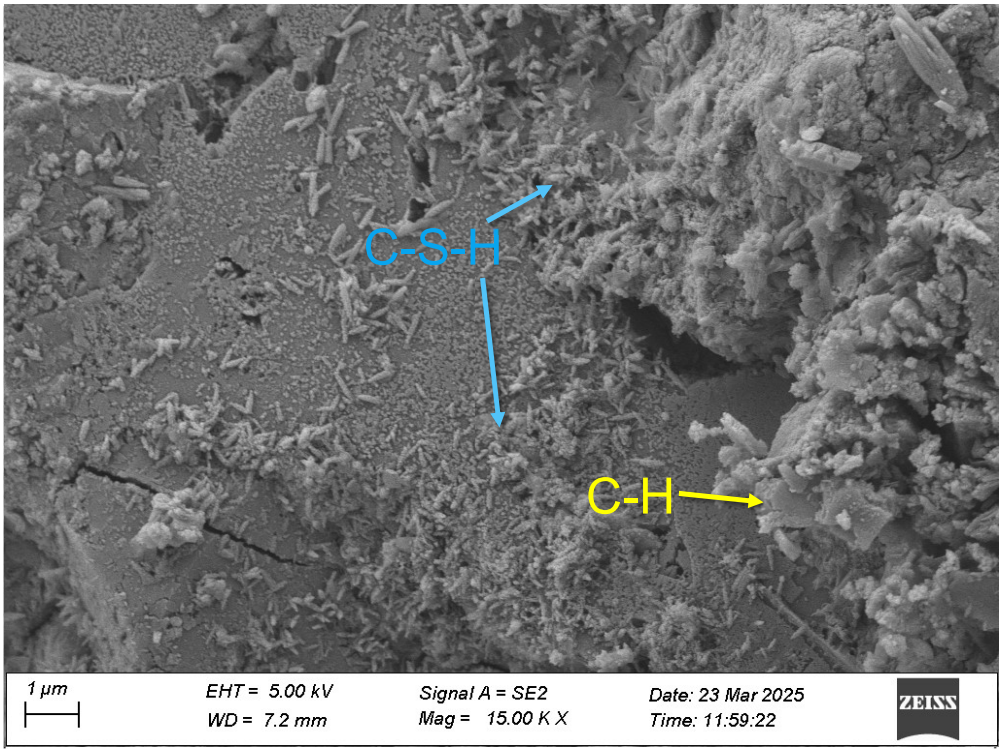


Figure 4.3 Frattini test result

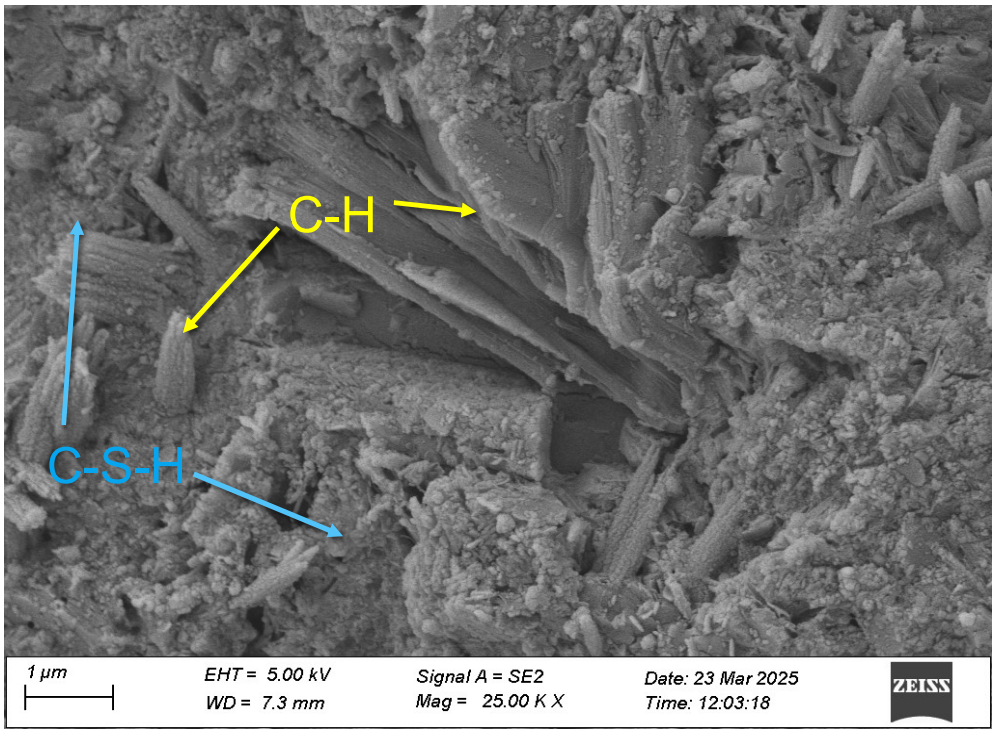
4.2 PASTE TEST RESULT

4.2.1 Scanning electron microscopy (SEM)

Scanning electron microscopy (SEM) images were obtained for cementitious samples with 0% (control), 1%, 2%, 3%, and 5% nano silica gel (NSG) replacements after 28 days of curing. The control sample exhibited larger pores and loosely bonded hydration products. With 1% NSG, the microstructure appeared denser, featuring more uniform and compact calcium silicate hydrate (C-S-H) gels occupying the pore spaces. At a 2% replacement rate, the matrix exhibited further refinement, with reduced cracking and void formation. Samples containing 3% and 5% NSG demonstrated highly dense, interlocked microstructures marked by continuous C-S-H formations and a notable decrease in visible needle-like ettringite. Fig (4.4, 4.5, 4.6, 4.7 and 4.8) shows an SEM image.

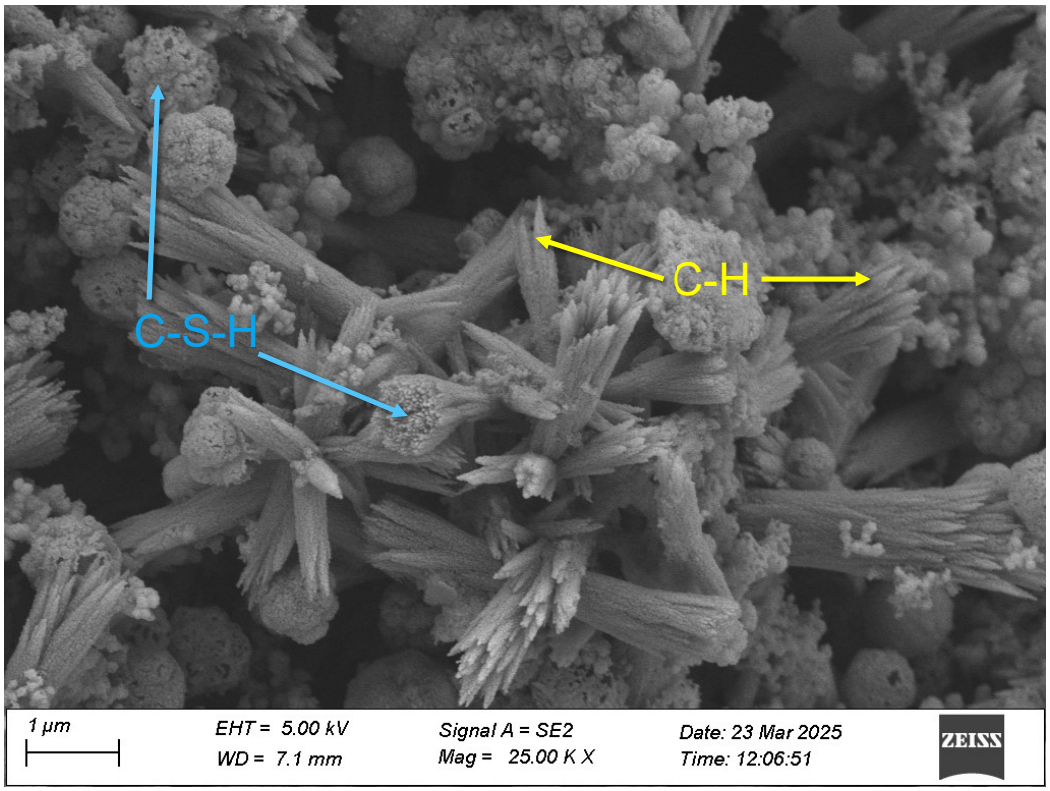


a) 15000x magnification

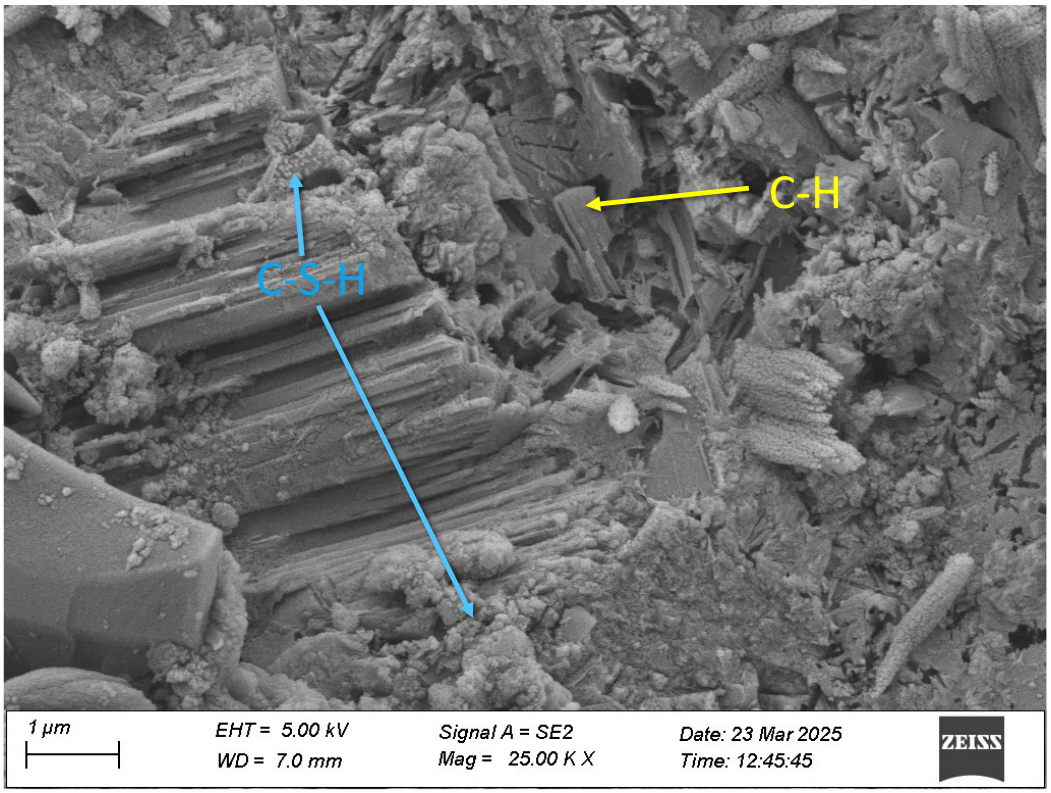


b) 25000x magnification

Figure 4.4 SEM image of the control paste

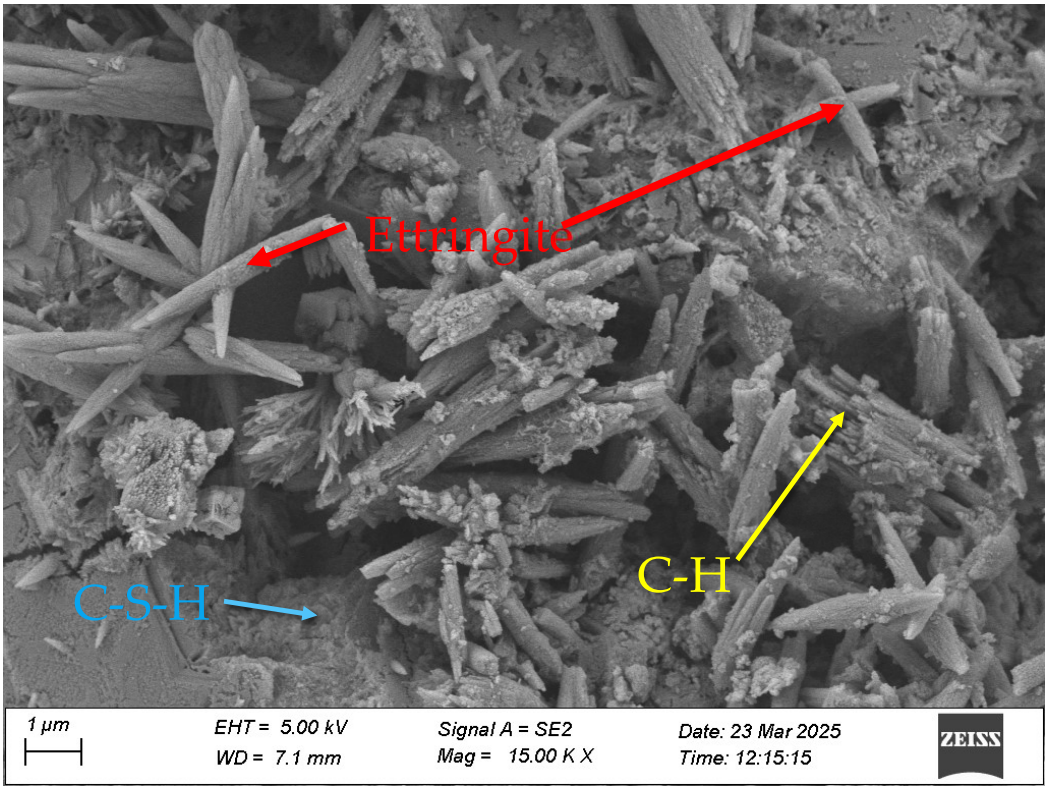


a) 25000x magnification

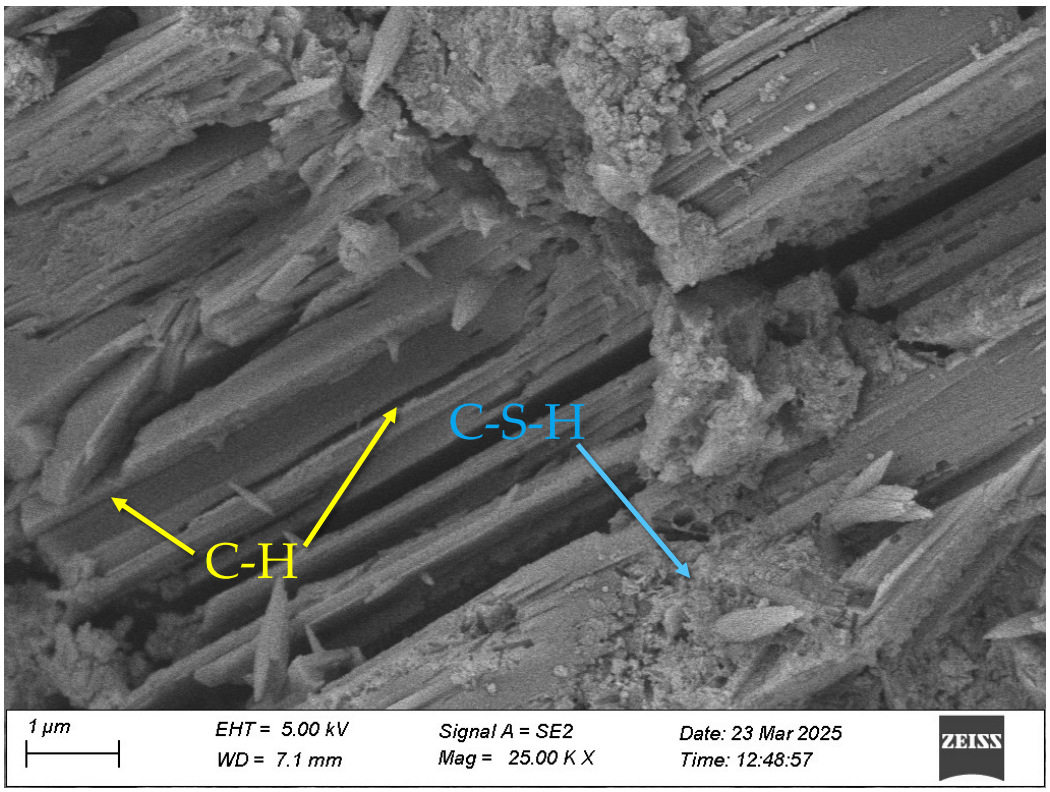


b) 25000x magnification

Figure 4.5 SEM image of 1% replacement of CEM-1 with NGS

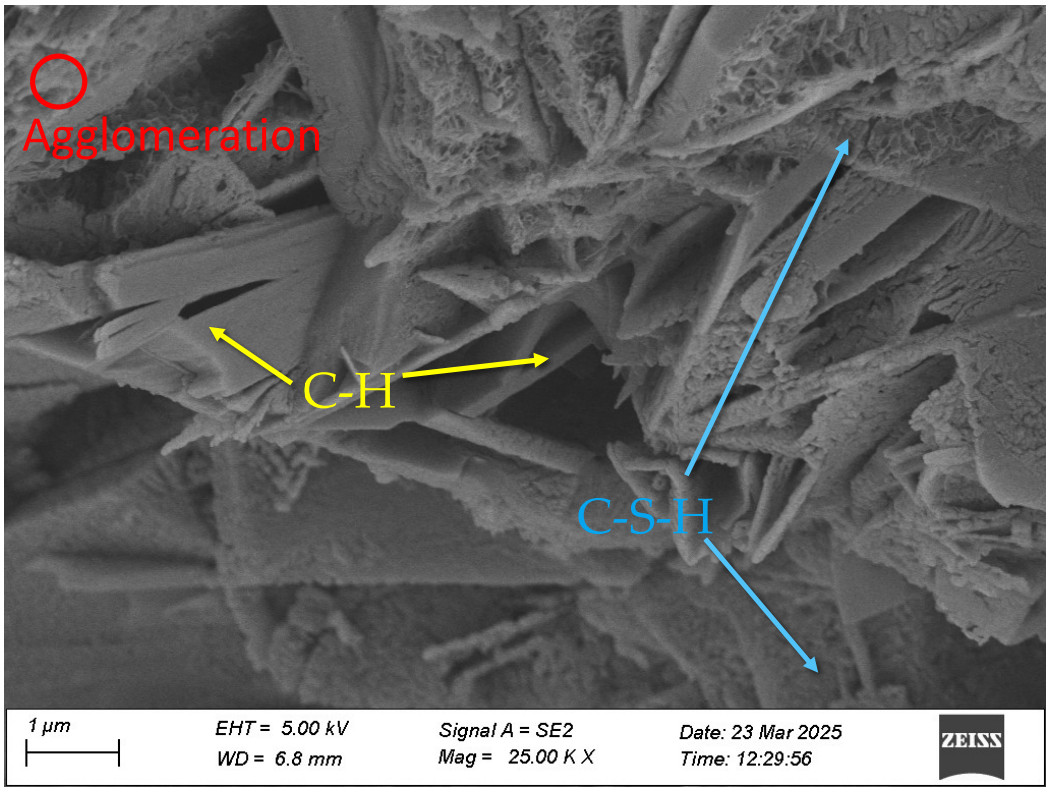


a) 15000x magnification

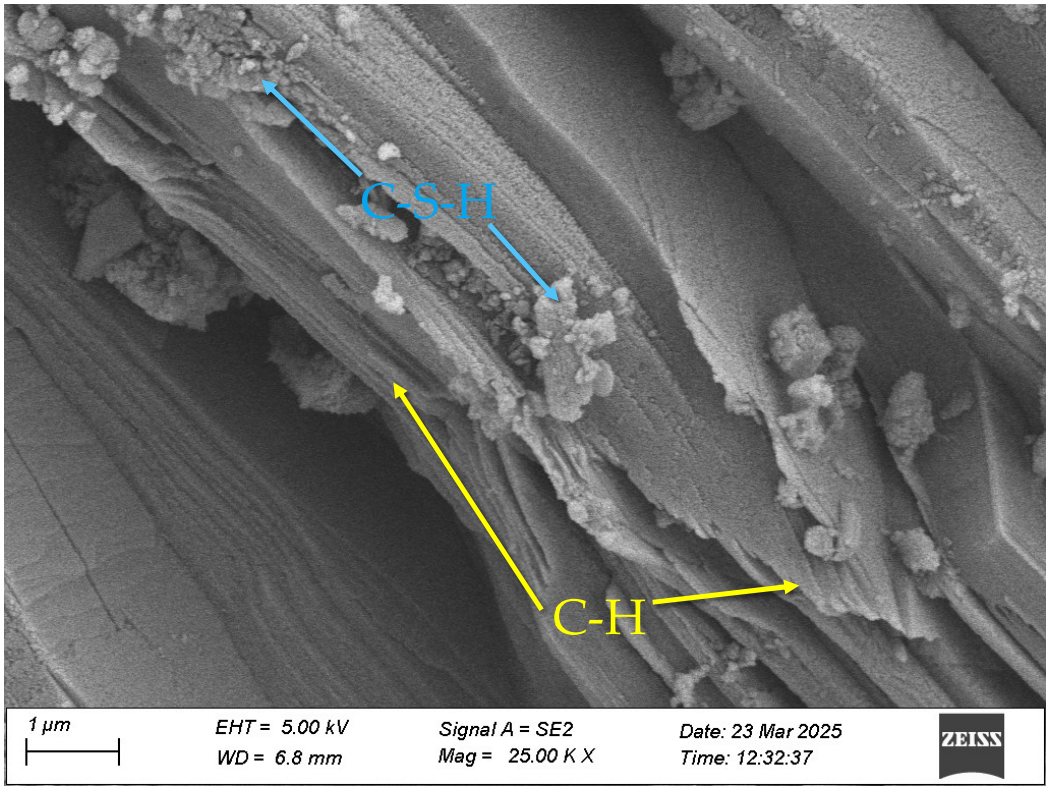


b) 25000x magnification

Figure 4.6 SEM image of 2% replacement of CEM-1 with NGS

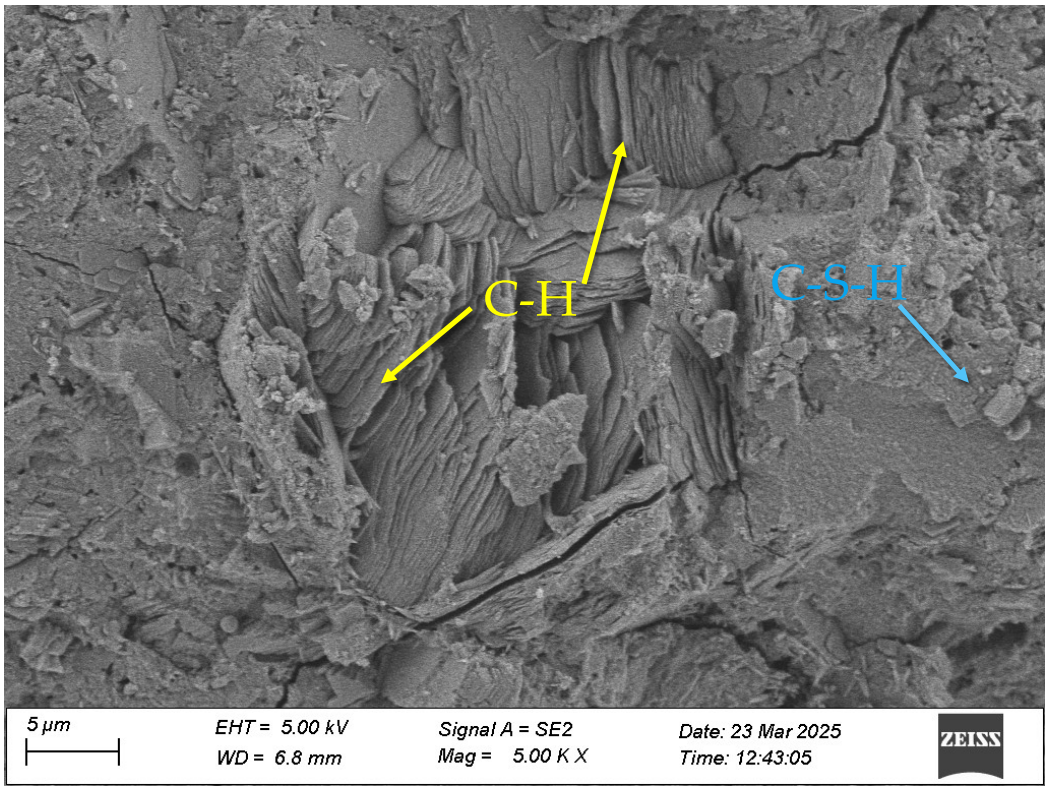


a) 25000x magnification

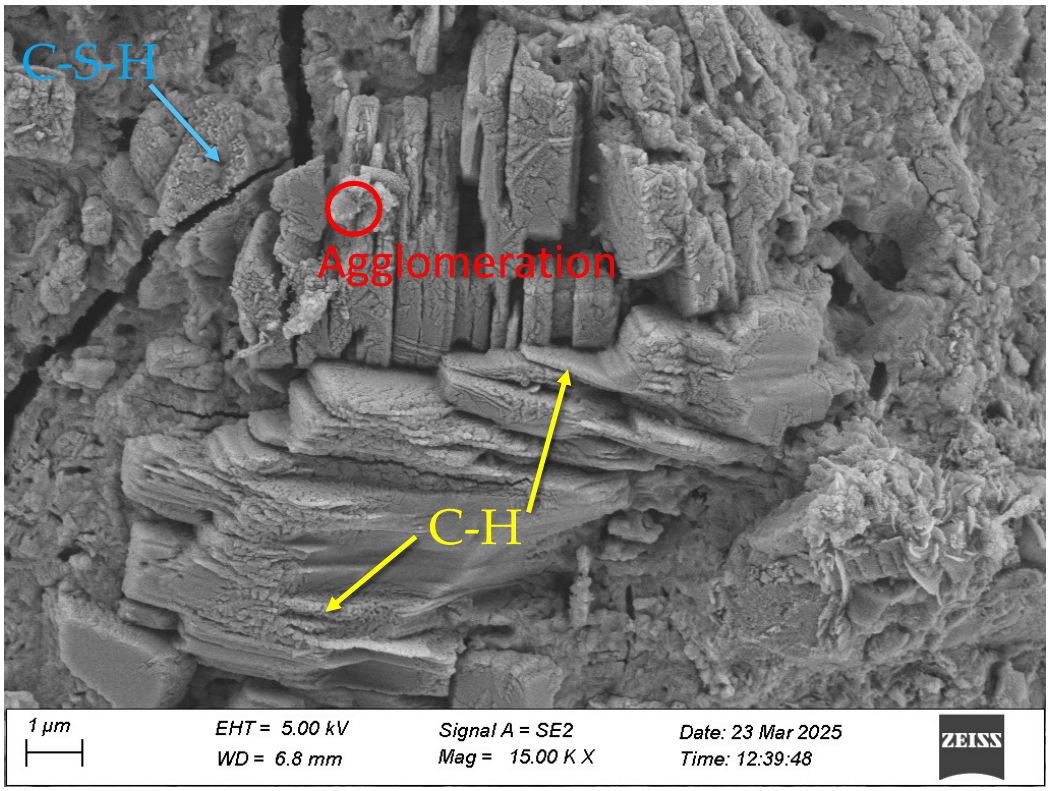


b) 25000x magnification

Figure 4.7 SEM image of 3% replacement of CEM-1 with NGS



a) 5000x magnification



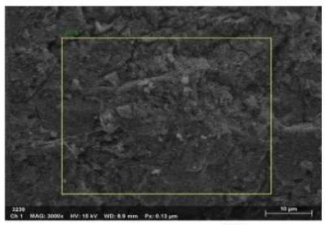
b) 15000x magnification

Figure 4.8 SEM image of 5% replacement of CEM-1 with NGS

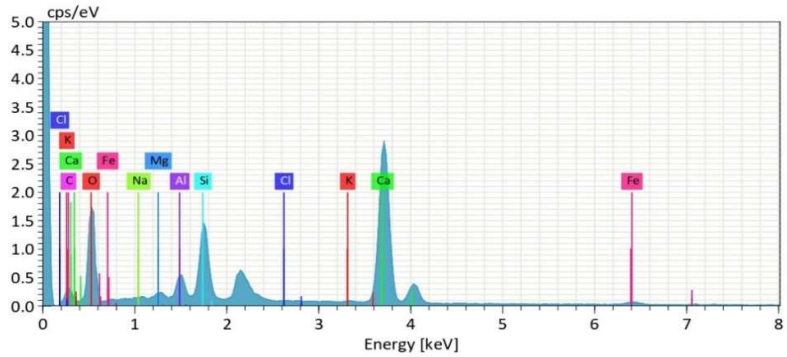
The SEM analysis confirms that NSG incorporation significantly improved the cement paste microstructure, especially at 2–5% replacement levels. NSG promoted the formation of a more compact and continuous C-S-H matrix, resulting in reduced porosity and greater uniformity in the hardened material. This enhancement is linked to the high surface area and strong pozzolanic reactivity of NSG, which accelerates hydration and refines the pore network (Yuvakkumar et al., 2014). Additionally, the diminished presence of needle-like ettringite at higher NSG contents indicates increased structural stability and reduced risk of expansion-related cracking (Al-Abboodi et al., 2020). These improvements contribute to better mechanical performance and durability, reinforcing the role of NSG as an effective supplementary cementitious material.

4.2.2 Energy-Dispersive X-ray Spectroscopy (EDX) Analysis

EDX analysis was performed on five representative regions of the nano silica samples using an accelerating voltage of 15.0 keV and a 3000x magnification (HV = 15.0 keV; WD = ~8.5–8.9 mm). The elemental composition consistently showed the presence of key elements: oxygen (O), silicon (Si), calcium (Ca), and aluminium (Al). The oxygen content was high across all samples, ranging from approximately 43% to 47%, while the silicon content ranged from ~7% to 9.5%, confirming a strong presence of silica. Calcium levels were notably high, ranging from ~32% to 36%, indicating the presence of calcium-rich compounds. Minor elements identified included carbon (C) (~6–9%), sodium (Na) (~0.03–0.85%), magnesium (Mg) (~0.46–0.99%), potassium (K) (~0.12–0.27%), iron (Fe) (~1.18–1.82%), and chlorine (Cl) (~0.04–0.07%). Fig (4.9, 4.10, 4.11, 4.12 & 4.13) shows energy-dispersive X-ray spectroscopy (EDX).

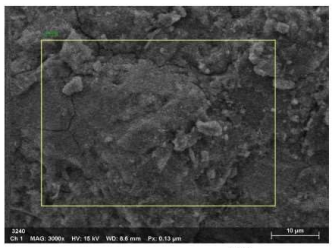


Name	Date	Time	HV [kV]	Mag	WD [mm]
3239	3/23/2025	12:44:39 PM	15.0 keV	3000x	8.9 mm

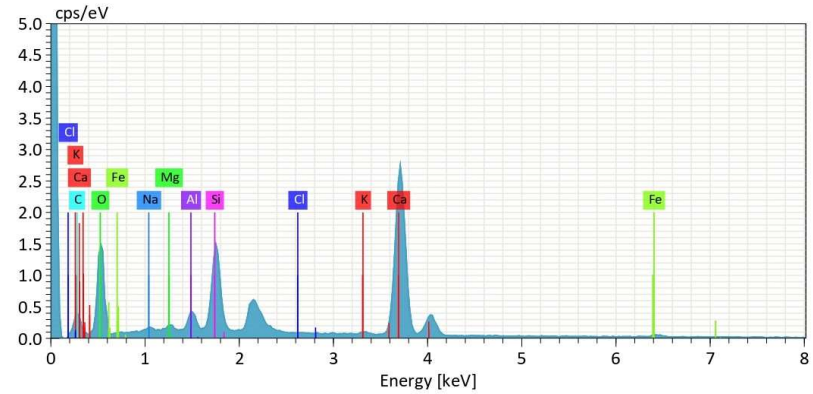


Spectrum	C	O	Na	Mg	Al	Si	Cl	K	Ca	Fe
3175	6.01	47.33	0.64	0.83	2.38	7.41	0.04	0.13	33.43	1.81

Figure 4.9 EDX of control sample

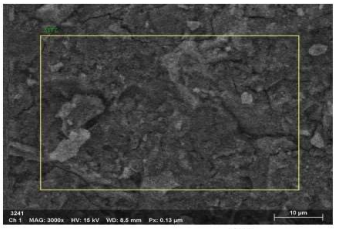


Name	Date	Time	HV [kV]	Mag	WD [mm]
3240	3/23/2025	12:50:12 PM	15.0 keV	3000x	8.6 mm

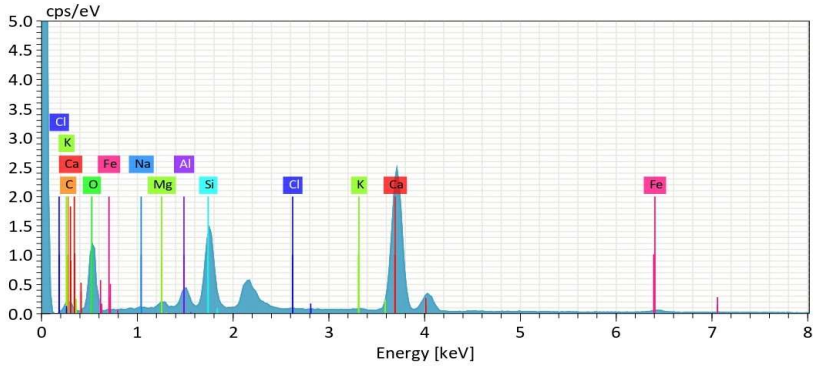


Spectrum	C	O	Na	Mg	Al	Si	Cl	K	Ca	Fe
3176	9.71	44.96	0.85	0.73	1.85	8.07	0.06	0.27	32.32	1.18

Figure 4.10 EDX of 1% CEM I replacement with NGS

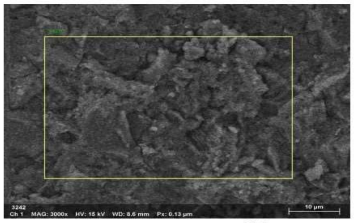


Name	Date	Time	HV [kV]	Mag	WD [mm]
3241	3/23/2025	12:53:31 PM	15.0 keV	3000x	8.5 mm

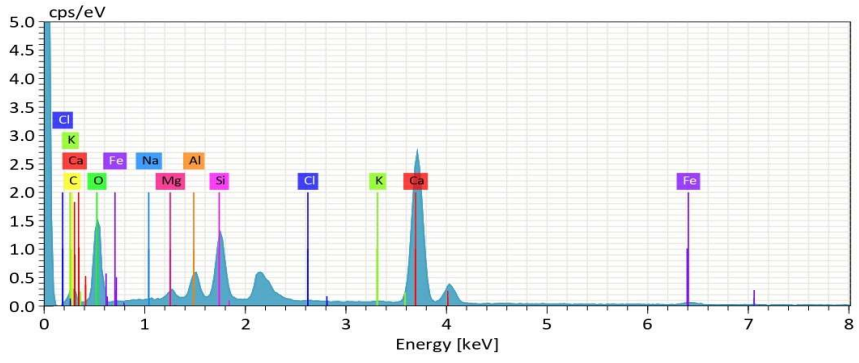


Spectrum	C	O	Na	Mg	Al	Si	Cl	K	Ca	Fe
3177	5.99	43.36	0.09	0.64	2.19	9.56	0.07	0.24	36.03	1.82

Figure 4.11 EDX of 2% CEM I replacement with NGS



Name	Date	Time	HV [kV]	Mag	WD [mm]
3242	3/23/2025	12:57:30 PM	15.0 keV	3000x	8.6 mm



Spectrum	C	O	Na	Mg	Al	Si	Cl	K	Ca	Fe
3178	7.13	46.93	0.03	0.99	2.82	7.27	0.05	0.12	33.24	1.42

Figure 4.12 EDX of 3% CEM I replacement with NGS

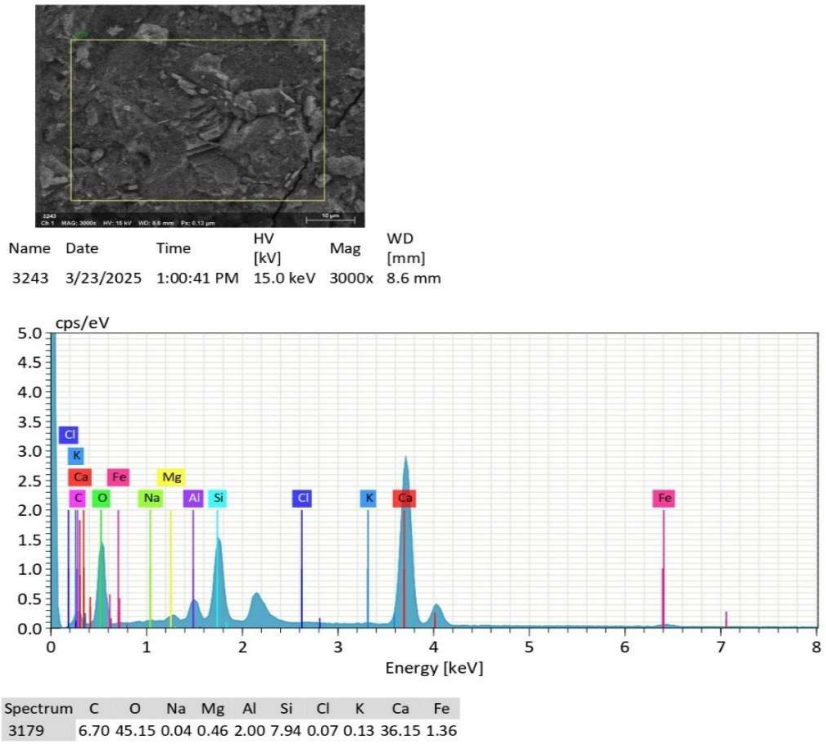


Figure 4.13 EDX of 5% CEM I replacement with NGS

The elevated levels of oxygen and silicon confirm the predominance of silica phases in the analyzed samples, consistent with the known composition of nano silica gel derived from rice husk ash and in agreement with findings from previous studies (Yuvakkumar et al., 2014). The significant presence of calcium (32–36%) likely corresponds to calcium silicate hydrate (C-S-H) or other calcium-bearing phases, contributing to the material's pozzolanic activity and compatibility in cementitious systems (Rahman & Padavettan, 2012). Trace elements such as Na, Mg, K, Fe, and Cl, though detected in low amounts, are likely remnants of synthesis additives or minor impurities from the rice husk ash source (Thuadaij & Nuntiya, 2008). The presence of carbon is expected due to residual organic content or carbon-based impurities. These results suggest that the NSG samples possess a chemical composition well-suited for pozzolanic use in cementitious materials, contributing to improved hydration

and strength through their reactive silica and the support of calcium-containing phases.

4.2.3 Normal Consistency

The normal consistency of cementitious mixtures incorporating different percentages of nano silica gel (NSG) derived from rice husk ash was evaluated to determine its effect on water demand. The control mix (0% NSG) exhibited a normal consistency of 27.00%. As NSG replacement levels increased, the consistency also increased progressively: 28.03% at 1% NSG, 28.80% at 2% NSG, 31.50% at 3% NSG, and 33.03% at 5% NSG. These results indicate a consistent trend of increased water demand with higher NSG content. Fig. 4 .14 shows the change in NC with varying levels of NSG.

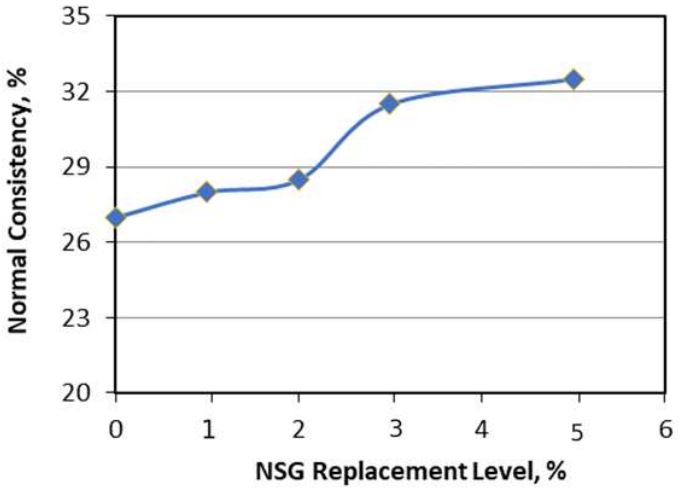


Figure 4.14 Normal consistency result

The progressive increase in normal consistency with higher NSG replacement aligns with existing literature highlighting the high surface area and water absorption capacity of nano silica particles (Quercia & Brouwers, 2010); Givi et al., 2010). The presence of fine, highly reactive nano silica enhances the particle packing density, which fills voids and reduces the availability of free water, thereby increasing the water requirement for achieving the desired consistency.

Moreover, the pozzolanic activity of NSG accelerates early hydration reactions, consuming more water and contributing to the observed trend (Nazari & Riahi, 2011).

At lower NSG levels (1%–2%), the increase in consistency is moderate, indicating manageable water adjustments and workability. However, at higher NSG levels (≥3%), the marked increase in consistency (up to 33.03% at 5% NSG) may necessitate the use of water-reducing admixtures or adjustments in water-to-binder ratio to ensure adequate workability. This finding is consistent with observations from (Quercia & Brouwers, 2010), who reported that amorphous nano silica enhances the water demand of cement-based mixes. Thus, careful optimization of the mix design is essential to balance the beneficial effects of NSG on microstructure and strength with the practical requirements of workability and ease of placement.

4.2.4 Setting Time

The setting time of cementitious mixtures incorporating varying percentages of nano silica gel (NSG) derived from rice husk ash was evaluated to assess its impact on hydration behaviour and workability. The control mix (0% NSG) exhibited an initial setting time of 85 minutes and a final setting time of 168 minutes. Introducing 1% NSG led to a slight reduction, with an initial setting time of 82 minutes and a final setting time of 160 minutes. With a 2% NSG replacement, the initial and final setting times dropped to 80 and 150 minutes, respectively. At 3% NSG, this effect became more evident, with initial and final setting times of 75 and 142 minutes. The most substantial reduction was observed at 5% NSG, where the initial setting time was 60 minutes and the final setting time was 125 minutes. These outcomes consistently indicate that increasing NSG content speeds up the setting process in cementitious systems.

This lowering in setting time is mainly due to the nano-scale particles and high surface reactivity of NSG, which accelerate the nucleation and development of calcium-silicate-hydrate (C-S-H) gel during early hydration. Nano silica promotes early-stage hydration by providing active nucleation sites and consuming calcium hydroxide (CH), thereby accelerating the stiffening process. Zhang and Islam (2012) reported that nano-silica significantly shortens the setting time through its impact on hydration kinetics. Fig 4.15 shows the influence of NSG replacement on setting time.

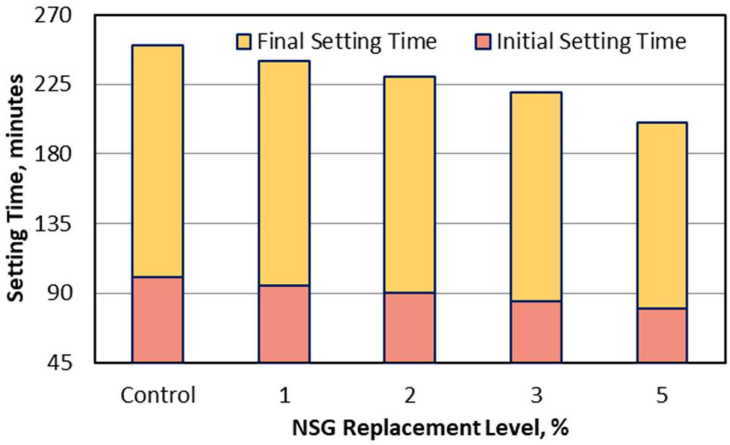


Figure 4.15 Setting Time Result

The reactivity of RHA-derived NSG further amplifies this effect. Torres-Carrasco et al. (2019) noted that RHA can achieve pozzolanic activity comparable to that of nano silica, facilitating faster CH consumption and C-S-H formation. Similarly, Tran et al. (2021) observed that NSG from RHA reduced both initial and final setting times in high-strength concrete due to its fine particle size and high silica concentration.

As NSG content exceeds 3%, the setting process is further accelerated not only by enhanced hydration but also by increased water demand. This reduces the amount of free water available, intensifying the drop-in setting time. This

combined effect, faster hydration and limited free water, leads to a quicker transition from a plastic to a rigid state, as also noted by (Anto et al., 2022a).

4.2.5 Soundness

The soundness of cementitious mixtures with varying percentages of nano-silica gel (NSG) derived from rice husk ash (RHA) was evaluated in terms of dimensional stability. The control mix (0% NSG) showed a consistent expansion of 1 mm. At 1% NSG, the expansion remained the same, indicating no notable effect on soundness. However, as the NSG content increased to 2%, the expansion increased to 1.4 mm, marking the beginning of measurable dimensional change. The expansion rose further to 1.8 mm at 3% NSG and reached 2.2 mm at 5%, indicating that higher NSG concentrations resulted in greater dimensional instability. Figure 4.16 shows soundness of various NSG-induced cement pastes.

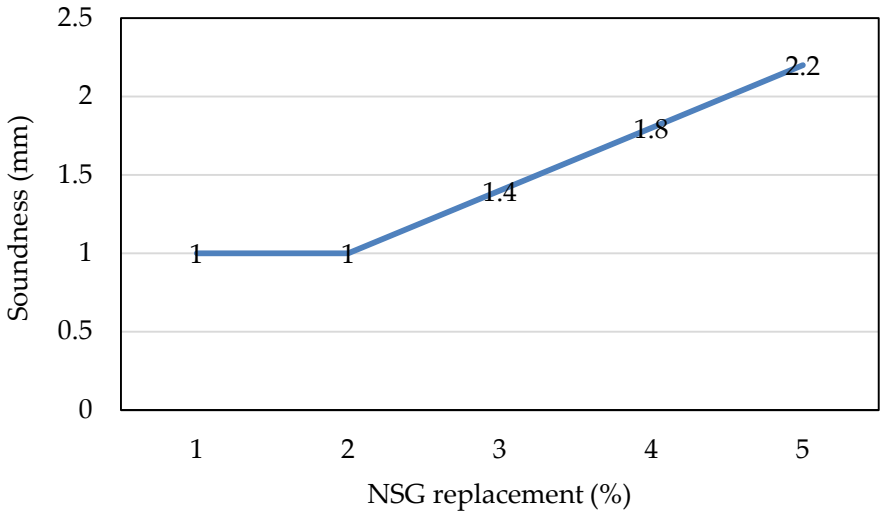


Figure 4.16 Soundness test results

In the discussion, a low NSG content (1%) had a minimal effect on dimensional stability. In contrast, higher dosages, particularly at 3% and 5%, resulted in significant increases in expansion, suggesting a trade-off between strength and

dimensional stability. Research has shown that low NSG dosages generally do not impact soundness, but higher amounts can lead to instability (Anto et al., 2022b); (Torres-Carrasco et al., 2019). Therefore, optimizing NSG content is essential to achieve a balance between performance and stability in cementitious materials.

4.2.6 Autoclave expansion

The autoclave expansion test, performed in accordance with ASTM C151, evaluated the dimensional stability of cementitious mixtures with different levels of NSG derived from rice husk ash. The control mix (0% NSG) exhibited the lowest expansion at 0.00737%, confirming excellent volumetric stability. Introducing 1% NSG resulted in a slight increase to 0.01156%, suggesting that low NSG content has a negligible effect on expansion. At 2% NSG replacement, expansion rose to 0.01965%, while 3% NSG replacement yielded 0.02491%, indicating a gradual increase in internal stresses with higher NSG content. The highest expansion occurred at 5% NSG, reaching a value of 0.03561%. Fig 4.17 shows the expansion found in the autoclave test for different NSG replacement.

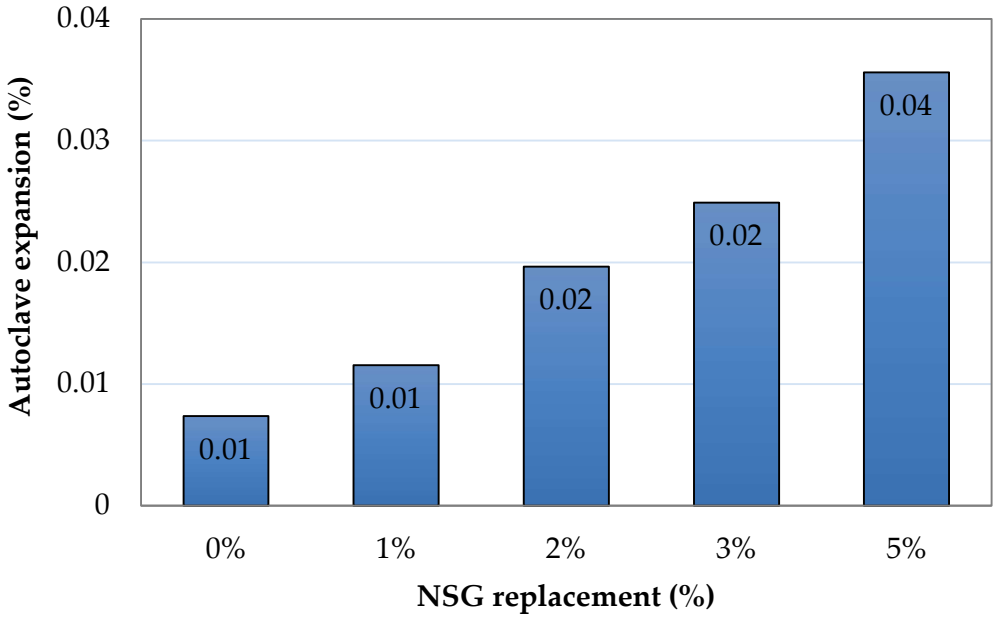


Figure 4.17 Autoclave expansion result

Despite the observed increases, all values remained well below the ASTM C1157 limit of 0.8%, confirming sound dimensional stability. The minor increase in expansion with NSG is attributed to the enhanced hydration reactions and the densification of the microstructure, which can lead to internal stresses. Endale et al. (2023) noted that cement blends incorporating RHA-based nano-silica yielded low expansion levels, particularly when maintained within optimal dosage ranges. Similarly, Danladi (2020) found that expansion due to RHA-derived nano-silica remained within safe limits, suggesting its suitability for volume-stable mortar and concrete formulations.

Additionally, Torres-Carrasco et al. (2019) discussed that the reactive silica of RHA, when used in nano-form, contributes to a controlled and uniform pozzolanic reaction, mitigating expansive tendencies even under autoclave conditions. Therefore, while NSG significantly enhances early-age reactivity, the results confirm that even at a 5% replacement level, dimensional stability remains within acceptable limits.

4.4 MORTAR TEST RESULT

4.4.1 The Flow Table Test

The flow table test results for mortar containing varying levels of nano silica gel (NSG) replacement provide key insights into water demand and workability. A consistent target flow value of ±5 mm from the control was maintained across all mixtures. Recorded flow values were 160 mm for 0% NSG, 156 mm for 1%, 165 mm for 2%, 156 mm for 3%, and 157 mm for 5%. These findings indicate that NSG content notably affects the water demand and flow characteristics of the mortar mixtures.

This trend agrees with the conclusions of Tran et al. (2021), who reported that NSG derived from rice husk ash significantly impacts water demand and rheological behaviour owing to its large surface area and reactivity. As the NSG

content increases, hydration kinetics speed up, and matrix densification improves, but workability may decline if adjustments like additional water or plasticizers are not made. Similarly, Danladi (2020) noted that fine NSG particles function as microfilmers, influencing the flow properties depending on the dosage and how effectively they are dispersed. The increased flow at 2% NSG might indicate an optimal packing density, whereas further increases in NSG lead to a reduction in fluidity once the critical threshold is surpassed. Fig 4.18 shows the flow value of different NSG-replaced mortars, and Fig 4.19 shows the water demand vs NSG replacement.

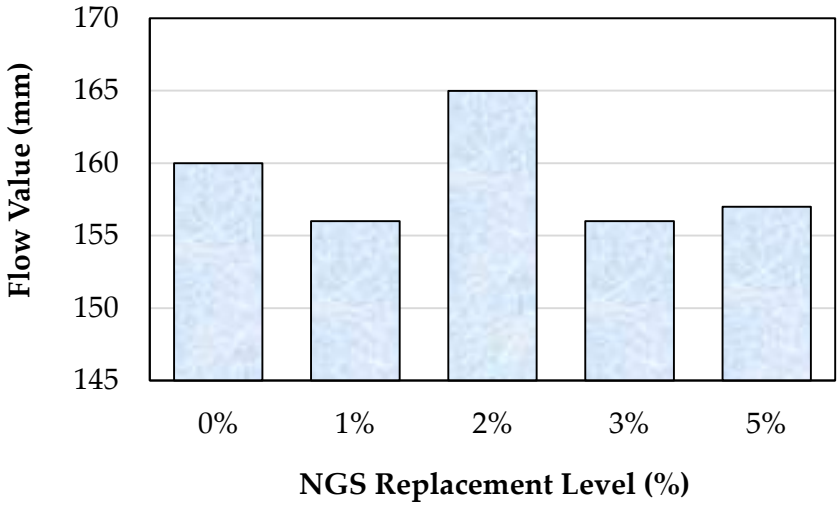


Figure 4.18 Flow value result

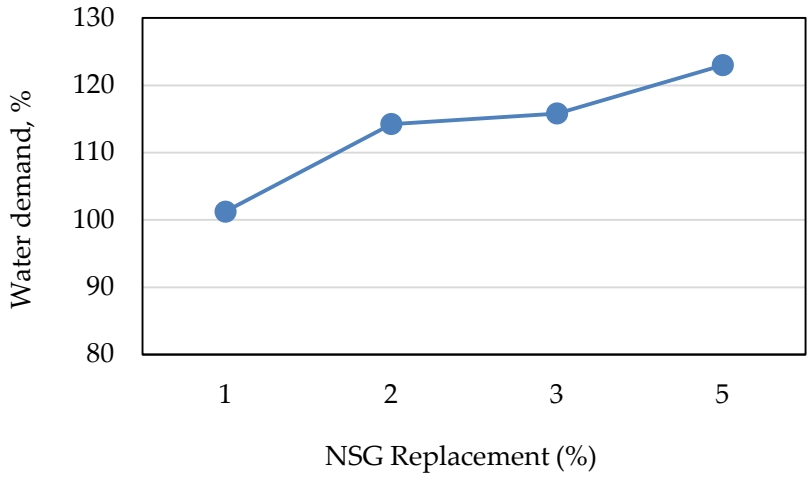


Figure 4.19 Water demand result

The findings of Najigivi et al. (2012) support this observation, noting that the effect of nano-silica combined with rice husk ash on workability can vary depending on dosage, particle agglomeration, and overall mix composition. Experimental results from this study showed a steady increase in water demand with rising NSG content in mortar mixes. Water consumption increased from 101.41 grams at 1% NSG replacement to 123 grams at 5%, marking a 21.3% rise. This increase is due to the ultra-fine particle size and large surface area of NSG, which enhances its water absorption and create a denser matrix that restricts flow, requiring more water to achieve workable consistency.

This outcome aligns with earlier research on cementitious materials. Quercia et al. (2012) noted that amorphous nano-silica substantially raises water demand due to its fine particle size and high reactivity, particularly in paste and mortar systems. Similarly, Alqamish & Al-Tamimi (2021) observed increased water requirements in mortar mixes containing up to 6% nano-silica, attributing this to particle agglomeration and heightened mixture viscosity. Hamada et al. (2023) confirmed that nano-silica reduces flow in mortar mixes, intensifying the need for water or superplasticizer to achieve adequate workability.

4.4.2 Fresh density of mortar

The fresh density of cementitious mortars incorporating different percentages of nano-silica gel (NSG) derived from rice husk ash was measured in accordance with BS EN 1015-3 standards. The control mix (0% NSG) exhibited the highest fresh density of 2295 kg/m^3. With 1% NSG replacement, the density slightly decreased to 2270 kg/m^3, while 2% NSG replacement resulted in a further decrease to 2245 kg/m^3. Notably, at 3% NSG replacement, the fresh density decreased to 2230 kg/m^3, while at 5% replacement, it decreased to 2210 kg/m^3. These variations suggest that NSG content has a variable impact on the

fresh density of mortar, showing both increases and decreases based on the level of replacement. Fig 4.20 shows the change in fresh density with NSG replacement in a bar chart.

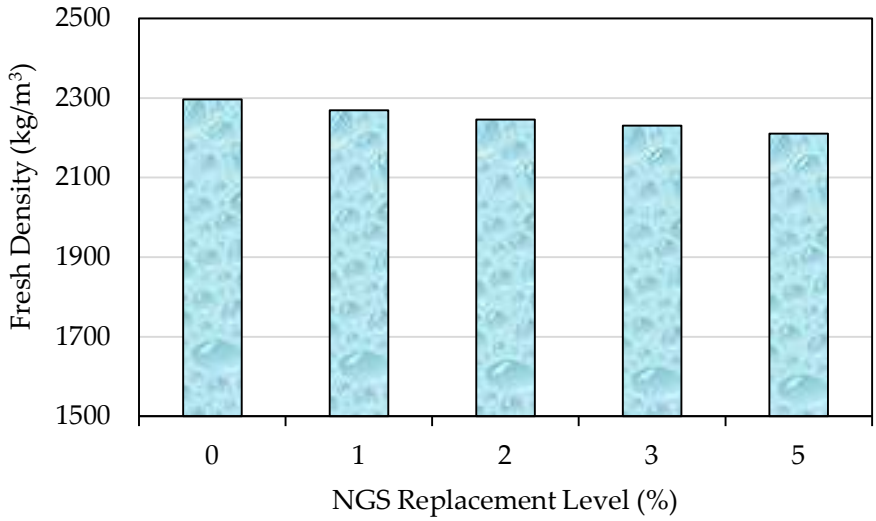


Figure 4.20 Fresh density of mortar

The observed variations in fresh density can be ascribed to the combined effects of fine particle size, high surface area, and water retention capacity of NSG, which influence packing density and matrix cohesion (Quercia & Brouwers, 2010; Givi et al., 2010). At lower replacement levels (1%–2%), the slight reduction in density is likely due to increased water demand and a potential dilution of cement content. This trend aligns with Givi et al. (2010), who found that nano silica can increase water requirements and enhance mix porosity.

At a 3% and 5% NSG replacement, a slight decrease in fresh density was observed, possibly due to increased air entrainment and greater water retention associated with the higher NSG content. Similar effects have been reported in previous studies, where excessive nano silica disrupted mix uniformity and introduced additional porosity (Quercia et al., 2012). Despite these fluctuations, all measured densities remained within the acceptable range for mortar (2200–

2300 kg/m³), indicating that NSG incorporation up to 3% maintains favourable workability and compaction. However, higher levels (≥5%) may require changes to the water-to-binder ratio or the incorporation of plasticizers to preserve optimal fresh mix properties.

4.4.3 Hardened Density of Mortar

The hardened density of cementitious mixtures incorporating different percentages of nano silica gel (NSG) was measured at 7, 28, and 90 days of curing. At 7 days, the control mix (0% NSG) exhibited the highest density of 2115 kg/m³. However, the density decreased progressively with increasing NSG content, reaching 2050 kg/m³ at 5% NSG replacement. This trend continued at 28 days, where the density ranged from 2125 kg/m³ (0% NSG) to 1985 kg/m³ (5% NSG), indicating continued hydration and microstructural changes. At 90 days, the hardened density further decreased, with values ranging from 2120 kg/m³ (0% NSG) to 1990 kg/m³ (5% NSG). These results consistently demonstrate a reduction in hardened density with higher NSG content at all curing ages.

Several factors cause the observed reduction in hardened density with increasing NSG content. Firstly, the high pozzolanic reactivity of NSG facilitates the formation of more calcium-silicate-hydrate (C-S-H) gel, which refines the pore structure and results in a denser overall microstructure yet paradoxically may decrease the bulk density as smaller gel products replace denser cement phases (Nazari & Riahi, 2011; Quercia et al., 2012). Secondly, the lower intrinsic density of NSG compared to cement (Yuvakkumar et al., 2014) directly contributes to the reduction in the overall density of the hardened matrix as the NSG content increases. Fig 4.20 shows the change in hardened density with NSG replacement level.

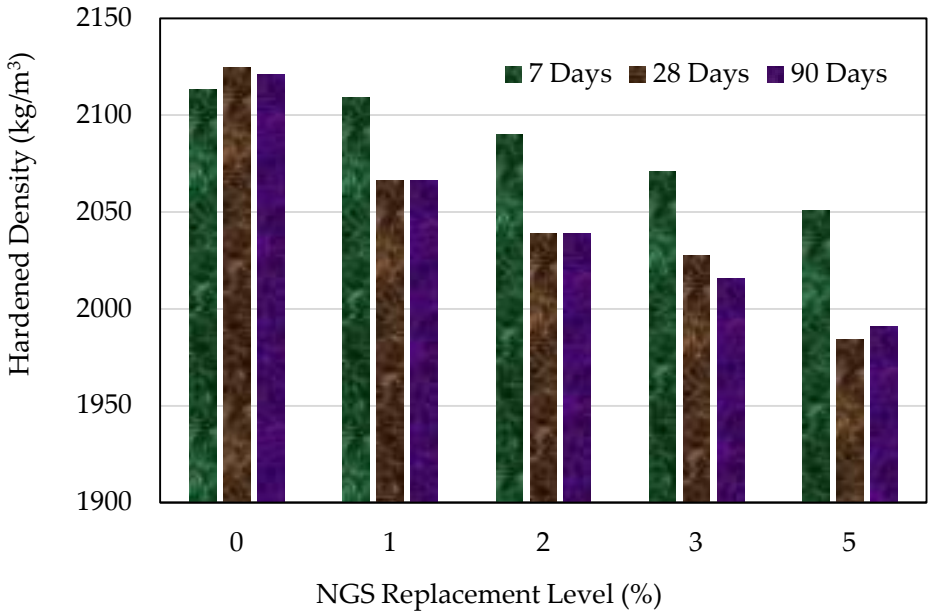


Figure 4.21 Hardened density test results

While a reduction in density can be beneficial for producing lightweight concrete with enhanced thermal insulation, excessive NSG replacement may compromise mechanical strength and durability due to increased porosity and a decrease in load-bearing capacity (Givi et al., 2010). The findings indicate that a 2% to 3% NSG replacement provides an optimal balance, offering microstructural refinement and pozzolanic activity without significantly affecting density. This aligns with previous studies, such as Qing et al. (2006), which emphasized the advantages of moderate nano silica content in optimizing hydration, porosity, and mechanical behaviour. Overall, these results highlight the importance of carefully controlling NSG dosage to achieve the best combination of structural integrity and performance in cementitious materials.

4.4.4 Flexural Strength Analysis

Fig 4.22 shows the variation of flexural strength of NSG induced mortar with age. The flexural strength of cementitious mortar with different nano silica gel

(NSG) replacement levels was assessed at 7, 28, and 90 days of curing. At 7 days, the control mix (0% NSG) recorded the highest flexural strength of 5.02 MPa. As the NSG content increased, a gradual reduction in strength was observed, with the 5% NSG mix reaching a strength of 4.65 MPa. At 28 days, the flexural strength increased overall, with the highest value recorded at 1% NSG replacement (6.3 MPa), surpassing the control mix (6.05 MPa). Beyond 1% replacement, the strength decreased progressively, reaching 5.37 MPa at 5% NSG. A parallel trend was observed at 90 days, with the highest strength again achieved at 1% NSG replacement (6.94 MPa), slightly exceeding the control (6.63 MPa). In contrast, the strength at 5% NSG replacement decreased to 5.67 MPa. The flexural strength data indicate that NSG content influences the tensile performance of cement-based materials at different curing ages.

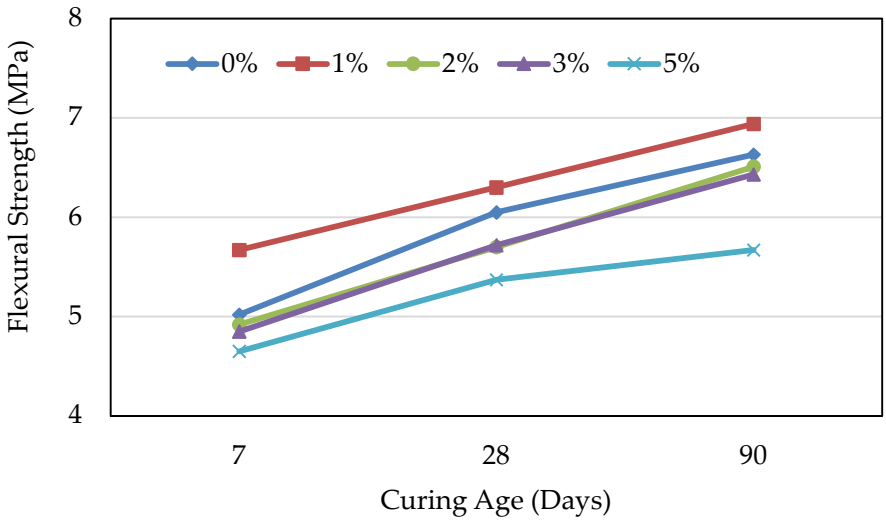


Figure 4.22 Flexural strength of NGS induced mortars at different ages

The initial reduction in flexural strength at 7 days with increasing NSG replacement can be attributed to limited calcium hydroxide (CH) availability for pozzolanic reactions during early hydration, which slows the progression of additional calcium-silicate-hydrate (C-S-H) gel (Quercia & Brouwers, 2010).

This aligns with previous research, which demonstrates that pozzolanic materials often require sufficient CH to contribute significantly to the development of strength at early ages (Givi et al., 2010).

As curing progresses, the pozzolanic activity of NSG becomes increasingly effective, resulting in microstructural refinement and enhanced bonding between hydration products. At 28 days and 90 days, 1% NSG replacement consistently yielded the highest flexural strength, suggesting that moderate NSG content optimizes the balance between pozzolanic reactivity and workability, enhancing the tensile performance of the cementitious matrix (Nazari & Riahi, 2011). However, at higher NSG levels (3% and 5%), the flexural strength reduced, possibly due to the agglomeration of fine particles, increased water demand, and potential porosity, which negatively affect matrix cohesion (Quercia & Brouwers, 2010; Givi et al., 2010).

4.4.5 Compressive Strength Analysis

The compressive strength of cementitious mortars incorporating nano silica gel (NSG) from rice husk ash was evaluated at 7, 28, and 90 days of curing. At 7 days, the control mix (0% NSG) exhibited a compressive strength of 47.0 MPa. Increasing the NSG replacement levels generally led to a modest increase in compressive strength: 50.2 MPa at 1% NSG, 46.0 MPa at 2% NSG, 45.4 MPa at 3% NSG, and 43.5 MPa at 5% NSG. At 28 days, the compressive strength of the control mix was 48.2 MPa. The strength improved at 1% NSG replacement (54.0 MPa), while at 2%, 3%, and 5% NSG replacement levels, the compressive strength was recorded as 47.4 MPa, 45.6 MPa, and 43.8 MPa, respectively.

At 90 days, the compressive strength of the control mix was 51.6 MPa. The highest strength was observed at a 1% NSG replacement level (54.0 MPa), while at 2%, 3%, and 5% NSG levels, the strength values were 50.6 MPa, 50.0 MPa, and 46.0 MPa, respectively.

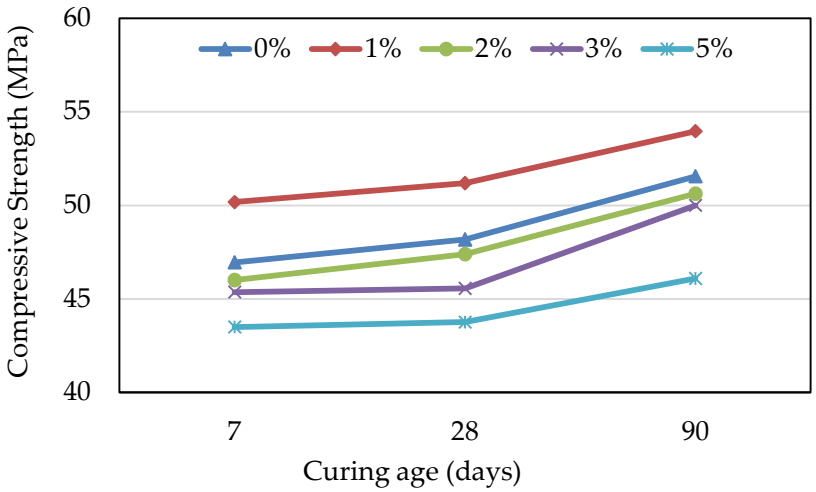


Figure 4.23 Compressive strength of mortars

The results indicate that low-level nano silica gel replacement (1% NSG) consistently improves compressive strength across all curing periods. This aligns with findings by Zhang et al. (2017) and Nazari and Riahi (2011), who reported that minor additions of nano-silica enhance microstructural refinement and increase the density of hydration products in cementitious systems. The strength improvement observed at 1% NSG is primarily attributed to its pozzolanic reaction with calcium hydroxide, generating additional calcium-silicate-hydrate (C-S-H) gel that contributes to a denser and more cohesive cement matrix (Quercia & Brouwers, 2010).

Conversely, at higher NSG replacement levels (≥2%), the compressive strength began to decline, likely due to agglomeration of NSG particles, increased water demand, and dilution of the cementitious phase (Givi et al., 2010). This trend suggests that while nano silica enhances early hydration and microstructural refinement, excessive replacement levels can disrupt the optimal packing density and pore structure, leading to increased porosity and reduced strength.

4.4.6 Strength Activity Index (SAI)

The Strength Activity Index (SAI) of cementitious mixtures containing various percentages of nano silica gel (NSG) was measured at 28 days to evaluate its pozzolanic effectiveness. The control mix (0% NSG) was assigned an SAI of 100% by default. At 1% NSG replacement, the SAI increased to 106.2%, reflecting an increase in compressive strength relative to the control. However, with higher NSG content, the SAI declined: 98.3% at 2%, 94.5% at 3%, and 90.9% at 5%. These results indicate that while a small addition of NSG (1%) positively influences strength development through enhanced pozzolanic reactivity, higher replacement levels may reduce strength due to factors such as increased water demand, particle agglomeration, or reduced cement content.

The SAI results demonstrate that incorporating NSG at low levels (1%) effectively enhances the compressive strength of cementitious systems by increasing pozzolanic activity and refining the microstructure (Nazari & Riahi, 2011). The recorded SAI of 106.2% at 1% NSG surpasses the ASTM C618 threshold of ≥75% for pozzolanic materials, confirming the suitability of NSG as a supplementary cementitious component at this level. These findings are consistent with those of Qing et al. (2006) and Givi et al. (2010), who noted that nano silica improves hydration kinetics and promotes C-S-H gel development, resulting in enhanced mechanical properties.

At higher NSG replacement levels (≥2%), the SAI values dropped below those of the control mix, suggesting that excessive NSG can cause problems such as particle agglomeration, elevated water demand, and dilution of the cementitious matrix. These factors collectively contribute to a reduction in compressive strength (Quercia et al., 2013). This decline in SAI highlights the trade-off between the benefits of microstructural refinement and the risks of increased porosity or weakened interfacial transition zones. These findings

emphasize the need to carefully optimize NSG dosage to achieve strength gains while maintaining workability and overall performance in cementitious systems.

4.4.7 Drying Shrinkage

Fig 4.29 shows the variation of drying shrinkage of NSG mortar with time. The drying shrinkage behaviour of cementitious mortar with varying nano silica gel (NSG) content derived from rice husk ash was monitored over 28 days at intervals of 7, 14, 21, and 28 days. At 7 days, the control mix (0% NSG) exhibited a shrinkage of 0.0303%. In contrast, the 1% NSG mix showed a slightly reduced shrinkage of 0.0259%, indicating a decrease in early-age shrinkage with the incorporation of low-level NSG. However, with higher NSG replacements, shrinkage values increased, with 2% NSG recording 0.0516% and 5% NSG at 0.0342%.

At 14 days, shrinkage increased across all mixes: 0.0408% for the control mix, 0.0498% for 1% NSG, and significantly higher shrinkage for 2% and 5% NSG (0.0823% and 0.0772%, respectively). By 21 days, the control mix reached 0.0689% shrinkage, while the 1% NSG mix increased to 0.0798%. Higher NSG levels continued to exhibit higher shrinkage, with 2% NSG at 0.1158% and 5% NSG at 0.0953%. At 28 days, the control mix exhibited a shrinkage of 0.077%, while the 1% NSG mixture showed moderate shrinkage at 0.127%. However, 2% NSG and 5% NSG exhibited the highest shrinkage levels, at 0.1358% and 0.1516%, respectively.

The progressive rise in drying shrinkage with time and higher NSG replacement levels can be ascribed to the high surface area and pozzolanic reactivity of NSG, which refines the pore structure but also leads to higher water absorption and gel formation, contributing to increased internal stresses during drying (Quercia et al., 2012; Givi et al., 2010). At low replacement levels

(1% NSG), the shrinkage remained relatively close to that of the control mix, indicating that moderate NSG additions enhance microstructure without significantly compromising dimensional stability. This finding aligns with previous studies that emphasize the optimal range for nano silica incorporation to control shrinkage while improving hydration and microstructure (Nazari & Riahi, 2011). However, at higher NSG replacement levels (≥2%), increased shrinkage was observed, likely due to a densification effect that promotes extensive gel formation, resulting in greater contraction stresses during moisture loss (ASTM C596).

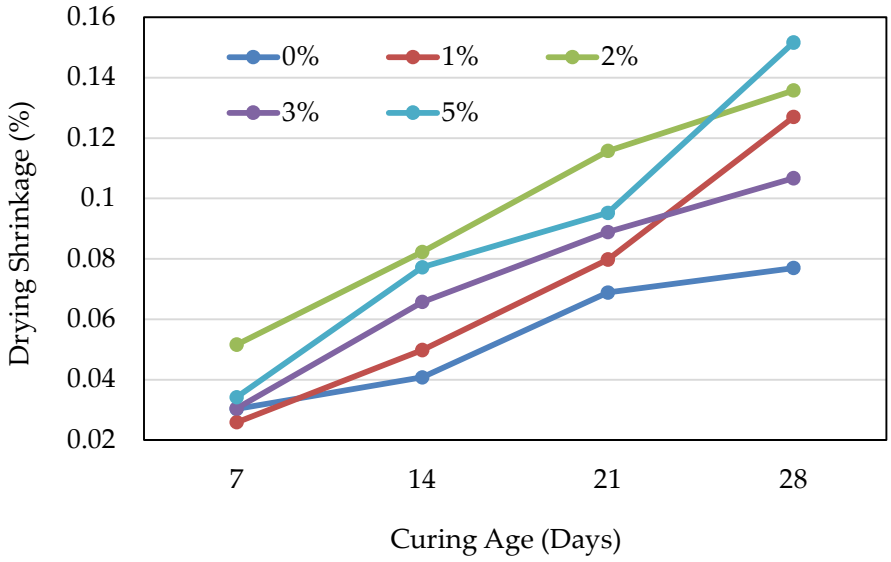


Figure 4.24 Drying shrinkage result

Excessive NSG content can lead to a tightly packed microstructure, which, although refined, becomes more susceptible to internal shrinkage and potential cracking, as also noted by Qing et al. (2006). These findings underscore the importance of optimizing NSG dosage to control drying shrinkage while still achieving the microstructural enhancements offered by nano silica.

4.4.8 Electrical Resistivity

The surface resistivity of cementitious samples containing different levels of Nano Silica Gel (NSG) replacement was measured to evaluate NSG's influence on durability and ionic permeability. The control mix (0% NSG) showed the highest surface resistivity at 4.15 kΩ·cm. With increasing NSG content, resistivity values declined progressively: 3.77 kΩ·cm at 1%, 3.47 kΩ·cm at 2%, 3.60 kΩ·cm at 3%, and 3.35 kΩ·cm at 5%. These results indicate that NSG replacement alters the microstructure and affects the ionic transport characteristics of the cementitious matrix. Fig 4.25 shows the resistivity of NGS-induced mortar samples.

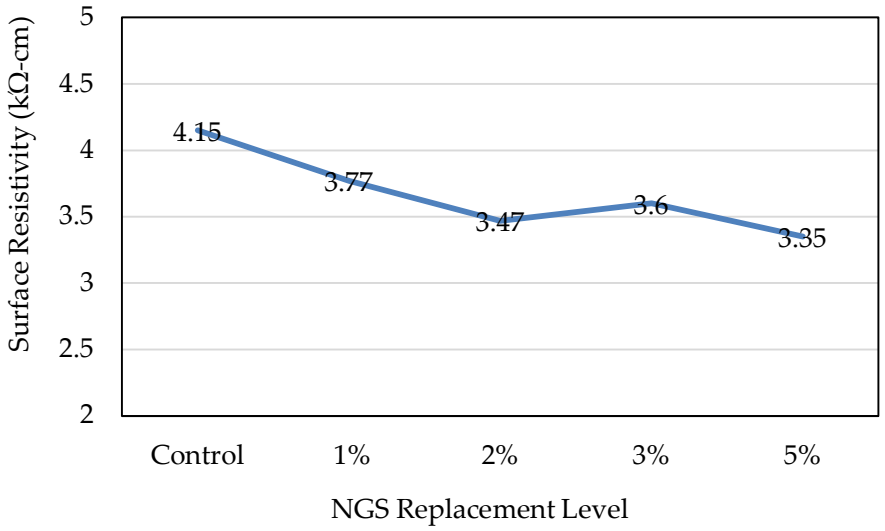


Figure 4.25 Surface resistivity of mortar

The observed reduction in surface resistivity with increasing NSG content suggests that higher NSG levels enhance the electrical conductivity of the cementitious matrix. This trend is typically associated with greater chloride ion penetrability and potentially reduced durability, especially under aggressive environmental conditions (Quercia et al., 2013). The control mix, with a resistivity of 4.15 kΩ·cm, is within the moderate durability classification as per

AASHTO T 358-15, indicating satisfactory resistance to chloride intrusion. However, the introduction of just 1% NSG resulted in a 9.2% decrease in resistivity, underscoring the sensitivity of the system to nano silica gel incorporation. Additionally, the 3% NSG mix showed a slight improvement over the 2% NSG mix (3.60 kΩ ·cm vs. 3.47 kΩ ·cm), possibly due to better dispersion and matrix densification at this concentration level. This aligns with previous studies suggesting that moderate NSG incorporation can refine pore structures and enhance the microstructure, thereby mitigating ionic conductivity to some extent (Givi et al., 2010). Nonetheless, at the highest replacement level (5%), the resistivity decreased further to 3.35 kΩ·cm, indicating a nearly 19.3% reduction compared to the control mix. This decrease suggests that excessive NSG may lead to increased pore connectivity, microstructural discontinuities, or particle agglomeration, which facilitates ion transport (Nazari & Riahi, 2011).

These findings emphasize that while the pozzolanic activity of NSG contributes to C-S-H gel formation and improved mechanical performance, excessive dosages can compromise the resistivity and, consequently, the chloride penetration resistance of the cementitious system (Quercia et al., 2013). Practically, a resistivity below 3 kΩ·cm is generally undesirable, as it correlates with high permeability and potential risks of reinforcement corrosion, especially in marine or de-icing environments.

4.5 SUMMARY OF EXPERIMENTAL RESULTS

In summary, the collective findings from Chapter 4 demonstrate that the incorporation of nano-silica gel (NSG) derived from rice husk ash has a nuanced effect on mortar performance, depending on the level of replacement. At low replacement levels (particularly 1%), NSG effectively refined the pore structure, reduced early-age drying shrinkage, and preserved or slightly

enhanced the dimensional stability of mortar. This dosage also maintained moderate surface resistivity, implying balanced durability and ionic permeability, while supporting microstructural improvements and mechanical gains. However, as the NSG content increased beyond 2%, the mortars exhibited a progressive increase in drying shrinkage and a marked reduction in surface resistivity, indicating a greater susceptibility to moisture-induced contraction and increased ionic transport, respectively.

These trends reflect the dual nature of NSG: its high pozzolanic reactivity and surface area enhance gel formation and densification; however, excessive amounts can lead to greater internal stresses, reduced pore connectivity, and potential durability concerns. The results from all tests thus underscore the importance of optimizing NSG dosage, showing that low-level additions can maximize performance benefits without compromising dimensional stability or long-term durability, while higher dosages may diminish these advantages by exacerbating shrinkage and permeability. This holistic analysis reinforces the recommendation of using low to moderate NSG contents to achieve the most favourable balance of mechanical, physical, and durability properties in sustainable cementitious systems.

Chapter 5: CONCLUSIONS

This chapter presents general remarks, comprehensive conclusions, key findings, limitations, implications, challenges, and guidelines for future investigations.

5.1 GENERAL

This study comprehensively investigated the incorporation of nano silica gel (NSG) derived from rice husk ash (RHA) as a partial substitute for cement in mortar formulations. Through a combination of standard laboratory tests and microstructural analyses (e.g., XRD, SEM and EDX), the research demonstrated that low-level NSG replacement (1%–2%) significantly enhances mechanical performance, including compressive and flexural strength, optimizes setting time, and refines the microstructure due to increased pozzolanic reactivity and generation of more calcium-silicate-hydrate (C-S-H) gel. This finding is particularly valuable, as it demonstrates a sustainable approach to repurposing agricultural waste while reducing cement usage, thereby supporting both environmental sustainability and cost efficiency. The study also indicates that higher NSG contents (≥3%) may contribute to increased shrinkage and lower surface resistivity, which could affect long-term durability, emphasising the importance of precise dosage control.

Overall, the research highlights the potential of RHA-derived NSG as an effective supplementary cementitious material (SCM), capable of improving both performance and service life of cement-based systems. The results stress the need to balance NSG content to fully leverage its pozzolanic benefits while mitigating issues such as elevated water demand and permeability. By establishing the optimal replacement level and showcasing the value of

agricultural waste utilization, this study serves as a meaningful contribution to the advancement of sustainable construction practices, offering practical insights for both academic research and industry application. Future studies should investigate the long-term durability of NSG in real environmental conditions, admixture compatibility, and large-scale implementation strategies to fully leverage the application of NSG in sustainable construction practices.

5.2 KEY FINDINGS

The experimental program included the synthesis and characterization of NSG and its application in mortar specimens at various replacement levels (0%, 1%, 2%, 3%, and 5%). Key physical, mechanical, and durability properties were studied analysed, including fresh consistency, setting time, soundness, density, compressive and flexural strength, drying shrinkage, and surface resistivity.
A 1% NSG replacement demonstrated the most favourable results across all parameters. It enhanced flexural strength (up to 6.94 MPa at 90 days), moderately reduced drying shrinkage, and maintained acceptable workability and setting characteristics.

1. The superior pozzolanic reactivity of NSG contributed to the formation of additional C-S-H gel, thereby improving the microstructure and strength development of cementitious materials.
2. Cement pastes and mortar mixes containing 1% NSG replacements exhibited significant improvements in both compressive strength and flexural strength, with approximately 10–15% higher compressive strength compared to the control mix.

3. When NSG replacement is 2% or more, it reduces flexural and compressive strength due to excessive C-S-H gel formation, higher water demand, particle agglomeration, and interference with cement hydration. These factors weaken the matrix and reduce compaction, leading to lower strength.
4. The study suggests that NSG derived from RHA can participate effectively in hydration reactions, promoting sustainable construction practices.

5.3 LIMITATION OF THE STUDY

While this study has yielded promising results, several limitations must be considered:

- The study focused on mortar specimens, limiting extrapolation to full-scale concrete applications.
- SEM imaging was limited for raw NSG due to instrument constraints, restricting early morphological assessment.
- The influence of NSG on long-term environmental resilience (e.g., freeze-thaw, chloride diffusion) was not explored in detail.

5.4 PRACTICAL IMPLICATION

- NSG, synthesized from agricultural waste (RHA), offers a sustainable supplementary cementitious material (SCM) for green construction.
- Incorporating 1%–2% NSG improves performance with minimal impact on workability, whereas higher dosages require adjustments to the mix (e.g., increased water content or admixtures).

- The use of NSG enhances early hydration, making it suitable for applications that require rapid setting or early strength development.

5.5 RECOMMENDATION FOR FURTHER STUDY

Given the limitations identified in this study, the following avenues for future research are recommended:

- To study the long-term durability of NSG-modified concrete under real environmental exposure conditions.
- To investigate the synergy of NSG with other SCMs such as fly ash, GGBS, or metakaolin in hybrid binder systems.
- To evaluate NSG performance in advanced concretes such as self-compacting, ultra-high-performance, or geopolymer concrete.
- To use nanoindentation and micro-CT scanning to better understand the pore structure and interfacial transition zone (ITZ) in NSG-containing systems

Reference

Al-Abboodi, S. M. T., Al-Shaibani, E. J. A., & Alrubai, E. A. (2020). Preparation and Characterization of Nano silica Prepared by Different Precipitation Methods. *IOP Conference Series: Materials Science and Engineering*, *978*(1). https://doi.org/10.1088/1757-899X/978/1/012031

Ali, T., Saand, A., Bangwar, D. K., Buller, A. S., & Ahmed, Z. (2021). Mechanical and durability properties of aerated concrete incorporating rice husk ash (Rha) as partial replacement of cement. *Crystals*, *11*(6). https://doi.org/10.3390/cryst11060604

Alqamish, H. H., & Al-Tamimi, A. K. (2021). Development and evaluation of nano-silica sustainable concrete. *Applied Sciences (Switzerland)*, *11*(7). https://doi.org/10.3390/app11073041

Al-saffar, F. Y., Wong, L. S., & Paul, S. C. (2023). An Elucidative Review of the Nanomaterial Effect on the Durability and Calcium-Silicate-Hydrate (C-S-H) Gel Development of Concrete. In *Gels* (Vol. 9, Issue 8). Multidisciplinary Digital Publishing Institute (MDPI). https://doi.org/10.3390/gels9080613

Amran, M., Fediuk, R., Murali, G., Vatin, N., Karelina, M., Ozbakkaloglu, T., Krishna, R. S., Kumar, A. S., Kumar, D. S., & Mishra, J. (2021). Rice husk ash-based concrete composites: A critical review of their properties and applications. In *Crystals* (Vol. 11, Issue 2, pp. 1–33). MDPI AG. https://doi.org/10.3390/cryst11020168

Anto, G., Athira, K., Nair, N. A., Sai, T. Y., Yadav, A. L., & Sairam, V. (2022a). Mechanical properties and durability of ternary blended cement paste containing rice husk ash and nano silica. *Construction and Building Materials*, *342*, 127732. https://doi.org/10.1016/J.CONBUILDMAT.2022.127732

Anto, G., Athira, K., Nair, N. A., Sai, T. Y., Yadav, A. L., & Sairam, V. (2022b). Mechanical properties and durability of ternary blended cement paste containing rice husk ash and nano silica. *Construction and Building Materials*, *342*, 127732. https://doi.org/10.1016/J.CONBUILDMAT.2022.127732

Azad, N. M., & Samarakoon, S. M. S. M. K. (2021a). Utilization of industrial by-products/waste to manufacture geopolymer cement/concrete. *Sustainability (Switzerland)*, *13*(2), 1–22. https://doi.org/10.3390/su13020873

Azad, N. M., & Samarakoon, S. M. S. M. K. (2021b). Utilization of industrial by-products/waste to manufacture geopolymer cement/concrete. *Sustainability (Switzerland)*, *13*(2), 1–22. https://doi.org/10.3390/su13020873

Bajpai, R., Choudhary, K., Srivastava, A., Sangwan, K. S., & Singh, M. (2020). Environmental impact assessment of fly ash and silica fume based geopolymer concrete. *Journal of Cleaner Production*, *254*. https://doi.org/10.1016/j.jclepro.2020.120147

Bernal, S. A., Juenger, M. C. G., Ke, X., Matthes, W., Lothenbach, B., De Belie, N., & Provis, J. L. (2017a). Characterization of supplementary cementitious materials by thermal analysis. *Materials and Structures/Materiaux et Constructions*, *50*(1). https://doi.org/10.1617/s11527-016-0909-2

Bernal, S. A., Juenger, M. C. G., Ke, X., Matthes, W., Lothenbach, B., De Belie, N., & Provis, J. L. (2017b). Characterization of supplementary cementitious materials by thermal analysis. *Materials and Structures/Materiaux et Constructions*, *50*(1). https://doi.org/10.1617/s11527-016-0909-2

Calabria-Holley, J., Paine, K., & Papatzani, S. (2015). Effects of nanosilica on the calcium silicate hydrates in Portland cement-fly ash systems. *Advances in Cement Research*, *27*(4), 187–200. https://doi.org/10.1680/adcr.13.00098

Danladi, M. A. (2020). Influence of silica-nano particles on properties of rice husk ash and calcium carbide waste binder based-mortar.

Davidovits, J. (2013). *GEOPOLYMER CEMENT*. www.geopolymer.org

Endale, S. A., Taffese, W. Z., Vo, D. H., & Yehualaw, M. D. (2023). Rice Husk Ash in Concrete. In *Sustainability (Switzerland)* (Vol. 15, Issue 1). MDPI. https://doi.org/10.3390/su15010137

Hamada, H. M., Abed, F., Binti Katman, H. Y., Humada, A. M., Al Jawahery, M. S., Majdi, A., Yousif, S. T., & Thomas, B. S. (2023). Effect of silica fume on the properties of sustainable cement concrete. *Journal of Materials Research and Technology*, *24*, 8887–8908. https://doi.org/10.1016/j.jmrt.2023.05.147

Hamada, H., Shi, J., Yousif, S. T., Al Jawahery, M., Tayeh, B., & Jokhio, G. (2023). Use of nano-silica in cement-based materials–a comprehensive review. In *Journal of Sustainable Cement-Based Materials* (Vol. 12, Issue 10, pp. 1286–1306). Taylor and Francis Ltd. https://doi.org/10.1080/21650373.2023.2214146

Hossam, ©, Alalaily, S., Eng, M., John's, S., & Newfoundland, C. (2017). *Service life of reinforced concrete exposed to chloride environment highlighting the effect of metakaolin in the mixture*.

Hu, K., Yi, J., Huang, B., & Wang, G. (2023). Grain-size effect on dislocation source-limited hardening and ductilization in bulk pure Ni. *Journal of Materials Science and Technology*, *154*, 9–21. https://doi.org/10.1016/j.jmst.2022.12.044

Iqbal Khan, M. (2018). Nanosilica/silica fume. *Waste and Supplementary Cementitious Materials in Concrete: Characterisation, Properties and Applications*, 461–491. https://doi.org/10.1016/B978-0-08-102156-9.00014-6

Labaran, Y. H., Atmaca, N., Tan, M., Atmaca, K., Aram, S. A., & Kaky, A. T. (2024). Nano-enhanced concrete: unveiling the impact of nano-silica on strength, durability, and cost efficiency. *Discover Civil Engineering*, *1*(1), 116. https://doi.org/10.1007/s44290-024-00120-9

Langebeck, A., Bohlen, A., Rentsch, R., & Vollertsen, F. (2020). Mechanical properties of high strength aluminum alloy en aw-7075 additively manufactured by directed energy deposition. *Metals*, *10*(5). https://doi.org/10.3390/met10050579

Li, G., & Zhao, X. (2002). *Properties of concrete incorporating fly ash and ground granulated blast-furnace slag*. www.elsevier.com/locate/cemconcomp

Lin, H., Chen, Y., Gao, X.-R., Xu, L., Lei, J., Zhong, G.-J., & Li, Z.-M. (2012). *Supporting Information A transparent, heat resistant, ductile, and self-reinforced polylactide through simultaneous formation of nanocrystals and orientated amorphous*.

Liu, D., Šavija, B., Smith, G. E., Flewitt, P. E. J., Lowe, T., & Schlangen, E. (2017). Towards understanding the influence of porosity on mechanical and fracture behaviour of quasi-brittle materials: experiments and modelling. *International Journal of Fracture*, *205*(1), 57–72. https://doi.org/10.1007/s10704-017-0181-7

Liu, X., Liu, L., Lyu, K., Li, T., Zhao, P., Liu, R., Zuo, J., Fu, F., & Shah, S. P. (2022). Enhanced early hydration and mechanical properties of cement-based materials with recycled concrete powder modified by nano-silica. *Journal of Building Engineering*, *50*. https://doi.org/10.1016/j.jobe.2022.104175

Lu, J. X., & Poon, C. S. (2018). Improvement of early-age properties for glass-cement mortar by adding nanosilica. *Cement and Concrete Composites*, *89*, 18–30. https://doi.org/10.1016/j.cemconcomp.2018.02.010

Mahdikhani, M., & Ramezanianpour, A. A. (2014). Mechanical properties and durability of self consolidating cementitious materials incorporating nano silica and silica fume. *Computers and Concrete*, *14*(2), 175–191. https://doi.org/10.12989/cac.2014.14.2.175

Maraveas, C., Kyrtopoulos, I. V., Arvanitis, K. G., & Bartzanas, T. (2024). The Aging of Polymers under Electromagnetic Radiation. In *Polymers* (Vol. 16, Issue 5). Multidisciplinary Digital Publishing Institute (MDPI). https://doi.org/10.3390/polym16050689

Moraes, C. A. M., Fernandes, I. J., Calheiro, D., Kieling, A. G., Brehm, F. A., Rigon, M. R., Berwanger Filho, J. A., Schneider, I. A. H., & Osorio, E. (2014). Review of the rice production cycle: By-products and the main applications focusing on rice husk combustion and ash recycling. In *Waste Management and Research* (Vol. 32, Issue 11, pp. 1034–1048). SAGE Publications Ltd. https://doi.org/10.1177/0734242X14557379

Mosaberpanah, M. A., & Umar, S. A. (2020). Utilizing Rice Husk Ash as Supplement to Cementitious Materials on Performance of Ultra High Performance Concrete: – A review. *Materials Today Sustainability*, *7–8*, 100030. https://doi.org/10.1016/J.MTSUST.2019.100030

Nurazzi, N. M., Asyraf, M. R. M., Fatimah Athiyah, S., Shazleen, S. S., Rafiqah, S. A., Harussani, M. M., Kamarudin, S. H., Razman, M. R., Rahmah, M., Zainudin, E. S., Ilyas, R. A., Aisyah, H. A., Norrrahim, M. N. F., Abdullah, N., Sapuan, S. M., & Khalina, A. (2021). A review on mechanical performance of hybrid natural fiber polymer composites for structural applications. In *Polymers* (Vol. 13, Issue 13). MDPI AG. https://doi.org/10.3390/polym13132170

Olivito, R. S., & Zuccarello, F. A. (2010). An experimental study on the tensile strength of steel fiber reinforced concrete. *Composites Part B: Engineering*, *41*(3), 246–255. https://doi.org/10.1016/j.compositesb.2009.12.003

Quercia, G., & Brouwers, H. J. H. (2010). *Application of nano-silica (nS) in concrete mixtures*.

Quercia, G., Hüsken, G., & Brouwers, H. J. H. (2012). Water demand of amorphous nano silica and its impact on the workability of cement paste. *Cement and Concrete Research*, *42*(2), 344–357. https://doi.org/10.1016/j.cemconres.2011.10.008

Rahman, I. A., & Padavettan, V. (2012). Synthesis of Silica nanoparticles by Sol-Gel: Size-dependent properties, surface modification, and applications in silica-polymer nanocompositesa review. In *Journal of Nanomaterials* (Vol. 2012). https://doi.org/10.1155/2012/132424

Scheibe, M., Dobrzynska, R., Urbaniak, M., & Bledzki, A. (2025). Polymer Structural Composites Reinforced with Hemp Fibres—Impact Tests of Composites After Long-Term Storage in Representative Aqueous Environments and Fire Tests in the Context of Their Disposal by Energy Recycling Methods. *Polymers*, *17*(3). https://doi.org/10.3390/polym17030276

Scrivener, K., Martirena, F., Bishnoi, S., & Maity, S. (2018). Calcined clay limestone cements (LC3). In *Cement and Concrete Research* (Vol. 114, pp. 49–56). Elsevier Ltd. https://doi.org/10.1016/j.cemconres.2017.08.017

Shaikh, F. U. A., & Supit, S. W. M. (2015). Chloride induced corrosion durability of high volume fly ash concretes containing nano particles. *Construction and Building Materials*, *99*, 208–225. https://doi.org/10.1016/j.conbuildmat.2015.09.030

Singh, L. P., Agarwal, S. K., Bhattacharyya, S. K., Sharma, U., & Ahalawat, S. (2011). *Preparation of Silica Nanoparticles and Its Beneficial Role in Cementitious Materials*. www.intechopen.com

Singh, L. P., Bhattacharyya, S. K., Kumar, R., Mishra, G., Sharma, U., Singh, G., & Ahalawat, S. (2014a). Sol-Gel processing of silica nanoparticles and their applications. In *Advances in Colloid and Interface Science* (Vol. 214, pp. 17–37). Elsevier B.V. https://doi.org/10.1016/j.cis.2014.10.007

Singh, L. P., Bhattacharyya, S. K., Kumar, R., Mishra, G., Sharma, U., Singh, G., & Ahalawat, S. (2014b). Sol-Gel processing of silica nanoparticles and their applications. In *Advances in Colloid and Interface Science* (Vol. 214, pp. 17–37). Elsevier B.V. https://doi.org/10.1016/j.cis.2014.10.007

Singh, S. P., & Murmu, M. (2010). *Eco-friendly concrete using by-products of steel industry*.

Sulka, G. D. (2023). Electrochemistry of Thin Films and Nanostructured Materials. In *Molecules* (Vol. 28, Issue 10). MDPI. https://doi.org/10.3390/molecules28104040

Tang, S., Wang, Y., Geng, Z., Xu, X., Yu, W., A, H., & Chen, J. (2021). Structure, fractality, mechanics and durability of calcium silicate hydrates. In *Fractal and*

Fractional (Vol. 5, Issue 2). MDPI AG. https://doi.org/10.3390/fractalfract5020047

Thomas, J. J., & Jennings, H. M. (2006). A colloidal interpretation of chemical aging of the C-S-H gel and its effects on the properties of cement paste. *Cement and Concrete Research*, *36*(1), 30–38. https://doi.org/10.1016/j.cemconres.2004.10.022

Thuadaij, N., & Nuntiya, A. (2008). Synthesis and Characterization of Nanosilica from Rice Husk Ash Prepared by Precipitation Method. In *CMU. J.Nat.Sci. Special Issue on Nanotechnology* (Vol. 7, Issue 1).

Torres-Carrasco, M., Reinosa, J. J., de la Rubia, M. A., Reyes, E., Alonso Peralta, F., & Fernández, J. F. (2019). Critical aspects in the handling of reactive silica in cementitious materials: Effectiveness of rice husk ash vs nano-silica in mortar dosage. *Construction and Building Materials*, *223*, 360–367. https://doi.org/10.1016/j.conbuildmat.2019.07.023

Tran, H. B., Le, V. B., & Phan, V. T. A. (2021). Mechanical properties of high strength concrete containing nano sio2 made from rice husk ash in Southern Vietnam. *Crystals*, *11*(8). https://doi.org/10.3390/cryst11080932

Yuvakkumar, R., Elango, V., Rajendran, V., & Kannan, N. (2014). High-purity nano silica powder from rice husk using a simple chemical method. *Journal of Experimental Nanoscience*, *9*(3), 272–281. https://doi.org/10.1080/17458080.2012.656709

Zareei, S. A., Ameri, F., Dorostkar, F., & Ahmadi, M. (2017). Rice husk ash as a partial replacement of cement in high strength concrete containing micro silica: Evaluating durability and mechanical properties. *Case Studies in Construction Materials*, *7*, 73–81. https://doi.org/10.1016/j.cscm.2017.05.001

Zhang, M. H., & Islam, J. (2012). Use of nano-silica to reduce setting time and increase early strength of concretes with high volumes of fly ash or slag. *Construction and Building Materials*, *29*, 573–580. https://doi.org/10.1016/j.conbuildmat.2011.11.013

Zhang, P., Wan, J., Wang, K., & Li, Q. (2017). Influence of nano-SiO2 on properties of fresh and hardened high performance concrete: A state-of-the-art review. *Construction and Building Materials*, *148*, 648–658. https://doi.org/10.1016/J.CONBUILDMAT.2017.05.059

Appendices

Appendix A: Property test of materials

1) Specific gravity test of Cement

Cement=64 gm

Initial Reading=0.8cm^3

Final Reading=21.5 cm^3

Specific Gravity= Weight/Reading Difference =64/(21.5-0.8)=3.0917=3.1

2) Specific gravity test of Nano Silica Powder

NS=44.5 gm

Initial Reading=0.3 cm^3

Final Reading=22.9 cm^3

Specific Gravity= Weight/Reading Difference =44.5/(22.9-0.3)=1.97

3) Water Content

Can + Wet NSG = 160 gm

Can weight = 72 gm

NSG = 160-72 = 88 gm

Can + Dry NSG = 86 gm

Dry Powder = 86-72 = 14 gm

Water = 88-14 = 74 gm

Water content = 74*100/88 = 84.09=84.1%

Appendix B: Mix Design

Target W/C ratio by weight = 0.5

Specific gravity of Cement = 3.1

Specific gravity of pozzolanic materials = 1.97

Density of water = 1 g/cm3 = 1000 kg/m3

Table B1: Summary of mix design for mortar

Materials	**Control sample**	**% Replacement of cement by NSG**			
		1%	**2%**	**3%**	**5%**
Water	225 gm	200.57 gm	176.14 gm	151.71 gm	103.0 gm
Cement	450 gm	445.50 gm	441.00 gm	436.50 gm	427.5 gm
NSG	---	27.29 gm	54.58 gm	81.87 gm	135.4 gm
Adjusted Water	---	15.00 gm	35.00 gm	40.00 gm	60.0 gm
CEN Sand	1350 gm	1350 gm	1350 gm	1350 gm	1350 gm

Appendix C: Test Result

Table C1: Flow table test

NSG	Flow Value (%)
Control	60
1% Replacement	56
2% Replacement	65
3% Replacement	56
5% Replacement	57

Table C2: Fresh density of mortar

NSG	Fresh Density (kg/m^3)
Control	2295
1% Replacement	2270
2% Replacement	2245
3% Replacement	2230
5% Replacement	2210

Table C3: Hardened density of mortar

NSG	Curing Intervals	Hardened Density (kg/m^3)
Control	7 Days	2115
1% Replacement		2110
2% Replacement		2090
3% Replacement		2070
5% Replacement		2050
Control	28 Days	2125
1% Replacement		2065
2% Replacement		2040
3% Replacement		2030
5% Replacement		1985
Control	90 Days	2120
1% Replacement		2065
2% Replacement		2040
3% Replacement		2015
5% Replacement		1990

Table C4: Flexural and compressive strength

NSG	Curing Age (days)	Flexural Strength (MPa)	Compressive Strength (MPa)	SAI (%)
0%	7	5.02	46.95	---
0%	28	6.05	48.18	---
0%	90	6.63	51.55	---
1%	7	5.67	50.17	106.86
1%	28	6.3	51.18	106.23
1%	90	6.94	53.96	104.68
2%	7	4.92	46.01	98.00
2%	28	5.7	47.39	98.36
2%	90	6.51	50.62	98.20
3%	7	4.85	45.36	96.61
3%	28	5.72	45.55	94.54
3%	90	6.43	49.99	96.97
5%	7	4.65	43.49	92.63
5%	28	5.37	43.76	90.83
5%	90	5.67	46.09	89.41

Table C5: Drying shrinkage

NSG	7 Days (%)	14 Days (%)	21 Days (%)	28 Days (%)
0%	0.0303	0.0408	0.0689	0.077
1%	0.0259	0.0498	0.0798	0.127
2%	0.0516	0.0823	0.1158	0.1358
3%	0.0305	0.0658	0.0889	0.1067
5%	0.0342	0.0772	0.0953	0.1516

Table C6: Water absorption

NSG	7 Days	28 Days	90 Days
0%	5.91%	6.80%	7.18%
1%	7.57%	8.50%	9.07%
2%	6.94%	9.77%	9.96%
3%	6.91%	9.44%	10.32%
5%	8.38%	12.79%	11.51%

Table C7: Normal consistency, setting time and soundness

NSG	Flow Value(mm)
0%	160
1%	156
2%	165
3%	156
5%	157

Table C8: Setting time

NSG	Initial Setting Time	Initial Setting Time
Control	85 Minutes	168 Minutes
1%	82 Minutes	160 Minutes
2%	80 Minutes	150 Minutes
3%	75 Minutes	142 Minutes
5%	60 Minutes	125 Minutes

Table C9: Soundness test results

NSG	Soundness (mm)
0%	1
1%	1
2%	1.4
3%	1.8
5%	2.2

Table C10: Autoclave expansion test

NSG	Expansion (%)
0%	0.00737
1%	0.01156
2%	0.01965
3%	0.02491
5%	0.03561

Table C11: Electrical resistivity

NSG	Surface Resistivity Readings (kΩ-cm)
Control	4.15
1% Replacement	3.77
2% Replacement	3.47
3% Replacement	3.6
5% Replacement	3.35

Table C12: Pozzolanic activity (Frattini)

NSG	Cao Concentration (millimoles per litre)	OH Concentration (millimoles per litre)
NSG	6.48	155.34
Cement	12.96	73.7
1% Replacement	9.99	97.83
2% Replacement	9.29	81.07
3% Replacement	8.91	65.74
5% Replacement	12.89	70.75